약학석사 학위논문

Stilbenoids and Flavonoid Glycosides from *Iris pallasii*

타래붓꽃에서 분리한 Stilbenoids 와 Flavonoid Glycosides 성분

2019 년 2 월

서울대학교 대학원

약학과 생약학 전공

김 수 성

Abstract

Iris pallasii var. chinensis (Fisch). Koidz (Iridacea) is an herbaceous perennid which is widely distributed in deep mountains of China, Korea, Japan and Russia. It has been found many places in Korea because of its developed root system. The dried seed of *Iris pallasii* traditionally used for the treatment of jaundice, diarrhea, hemoptysis, leucorrhea and pharyngitis. The previous phytochemical studies of *Iris* species identified the presence of flavonoids, xanthones, triterpenoids, stilbenoids and quinones. Nowadays, more attention has been focused on the stilbene oligomers because they showed a various pharmacological property like neuroprotective, anti-proliferative, antivirus activities. Based on these biological activity, seeds of *Iris pallasii* have been evaluated for the treatment of dementia. In this research, we isolated ten stilbenoids (**1 - 10**), two catechin (**11** – **12**) four flavonoid glycosides (**13 - 16**) from *Iris pallasii* seeds, flower and leaves. Among them, *cis*-ε-viniferin-13b-11a-O-*β*-D-diglucopyranoside (**1**) and *cis*-vitisin B-13b-*O*-*β*-D-glucopyranoside (**2**) were reported for the first time from nature. The isolated compounds were tested their neuraminidase inhibitory activities against H1N1 viral strains. Compounds **7-10** corresponding to stilbene tetramers showed significant virus inhibition effect than other stilbenoids compounds and flavonoid glycosides at the low range of concentration (25 μM). Among them, compounds **9** and **10** with *trans* type olefinic tetramers were evalutated higher neuraminidase inhibitory effects than the others. Especially, Compound **9** showed potent neuraminidase activity.

Keyword: *Iris pallasii*, Iridaceae, stilbenoid, flavonoid glycosides, neuraminidase inhibitiory activities

Student Number: 2017-22999

Table of Contents

List of Abbreviations

ACN: acetonitrile

brd: broad doublet

$CHCl_3$: chloroform

COSY: correlation spectroscopy

DMSO: dimethyl sulfoxide

d: doublet

dd: doublet of doublet

dt: doublet of triplet

EtOAc: ethyl acetate

HMBC: heteronuclear multi-bond correlation

HPLC: high performance liquid chromatography

HRESIMS: high-resolution electrospray ionization mass spectrometry

HSQC: heteronuclear single quantum coherence

Hz: hertz

IC_{50}: the half maximal inhibitory concentration

m: multiplet

CH_3OH: methanol

MS: mass spectrometry

n-BuOH: *n*-butanol

NMR: nuclear magnetic resonance

NP: normal phase

qTOF: quadrupole-time of flight

RP: reverse phase

NOESY: nuclear overhauser effect spectroscopy

s: singlet

sept: septet

TLC: thin layer chromatography

t_R: retention time (RT)

UPLC: ultra high performance liquid chromatography

UV: ultraviolet absorption spectroscopy

List of Figures

List of Tables

List of Schemes

I. Introduction

1. *Iris pallasii var. chinensis* Fischer (Iridaceae)

The monocotyledon family Iridaceae comprise some 1800 species in 60 genera, representing one of the largest families of the superorder Lilianae (Goldblatt 2000). Members of Iridaceae are worldwide in distribution, particularly diverse in Africa which are restricted to southern Africa (Reeves et al. 2001). *Iris pallasii var chinensis* have its place to the family of Iridaceae, is an herbaceous perennid native to East asia such as China, Russia and Japan (Lv et al. 2015). It grows in a dry place of mountain, because of its developed root system for conserving water. The previous phytochemical reports of Iris species revealed the existence of flavones (Rahman et al. 2000), triterpenes (Wong et al. 1986), stilbenes and quinone (Seki et al. 1995).

The dried seeds of *Iris pallasii* have the effects of curing poison, lowering heat, haemostatic, removing dampness. Because of these feature, it has been used for treatment of jaundice, diarrhea, hemoptysis, leucorrhea (Lv et al. 2015). The secondary metabolites that are mainly made in the seeds of *Iris pallasii* are stilbenoids. Naturally biosynthetic oligostilbenes are obtaing more attention because they show several beneficial effects for health, including hepatoprotective, antitumor, anti-adipogenic, antioxidant, antiaging, anti-inflammatory, anti-microbial, antiviral, immunosuppressive and neuroprotective activities (Lv et al. 2016). This type of stilbene oligomers are made in very small amounts in herbals and not commercially obtainable (Lv et al. 2016). In addition, they have been studied much less than the monomer such as resveratrol.

2. Stilbenoid

Most phytochemical studies on stilbenoids made on the grapevines, and the structures are one of the important class of grape polyphenols. In general stilbenes act as phytoalexins in soft tissues. Viniferin, well known resveratrol dimer, can also shape in grape inner tissues by oligomerization as dynamic shield against exogenous attacks.

Flavonoid glycoside derivatives

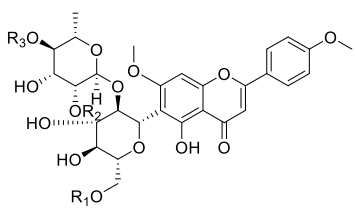

R_1=R_2=H, R_3=Ac: 4‴-*O*-acetyl-embinin
R_1=H, R_2=Ac, R_3=H: 2‴,4‴-*O*-diacetyl-embinin
R_1=Ac, R_2=H, R_3=Ac: 6″,4‴-*O*-diacetyl-embinin
R_1=R_2=R_3=H: embinin

Triterpenes

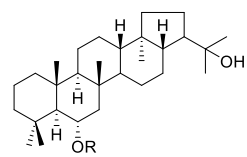

R=H: Zeorin
R=OAc: Zeorin acetate

Stilbenoids

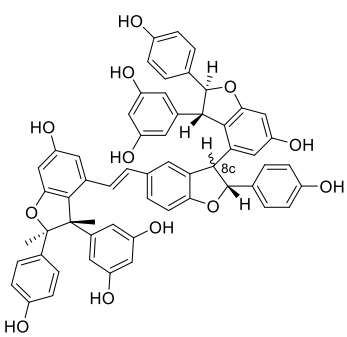

8c=α: Vitisin B
8c=β: Vitisin C

Quinones

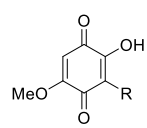

R=$C_{16}H_{33}$: Irisoquin A
R=$C_{17}H_{35}$: Irisoquin B
R=$C_{18}H_{37}$: Irisoquin C
R=$C_{19}H_{39}$: Irisoquin D

Figure 1. Structures of chemical constituents reported in Iridaceae

(Flamini et al. 2015). Among numerous natural stilbenoids, Resveratrol shares a general biosynthetic route responsible for the production of cinnamic acids and flavonoids through the phenylpropanoid pathway (Vogt 2010). Phenylalanine has undergone quite a few enzymatic reactions to produce linear intermediate. These intermediate plays an important role in biosynthesis of flavonoids or biosynthesis of stilbenes, depending on the situation. Stilbene synthase is programed to be induced when the situation of stimuli such as physical injury, UV irradiation, or pathogenic invasion (Vannozzi et al. 2012). Because of these properties, resveratrol and its oligomeric derivatives are located in lignified stem tissues that are not photo-synthetic like flowers or leaves where they have been exhibited to disturb with ion transport and related redox process (Gorham and J. Coughlan 1980). Resveratrol has undergone several structural changes such as glycosylation after it has been biosynthesized. Piceid, the resveratrol glycoside derivatives, is thought to support in the translocating the metabolites and storage of resveratrol within the cell tissues as well as defend resveratrol from radical oxidation (Regev-Shoshani et al. 2003).

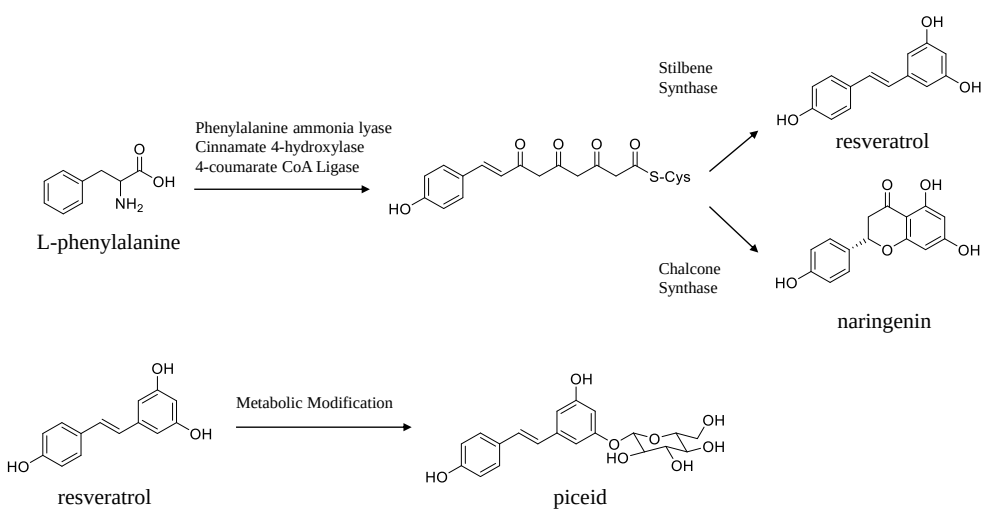

Figure 2. Resveratrol biosynthesis and modification

The majority of naturally appearing stilbenes have several benzene groups and can be prenylated or geranylated. These prenylated (geranylated) oligomers, compounds result from the oxidative coupling of *trans*-resveratrol or other monomeric stilbene units, such as oxyresveratrol, isorhapontigenin or piceatannol, have attracted interest due to their complex structural configurations (Shen et al. 2009). Basically, the monomeric stilbene units are linked by either C-C or C-O-C bonds with two, four, six or eight linkage points (Shen et al. 2009). These units can also form various types of trimers (Figure 3) and tetramers (Figure 4). Given the nature of these structures, they have strong anti-oxidant/radical scavenging properties and are easily polymerized by oxidative coupling to form oligomers (Shen et al. 2009). Due to their varied pattern and complexity of making oligomers, a wide range of oligostilbenoids are possible. Stilbenes are being studied as a source for developing new drugs and medicines. The new stilbene compounds isolated recently have shown diverse bioactivities, among them, monomeric stilbenes are tested as candidates for dementia and cancer treatment. Given this, a larger unit of stilbene structures are also expected to be a potential candidate for treatment for intractable diseases.

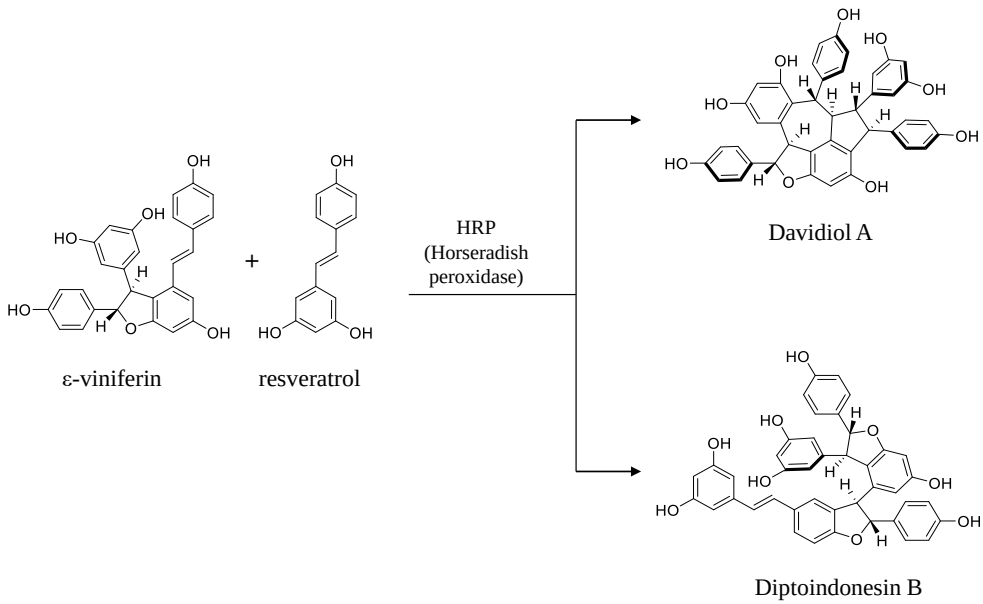

Figure 3. Studies of the biosynthesis of stilbene trimer

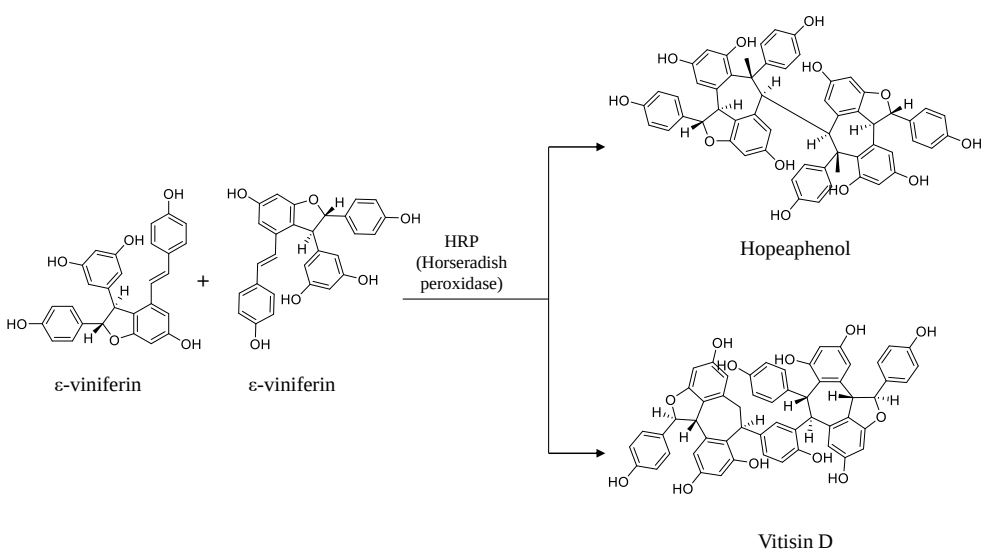

Figure 4. Studies of the biosynthesis of stilbene tetramer

3. Flavonoid

Flavonoids are typical secondary metabolite high in vegetables, fruits, wines and tea. Flavonols are among the principal classes of bioactive polyphenols and are mainly present in the aerial parts of *Iris* species. Flavonoids are divided into 6 sub-groups (flavone, flavonol, flavan-3-ol, flavanone, isoflavone, anthocyanidin, and catechin) and depending on where the sugar is attached, the type changes. Four known C-glycosylflavones, embinin derivatives are isolated from the leaves and flos of *Iris pallasii*. They showed duplication of signals at a certain rate in the ^{1}H and ^{13}C-NMR spectra in room temperature. Similar examinations had been made previously on another C-glycosylflavone, spinosyn, and attributed to the existence of two rotamers which were gradually interconverting via rotation about the C-glycosidic bond (Lewis et al. 2000). Rotamers happen when rotation is deterred by a rotational energy barrier (Frank et al. 2012) (Figure 5). Flavonoid C-glycosides displayed considerable antioxidant activity, carcinostatic activity and antitumor activity, and other biological effects (Xiao et al. 2016).

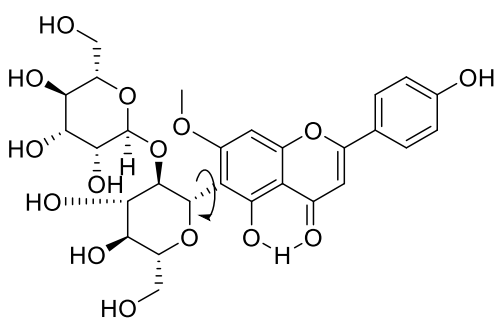

Figure 5. Rotation of Flavonoid C-glycoside

4. Neuraminidase assay and its purpose of study

The infection of viruses and bacteria has been recognized as a constant danger to human health. This is because these microbes evolved over generations to develop resistance to existing traditional drugs. Thus, discovery of lead compounds with inhibition abilities against key enzymes essential for infectivity is a massive interest to the medicinal group (Yuk et al. 2013). Neuraminidase (NA) is one of the greatest promising drug targets in pharmaceutical and agricultural chemistry since this key

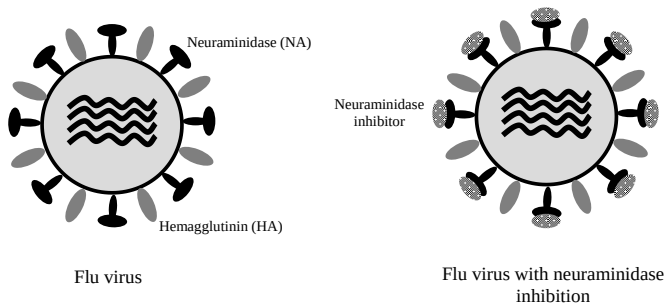

Figure 6. Diagram of an influenza virus with the location of neuraminidase (NA) and hemagglutinin (HA) glycoproteins

enzyme is involved in many biological and pathological processes (Paulson and Kawasaki 2011). The NA is responsible for cutting sialic acids, the residue of glycoconjugate on the surface of the cell. This process is associated with cell signals and recognition (Yuk et al. 2013). In this study, the seeds of *Iris pallasii* extractions and isolated compounds were exhibit neuraminidase inhibitory properties. Since the seeds of *Iris pallasii* have long been used as a cure for diarrhea and sore throat, a disease linked to the virus, we have tested their inhibitory activity. To clarify the link between the traditional usage and the structure of isolated compounds, all isolates were tested for their inhibition activities against H1N1 type neuraminidases viral strain.

II. Meterials and Methods

1. Plant materials

Iris pallasii var. chinensis Fischer were collected at the Medicinal Plant Garden (Seoul National University, Koyang, Republic of Korea). The sample was identified by S. I. Han (The medicinal Plant Garden, College of Pharmacy, Seoul National University), and a voucher specimen (SNU-2016-09) has been deposited at the Herbarium in the Medicinal Plant Garden.

2. Chemicals, reagents and chromatography

2-1. Chemical reagents

- Sephadex™ LH-20 (bead size 25-100 μm, GE Healthcare, IL, USA)
- TLC Silicagel 60 F_{254} (Art. 5715, Merck, Germany)
- TLC Silicagel 60 C-18F_{254} (Art. 15389, Merck, Germany)
- TLC visualization reagent: Anisaldehyde-H_2SO_4
- HP-20 (Mitsubishi Chemical Industries Ltd., Tokyo, Japan)
- MPLC Reveleris flash cartridges Silica 120g (Grace, USA)
- MPLC Reveleris flash cartridges Silica C-18 120g (Grace, USA)
- All Solvents used for extraction, fractionation and isolation (n-hexane, $CHCl_3$, EtOAc, n-BuOH, MeOH) were first grade (Daejung, Si-heung, Republic of Korea)
- Solvents used for HPLC chromatography (ACN, MeOH) were purchased from J. T. Baker Chemical Corp. (Center valley, PA, USA)
- NMR solvents ($CDCl_3$, CD_3OD, DMSO-d_6) were purchased from Merck (Darmstadt, Germany)

2-2. Bioassay reagent

- Dulbecco's Modified Eagle's Medium (DMEM), (Hyclone, Logan, UT, USA).
- Fetal bovine serum (FBS) (Hyclone, Logan, UT, USA)
- PEI transfection reagent (Polyscience, Inc., Warrington, PA, USA
- Phosphate-buffered saline (PBS) (Takara, Shiga, Japan).
- EDTA (Ethylene Diamine Tetra Acetic acid) (Sigma-Aldrich Co., St Louis, MO, USA).
- Trypsin (Hyclone, Logan, UT, USA)
- Bovine serum albumin (BSA) (sigma-Aldrich Co., St Louis, MO, USA).
- Formaldehyde (Junsei Chemical Co. Ltd, City, Japan).
- 2-(4-methylumbelliferyl)-α-D-N-acetyl neuraminic acid (4-MU-NANA) (Sigma-Aldrich Co., St Louis, MO, USA).

- MES (2-(*N*morpholino)ethane sulfonic acid) (Sigma-Aldrich Co., St Louis, MO, USA).
- Glycine (Junsei Chemical Co. Ltd, City, Japan)

3. Experimental instruments

- Analytical balance: Mettler AE 50 (Switzerland)
- Autoclave: Sanyo MLS 3000 (Japan)
- Centrifuge: Effendroff centrifuge 5810 (Germany)
- Evaporator: EYELA NE (USA)
- Ultrasonicator: Branson 8510 (USA)
- Analytical HPLC system
    - HPLC: Dionex 3000 Ultimate RLSC system, Thermo Dionex (St. Albans, UK)
    - Column: YMC triart C-18 column, 4.6 × 250mm, 5μm (YMC Co. Ltd., Japan)
- MPLC: MPLC-Reveleris system (Grace, USA)
- NMR: JEOL JMN-LA300 Spectrometer 300 (JEOL, Japan)
  Bruker AVANCE digital Spectrometer 300 (Bruker, Germany)
  Bruker AVANCE digital Spectrometer 400 (Bruker, Germany)
  Bruker AVANCE digital Spectrometer 600 (Bruker, Germany)
  Bruker AVANCE digital Spectrometer 800 (Bruker, Germany)
- Polarimeter: Jasco P-2000 polarimeter (Jasco, USA)
- Preparative HPLC system
    - Waters Delta Prep coupled with Waters 2489 UV/vis detector (USA)
    - Gilson 321 Pump and UV/vis detector (USA)
    - Column: YMC triart C-18 column, 20 × 250nm, 5 μm (YMC Co. Ltd., Japan)
- UPLC-qTOF MS system
    - Waters Acquity UPLC® system (Waters Co., Milford, MA, USA)
    - Column: Waters Acquity UPLC BEH C-18, 2.1 mm × 100 mm, 1.7 μm
    - Waters Xevo G2 qTOF mass spectrometer (Waters MS Technologies, Manchester, UK)

4. Extraction, Fractionation and isolation of *Iris pallasii*

4-1. Extractions, fractionation of the seeds of *Iris pallasii*

The air-dried seedcases of *Iris pallasii* (2 kg) were chopped and extracted with 70% EtOH in water at room temperature for 2 days. The filtrate was concentrated *in vacuo* to yield a brown gum. This crude extract (50.0 g) was deposited in distilled water and followed by fractionation with *n*-hexane (2.9g), chloroform (2.4g), EtOAc (20g), *n*-BuOH(7g) and water (Scheme 1).

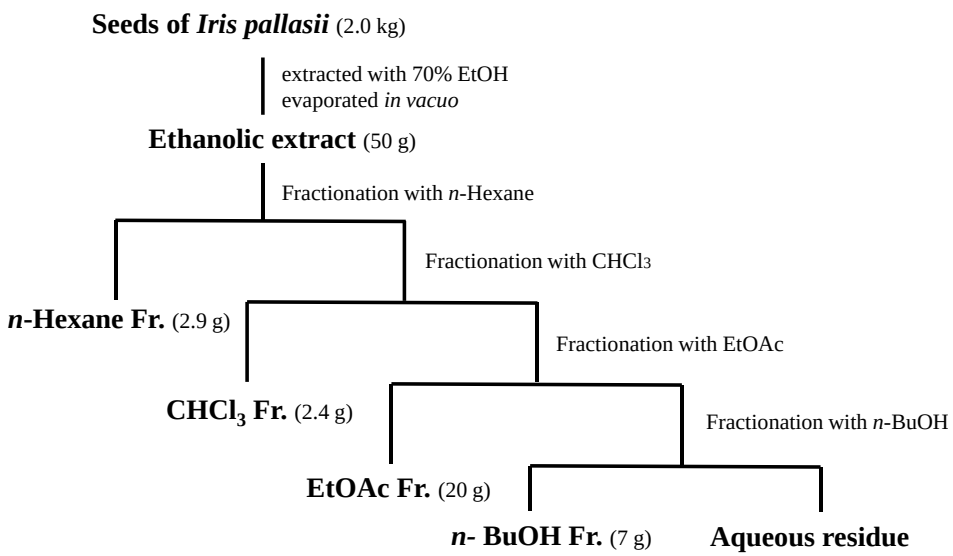

Scheme 1. Extraction, fractionation of the seeds of *Iris pallasii*

4-1-1 Isolation of compounds from EtOAc fraction of the seeds of *Iris pallasii*

The EtOAc fraction (20.0 g) was chromatographed with a reverse phase MPLC [A:B gradient from 30:70 to 100:0, acetonitrile (A), H_2O with 0.1% formic acid (B); flow rate 80 ml/min], to yield 4 fraction (EA1 – EA4). Compound **11** (210 mg), **12** (9 mg) were isolated from EA 1 fraction through preparative HPLC [0-30min: A:B (79:21) isocratic, acetonitrile (A), 0.1% formic acid in H_2O (B); flow rate 13 ml/min; UV detection at 210 nm]. EA 2 fraction was applied to Sephadex LH-20 with 100% MeOH to separate two subfraction, one of which separated compound **1** (7.1 mg). The other subfraction then subjected to semi-preparative HPLC [0-15min: A:B (29:71) isocratic, acetonitrile (A), 0.1% formic acid in H_2O (B); flow rate 4ml/min], to afford compounds **2** (3.9 mg) and **4** (11.1 mg). Compounds **3** (340 mg) and **4** (410 mg) were show major peak on UV chromatogram and the MPLC was used once again, inferred that the amount would be large. The condition of MPLC was A:B gradient from 45:55 isocratic MeOH (A), H_2O with 0.1% formic acid (B); flow rate 40 ml/min, UV detection at 254 nm. In the EA 4 fraction, prep HPLC [0-25min: A:B (30:70) isocratic, acetonitrile (A), 0.1% formic acid in H_2O (B)] was performed to obtain two subfraction depending on the polarity and four compounds were separated each through semi-preparative HPLC [0-25min: A:B (25:75) isocratic, acetonitrile (A), 0.1% formic acid in H_2O (B)], [0-25min: A:B (34:66) isocratic, acetonitrile (A), 0.1% formic acid in H_2O (B)] each (Scheme 2).

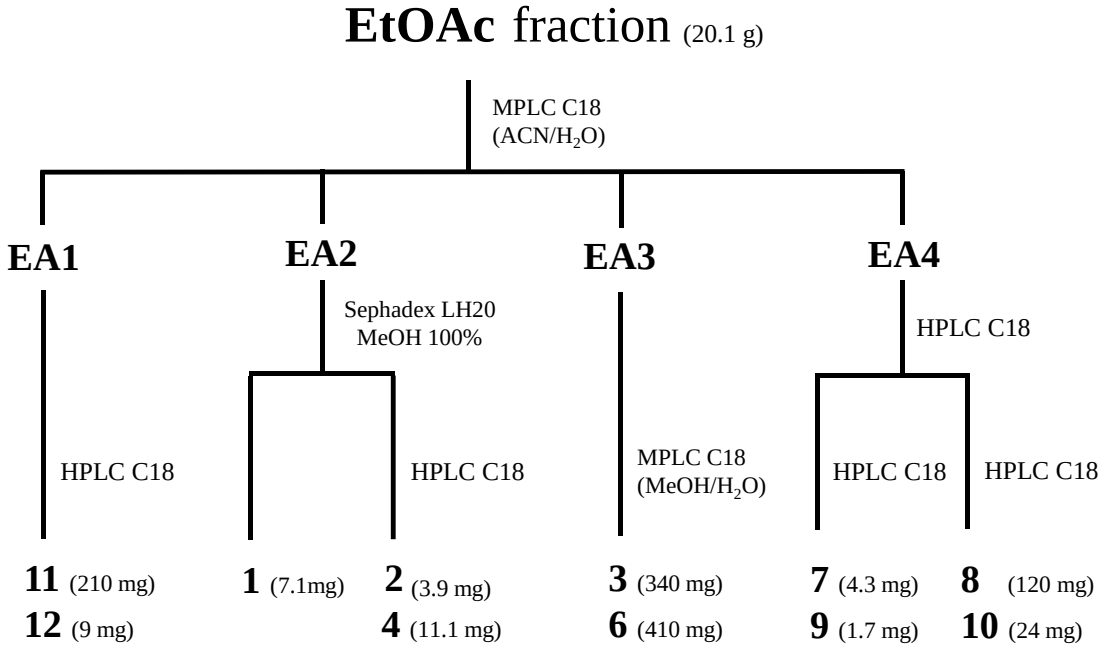

Scheme 2. Isolation of compounds from the EtOAc fraction of the seeds of *Iris pallas*

4-1-2 Isolation of compounds from *n*-BuOH fraction of the seeds of *Iris pallasii*.

The *n*-BuOH fraction was fractionated into two fractions by using ODS silica gel MPLC [A:B gradient from 30:70 to 90:0, acetonitrile (A), H_2O with 0.1% formic acid (B); flow rate 60 ml/min] and compound **5** (28.3 mg) was isolated from BU 1 subfraction (Scheme 3).

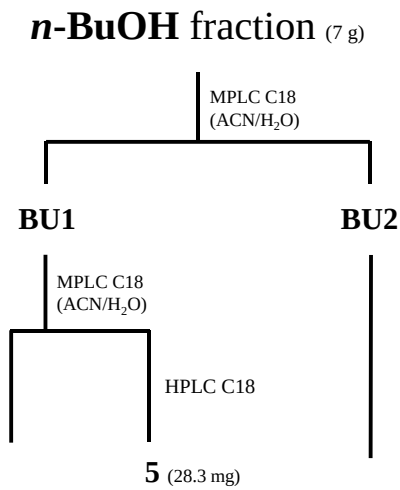

Scheme 3. Isolation of compounds from the *n*-BuOH fraction of the seeds of *Iris pallasii*

4-2. Extractions and isolation of the flowers and leaves of *Iris pallasii*

The dried flowers and leaves of *Iris pallasii* (100g) were extracted with 70% EtOH in ultrasonic apparatus. Each ethanolic extracts were successively partitioned with *n*-hexane, chloroform, EtOAc, *n*-BuOH and water like seeds. The EtOAc fr. of flowers (740 mg) was chromatographed with a Sephadex LH 20 with MeOH 100%, to yield four fractions (1-4). Compounds **13** (24.3 mg) and **14** (48.3 mg) were obtained from fraction 2 respectively by ODS silica gel HPLC [A:B gradient 32:68 isocratic, acetonitrile (A), H_2O with 0.1% formic acid (B); flow rate 14 ml/min]. The $CHCl_3$ fraction of leaves also fractionated with Sephadex LH 20 with MeOH 100% to yield 5 subfraction. Fraction 4 then chromatographed with MPLC [A:B gradient from 35:65 to 80:0, acetonitrile (A), H_2O with 0.1% formic acid (B); flow rate 60 ml/min] and successively separated by the semi-preparative HPLC [A:B gradient 35:65 isocratic, acetonitrile (A), H_2O with 0.1% formic acid (B); flow rate 4 ml/min] which yielded compounds **15** (16.3 mg) and **16** (40.3 mg) (Scheme 4).

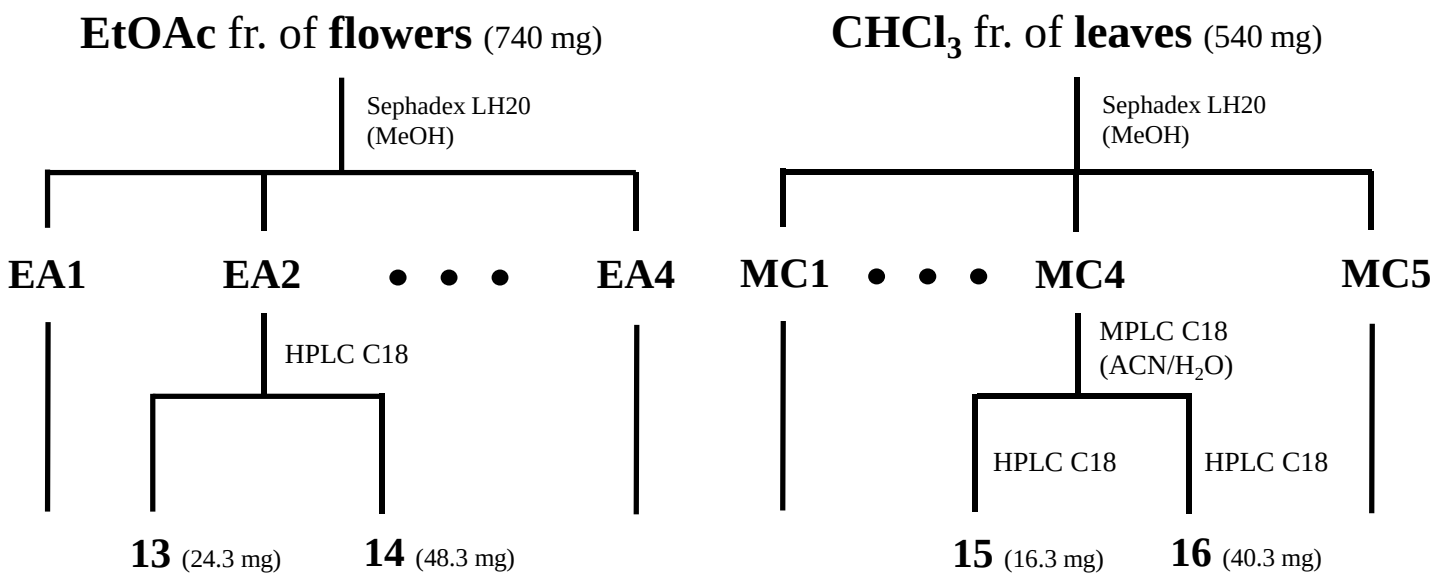

Scheme 4. Isolation of compounds from the *n*-BuOH fraction of the seeds of *Iris pallasii*

4-3. Chemical and spectral properties of isolated compounds

4-3-1. Compound **1**

Brown amorphous powder

$[\alpha]_{\mathrm{D}}^{20}$ + 61.2 (*c* 0.1, MeOH)

HRESIMS *m/z* 777.2388 $[M-H]^-$ (calcd for $C_{40}H_{42}O_{16}$ 777.2395, 0.9 ppm)

UV (MeOH) λ_{max} (log ε) 230 (sh), 204 (4.7), 287 (4.2) nm

ECD (MeOH) λ_{max} (Δε) 206 (20.5), 236 (15.1), 311 (−2.9) nm

^{1}H NMR (600 MHz, CD_3OD) see Table 1

^{13}C NMR (150 MHz, CD_3OD) see Table 2

4-3-2. Compound **2**

Brown amorphous powder

$[\alpha]_{\mathrm{D}}^{20}$ – 18.1 (*c* 0.1, MeOH)

HRESIMS *m/z* 1067.3148 $[M-H]^-$ (calcd for $C_{62}H_{52}O_{17}$ 1067.3126, 2.1 ppm)

UV (MeOH) λ_{max} (log ε) 225 (sh), 208 (4.9), 285 (4.3) nm

ECD (MeOH) λ_{max} ($\Delta\varepsilon$) 208 (11.8), 222 (-11.2), 295 (−5.7) nm

^{1}H NMR (600 MHz, CD_3OD) see Table 3

^{13}C NMR (150 MHz, CD_3OD) see Table 4

4-3-3. Compound **3**

Brown amorphous powder

$[\alpha]_{D}^{20}$ + 69.4 (*c* 0.1, MeOH)

HRESIMS *m*/*z* 453.1342 $[M-H]^-$ (calcd for $C_{30}H_{26}O_{12}$ 453.1338, 0.9 ppm)

UV (MeOH) λ_{max} (log ε) 240 (sh), 207 (4.5), 325 (4.3) nm

ECD (MeOH) λ_{max} ($\Delta\varepsilon$) 209 (11.4), 239 (29.1), 296 (−4.2) nm

^{1}H NMR (850 MHz, CD_3OD) see Table 1

^{13}C NMR (212.5 MHz, CD_3OD) see Table 2

4-3-4. Compound **4**

Brown amorphous powder

$[\alpha]_D^{20}$ + 33.2 (*c* 0.1, MeOH)

HRESIMS *m/z* 615.1863 $[M-H]^-$ (calcd for $C_{34}H_{32}O_{11}$ 615.1866, 0.5 ppm)

UV (MeOH) λ_{max} (log ε) 230 (sh), 204 (4.6), 324 (4.2) nm

ECD (MeOH) λ_{max} (Δε) 207 (15.8), 238 (19.7), 308 (−3.7) nm

^{1}H NMR (600 MHz, CD_3OD) see Table 1

^{13}C NMR (150 MHz, CD_3OD) see Table 2

4-3-5. Compound **5**

Brown amorphous powder

$[\alpha]_D^{20}$ – 11.1 (*c* 0.1, MeOH)

HRESIMS *m/z* 777.2388 $[M-H]^-$ (calcd for $C_{20}H_{27}O_2$ 777.2395, 0.3 ppm)

UV (MeOH) λ_{max} (log ε) 250 (sh), 203 (4.7), 325 (4.2) nm

ECD (MeOH) λ_{max} (Δε) 206 (14.5), 239 (14.9), 310 (−2.4) nm

^{1}H NMR (600 MHz, $CDCl_3$) see Table 1

^{13}C NMR (150 MHz, $CDCl_3$) see Table 2

4-3-6. Compound **6**

Brown amorphous powder

$[\alpha]_D^{20}$ + 285 (c 0.1, MeOH)

HRESIMS m/z 905.2591 $[M-H]^-$ (calcd for $C_{56}H_{42}O_{12}$ 905.2598, 0.8 ppm)

UV (MeOH) λ_{max} (log ε) 230 (sh), 210 (4.9), 285 (4.3) nm

ECD (MeOH) λmax (Δε) 236 (42.3), 290 (0.85) nm

^{1}H NMR (800 MHz, CD_3OD): δ 7.15 (H-2a/6a, d;8.6), 7.10 (H-2c/6c, d;8.6), 7.03 (H-2d/6d, d;8.2), 6.80 (H-3a/5a, d;8.6), 6.75 (H-6b, dd;8.5, 2.0), 6.74 (H-3c/5c, d;8.6), 6.65 (H-3d/5d, d;8.6), 6.63 (H-5b, d;8.5), 6.47 (H-14b, d;1.9), 6.34 (H-7b, d;16.2), 6.30 (H-8b, d;16.2), 6.21 (H-12a, t;2.1) 6.21 (H-2b, d;2.1), 6.15 (H-12b, d;1.6), 6.12 (H-2d/6d, d;8.2), 6.12 (H-14a, d;2.1), 6.09 (H-14d, d;2.1), 6.07 (H-12c, d;2.0), 5.98 (H-12d, d;2.2), 5.97 (H-14c, d;2.0), 5.83 (H-7d, d;11.5), 5.44 (H-8c, d;3.8), 5.33 (H-7a, d;6.4), 5.27 (H-7c, d;3.4), 4.28 (H-8a, d;6.4), 4.15 (H-8d, d;11.6)

^{13}C NMR (200 MHz, CD_3OD): δ

161.6 (C-11b), 159.0 (C-13b), 158.5 (C-11a), 158.5 (C-13a), 158.2 (C-4a), 157.4 (C-4b), 157.4 (C-4c), 157.2 (C-11d), 157.1 (C-13d), 155.5 (C-11c), 155.4 (C-4d), 154.2 (C-13c), 145.9 (C-9a), 141.2 (C-9c), 140.3 (C-9d), 135.8 (C-9b), 134.7 (C-1d), 132.6 (C-1a), 131.5 (C-3b), 131.4 (C-2b), 129.9 (C-8b), 129.7 (C-1c), 128.9 (C-1b), 128.9 (C-2c), 128.9 (C-6c), 127.9 (C-6b), 127.8 (C-2a), 127.8 (C-6a), 126.9 (C-2d), 126.9 (C-6d), 122.2 (C-7b), 121.1 (C-10c), 119.7 (C-10d), 119.7 (C-10b), 118.1 (C-5b), 114.9 (C-3a), 114.9 (C-5a), 114.8 (C-3c), 114.8 (C-5c), 114.2 (C-3d), 114.2 (C-5d), 109.1 (C-14c), 107.2 (C-14d), 106.0 (C-10a), 106.0 (C-14a), 102.9 (C-14b), 100.9

(C-12a), 99.6 (C-12d), 95.2 (C-12b), 94.8 (C-12c), 93.4 (C-7a), 87.7 (C-7d), 56.8 (C-8a), 48.5 (C-8d), 40.3 (C-8c), 39.9 (C-7c)

4-3-7. Compound **7**

Brown amorphous powder

$[\alpha]_{\mathrm{D}}^{20}$ – 16.2 (*c* 0.1, MeOH)

HRESIMS *m*/*z* 905.2589 $[M-H]^-$ (calcd for $C_{56}H_{42}O_{12}$ 905.2598, 1.0 ppm)

UV (MeOH) λ_{max} (log ε) 241 (sh), 205 (4.8), 284 (4.1) nm

ECD (MeOH) λ_{max} (Δε) 207 (18.3), 221 (-11.8), 309 (−7.5) nm

^{1}H NMR (800 MHz, CD_3OD) see Table 3

^{13}C NMR (200 MHz, CD_3OD) see Table 4

4-3-8. Compound **8**

Brown amorphous powder

$[\alpha]_{\mathrm{D}}^{20}$ + 841.0 (*c* 0.1, MeOH)

HRESIMS *m*/*z* 905.2578 $[M-H]^-$ (calcd for $C_{56}H_{42}O_{12}$ 905.2598, 0.1 ppm)

UV (MeOH) λ_{max} (log ε) 230 (sh), 208 (4.3), 286 (4.3) nm

ECD (MeOH) λ_{max} (Δε) 207 (14.7), 239 (49.7), 306 (−1.5) nm

^{1}H NMR (800 MHz, CD_3OD) see Table 3

^{13}C NMR (200 MHz, CD_3OD) see Table 4

4-3-9. Compound **9**

Brown amorphous powder

$[\alpha]_D^{20}$ – 66.1 (*c* 0.1, MeOH)

HRESIMS *m*/*z* 905.2604 $[M-H]^-$ (calcd for $C_{56}H_{42}O_{12}$ 905.2598, 0.7 ppm)

UV (MeOH) λ_{max} (log ε) 210 (sh), 206 (4.8), 320 (4.2) nm

ECD (MeOH) λ_{max} (Δε) 207 (14.7), 221 (−5.1), 309 (−7.5) nm

^{1}H NMR (600 MHz, CD_3OD) see Table 3

^{13}C NMR (150 MHz, CD_3OD) see Table 4

4-3-10. Compound **10**

Brown amorphous powder

$[\alpha]_{\mathrm{D}}^{20}$ + 181.5 (*c* 0.1, MeOH)

HRESIMS *m/z* 905.2704 $[M-H]^-$ (calcd for $C_{56}H_{42}O_{12}$ 905.2598, 0.8 ppm)

UV (MeOH) λ_{max} (log ε) 230 (sh), 205 (4.8), 319 (4.2) nm

ECD (MeOH) λmax (Δε) 205 (15.8), 239 (31.1), 309 (2.5) nm

^{1}H NMR (600 MHz, CD_3OD) see Table 3

^{13}C NMR (150 MHz, CD_3OD) see Table 4

4-3-11. Compound **11**

Brown amorphous powder

$[\alpha]_{\mathrm{D}}^{20}$ – 21 (*c* 0.1, MeOH)

HRESIMS *m/z* 289.0701 $[M-H]^-$ (calcd for $C_{15}H_{14}O_6$ 289.0712, 3.5 ppm)

UV (MeOH) λ_{max} (log ε) 221 (sh), 210 (4.4), 280 (3.5) nm

ECD (MeOH) λ_{max} (Δε) 208 (5.1), 225 (−6.5), 282 (−1.1) nm

^{1}H NMR (500 MHz, CD_3OD): δ 6.83 (H-2′, d;1.8), 6.75 (H-5′, d;8.1), 6.71 (H-6′, d;8.1, 1.8), 5.84 (H-6, d;2.2), 4.55 (H-2, d;7.5), 3.96 (H-3, m), 2.87 (H-4, dd;16.1, 5.4), 2.50 (H-4, dd;16.1, 8.1)

^{13}C NMR (125 MHz, CD_3OD): δ 157.9 (C-8a), 157.6 (C-7), 156.9 (C-5), 146.2 (C-4′), 146.2 (C-3′), 132.2 (C-1′), 120.0 (C-6′), 116.1 (C-5′), 115.2 (C-2′), 100.8 (C-4a), 96.3 (C-6), 95.5 (C-8), 82.9 (C-2), 68.9 (C-3), 28.5 (C-4)

4-3-12. Compound **12**

Brown amorphous powder

$[\alpha]_{\mathrm{D}}^{20}$ – 214 (*c* 0.1, MeOH)

HRESIMS *m/z* 577.1334 $[M-H]^-$ (calcd for $C_{30}H_{26}O_{12}$ 577.1346, 2.1 ppm)

UV (MeOH) λ_{max} (log ε) 230 (sh), 209 (4.0), 268 (3.8) nm

ECD (MeOH) λ_{max} (Δε) 206 (4.1), 225 (− 38.4), 290 (−1.5) nm

^{1}H NMR (500 MHz, CD_3OD): δ 6.74 (H-2‴, d;1.8), 6.68 (H-5′, dd;8.2, 1.8), 6.68 (H-5‴, d;8.1, 1.8), 6.59 (H-2′, d;1.8), 6.47 (H-6‴, dd;8.2, 1.9), 6.26 (H-6′, dd;8.2, 1.8), 6.08 (H-6, s), 5.89 (H-6″, d;2.4), 5.79 (H-8″, d;2.4), 4.54 (H-4″, d;7.4), 4.42 (H-2, d;7.8), 4.37 (H-3″, dd;9.6, 7.4), 4.26 (H-2″, d;9.6), 3.80 (H-3, dd; 13.3, 7.6), 2.77 (H-4, dd;16.3, 5.5), 2.49 (H-4, dd;16.2, 8.0), 1.29 (H-1‴, s)

^{13}C NMR (125 MHz, CD_3OD): δ 158.6 (C-8″a), 157.1 (C-7″), 157.0 (C-8a), 155.8 (C-7), 155.6 (C-5), 154.9 (C-5″), 146.2 (C-3‴), 146.0 (C-4‴), 145.8 (C-3′), 145.6

(C-4′), 132.6 (C-1‴), 131.8 (C-1′), 120.6 (C-6‴), 119.8 (C-6′), 116.4 (C-5‴), 116.2 (C-5′), 116.0 (C-2‴), 115.5 (C-2′), 108.1(C-8), 107.2 (C-4″a), 102.2 (C-4a), 97.3 (C-6″), 96.8 (C-8″), 96.0 (C-6), 83.9 (C-2″), 82.4 (C-2), 73.7 (C-3″), 68.9 (C-3), 38.5 (C-4″), 28.8 (C-4)

4-3-13. Compound **13**

Yellow amorphous powder

$[\alpha]_{\mathrm{D}}^{20}$ – 20.4 (*c* 0.1, MeOH)

HRESIMS *m*/*z* 591.1725 $[M-H]^-$ (calcd for $C_{28}H_{32}O_{14}$ 591.1714, 1.9 ppm)

UV (MeOH) λ_{max} (log ε) 213 (4.5), 273 (4.3), 335 (4.2) nm

ECD (MeOH) λmax (Δε) 222 (−4.0), 282 (2.2), 315 (−1.5)

^{1}H NMR (400 MHz, CD_3OD) see Table 5

^{13}C NMR (100 MHz, CD_3OD) see Table 6

4-3-14. Compound **14**

Yellow amorphous powder

$[\alpha]_{\mathrm{D}}^{20}$ – 24 (*c* 0.1, MeOH)

HRESIMS *m/z* 605.1879 $[M-H]^-$ (calcd for $C_{29}H_{34}O_{14}$ 605.1870, 1.5 ppm)

UV (MeOH) λ_{max} (log ε) 214 (4.4), 273 (4.3), 330 (4.2) nm

ECD (MeOH) λmax (Δε) 212 (−2.6), 273 (−3.0), 339 (0.6)

^{1}H NMR (400 MHz, CD_3OD) see Table 5

^{13}C NMR (100 MHz, CD_3OD) see Table 6

4-3-15. Compound **15**

Brown amorphous powder

$[\alpha]_D^{20}$ – 25 (*c* 0.1, MeOH)

HRESIMS *m/z* 689.2087 $[M-H]^-$ (calcd for $C_{33}H_{38}O_{16}$ 689.2087, 0.7 ppm)

UV (MeOH) λ_{max} (log ε) 213 (4.5), 273 (4.3), 331 (4.4) nm

ECD (MeOH) λ_{max} (Δε) 219 (−4.2), 274 (− 2.5), 336 (−0.1)

^{1}H NMR (400 MHz, CD_3OD) see Table 5

^{13}C NMR (100 MHz, CD_3OD) see Table 6

4-3-16. Compound **16**

Brown amorphous powder

$[\alpha]_{\mathrm{D}}^{20}$ – 52 (*c* 0.1, MeOH)

HRESIMS *m/z* 689.2092 $[M-H]^-$ (calcd for $C_{33}H_{38}O_{16}$ 689.2082, 1.5 ppm)

UV (MeOH) λ_{max} (log ε) 212 (4.4), 273 (4.2), 331 (4.3) nm

ECD (MeOH) λ_{max} (Δε) 212 (−5.6), 271 (−4.9), 284 (0.6)

^{1}H NMR (400 MHz, CD_3OD) see Table 5

^{13}C NMR (100 MHz, CD_3OD) see Table 6

Table 1. ^{1}H NMR data of compounds **1**, **3, 4** and **5** in CD_3OD (δ in ppm)

position	**1**[a]	**3**[b]	**4**[a]	**5**[a]
1a				
2a/6a	6.96 (d, 8.6)	7.17 (d, 8.4)	7.13 (d, 8.4)	7.17 (d, 8.5)
3a/5a	6.73 (d, 8.5)	6.79 (d, 8.5)	6.76 (d, 8.7)	6.77 (d, 8.5)
7a	5.24 (d, 6.1)	5.39 (d, 6.6)	5.40 (d, 6.7)	5.39 (d, 6.3)
8a	3.33 (d, 6.1)	4.37 (d, 6.6)	4.37 (d, 6.7)	4.48 (d, 6.3)
9a				
10a	6.22 (brs)	6.19 (d, 1.7)	6.15 (d, 2.2)	6.42 (brs)
11a				
12a	6.41 (t, 2.1)	6.21 (t, 1.7)	6.19 (t, 2.2)	6.48 (t, 2.1)
13a				
14a	6.12 (brs)	6.19 (d, 1.7)	6.15 (d, 2.2)	6.35 (d, 1.6)
1b				
2b/6b	6.92 (d, 8.5)	7.06 (d, 8.5)	7.05 (d, 8.6)	7.06 (d, 8.6)
3b/5b	6.60 (d, 8.6)	6.67 (d, 8.5)	6.64 (d, 8.7)	6.66 (d, 8.6)
7b	6.25 (d, 11.9)	6.84 (d, 16.3)	6.91 (d, 16.3)	6.92 (d, 16.4)
8b	6.07 (d, 12.0)	6.59 (d, 16.3)	6.59 (d, 17.0)	6.57 (d, 16.4)
9b				
10b				
11b				
12b	6.54 (d, 1.7)	6.28 (d, 1.5)	6.57 (d, 1.9)	6.58 (d, 1.9)
14b	6.55 (d, 1.7)	6.66 (d, 1.4)	7.01 (d, 2.1)	7.02 (d, 1.9)
13b-Glc				
1′	4.73 (d, 7.1 Hz)		4.92 (d, 7.6)	4.72 (d, 7.3)
2′	3.40 - 3.50 (m)		3.40 - 3.50 (m)	3.40 - 3.50 (m)
3′	3.40 - 3.50 (m)		3.40 - 3.50 (m)	3.40 - 3.50 (m)
4′	3.40 - 3.50 (m)		3.40 - 3.50 (m)	3.40 - 3.50 (m)
5′	3.40 - 3.50 (m)		3.40 - 3.50 (m)	3.40 - 3.50 (m)
6′	3.81 (dd, 12.1, 2.2) 3.70 (dd, 12.1, 5.1)		3.95 (dd, 12.1, 2.1) 3.71 (dd, 12.1, 6.1)	3.95 (dd, 12.1, 2.2) 3.70 (dd, 12.1, 5.5)

Table 1. Continued

11a-Glc		
1″	4.76 (d, 7.1)	4.94 (d, 7.3)
2″	3.40 - 3.50 (m)	3.40 - 3.50 (m)
3″	3.40 - 3.50 (m)	3.40 - 3.50 (m)
4″	3.40 - 3.50 (m)	3.40 - 3.50 (m)
5″	3.40 - 3.50 (m)	3.40 - 3.50 (m)
6″	3.84 (dd, 12.1, 2.2) 3.65 (dd, 12.1, 5.1)	3.78 (dd, 12.1, 2.2) 3.70 (dd, 12.1, 5.5)

ppm, *J* in Hz. [a]Recorded in 600 MHz. [b]Recorded in 850 MHz.

Table 2. ^{13}C NMR data of compounds **1**, **3, 4** and **5** in CD_3OD (δ in ppm)

position	**1**[a]	**3**[b]	**4**[a]	**5**[a]
1a	133.5	132.5	133.6	134.5
2a/6a	128.5	127.4	128.2	129.0
3a/5a	116.3	115.0	116.3	117.2
4a	158.5	157.1	158.6	159.5
7a	94.9	93.4	94.9	95.7
8a	57.6	56.9	58.2	58.7
9a	147.0	146.0	146.9	147.8
10a	108.4	106.1	107.5	109.7
11a	160.3	158.7	160.1	161.7
12a	103.4	100.8	102.9	104.6
13a	159.6	158.7	160.1	160.8
14a	110.0	106.1	107.5	111.0
1b	130.0	129.0	130.3	131.0
2b/6b	131.2	126.8	128.9	129.8
3b/5b	116.1	114.9	116.4	117.3
4b	157.9	157.0	158.5	159.4
7b	132.2	129.0	131.0	132.1
8b	126.4	122.3	123.2	124.0
9b	137.5	135.5	137.0	137.9
10b	123.2	118.7	122.9	123.4
11b	162.6	161.4	162.5	163.4
12b	98.3	95.5	98.5	99.3
13b	160.4	158.4	160.6	161.5
14b	110.6	103.0	106.1	107.1
13b-Glc				
1′	102.4		102.3	103.4
2′	74.8		75.0	75.8
3′	77.9		78.0	78.8
4′	71.1		71.5	72.4
5′	78.0		78.3	79.2
6′	62.3		62.6	63.4

Table 2. Continued

11a-Glc		
1″	102.6	103.6
2″	74.8	75.6
3″	77.8	78.8
4″	71.1	71.9
5″	78	78.86
6″	62.2	63.08

ppm, *J* in Hz. [a]Recorded in 150 MHz. [b]Recorded in 212.5 MHz.

Table 3. ^{1}H NMR data of compounds **2**, **7, 8, 9** and **10** in CD_3OD (δ in ppm)

position	**2**[b]	**7**[a]	**8**[a]	**9**[b]	**10**[b]
1a					
2a/6a	7.00 (d, 8.6)	7.02 (d, 8.5)	6.99 (d, 8.5)	7.14 (d, 8.6)	7.14 (d, 8.6)
3a/5a	6.74 (d, 8.6)	6.75 (d, 8.5)	6.74 (d, 8.5)	6.77 (d, 8.6)	6.76 (d, 8.6)
4a					
7a	5.26 (d, 6.5)	5.22 (d, 6.2)	5.21 (d, 5.5)	5.37 (d, 6.6)	5.35 (d, 6.2)
8a	3.91 (d, 6.5)	3.85 (d, 6.2)	3.76 (d, 5.5)	4.34 (d, 6.6)	4.36 (d, 6.2)
9a					
10a	5.92 (d, 2.2)	5.94 (d, 2.2)	5.99 (d, 2.1)	5.99 (d, 1.6)	5.87 (d, 1.9)
11a					
12a	6.10 (t, 2.1)	6.11 (t, 2.2)	6.10 (t, 2.1)	6.07 (t, 2.1)	6.17 (t, 2.1)
13a					
14a	5.92 (d, 2.2)	5.94 (d, 2.2)	5.99 (d, 2.1)	5.99 (d, 1.6)	5.87 (d, 1.9)
1b					
2b	6.51 (m)	6.54 (d, 2.2)	6.51 (brs)	6.67 (m)	6.59 (d, 1.6)
3b					
4b					
5b	6.56 (d, 8.3)	6.56 (d, 8.6)	6.45 (d, 8.3)	6.68 (d, 8.6)	6.63 (d, 8.4)
6b	6.91 (dd, 8.3, 1.3)	6.92 (dd, 8.3, 1.1)	6.83 (brd, 8.3)	6.99 (dd, 8.4, 1.5)	6.99 (dd, 8.4, 1.5)
7b	6.08 (d, 12.3)	6.07 (d, 12.2)	6.17 (d, 12.0)	6.52 (d, 16.4)	6.73 (d,15.2)
8b	5.96 (d, 12.2)	5.97 (d, 12.2)	6.02 (d, 12.0)	6.69 (d, 17.0)	6.55 (d,16.3)
9b					
10b					
11b					
12b	6.47 (d, 2.1)	6.19 (d, 2.1)	6.24 (brs)	6.23 (d, 2.1)	6.25 (brs)
13b					
14b	6.48 (d, 1.9)	6.21 (d, 2.1)	6.24 (brs)	6.11 (d, 2.1)	6.13 (d, 1.9)
1c					
2c/6c	6.60 (d, 8.5)	6.61 (d, 8.5)	7.01 (d, 8.5)	6.59 (d, 8.4)	6.96 (d, 8.4)
3c/5c	6.55 (d, 8.6)	6.56 (d, 8.5)	6.68 (d, 8.5)	6.53 (d, 8.7)	6.66 (d, 8.5)
4c					
7c	5.44 (d, 5.8)	5.45 (d, 5.6)	5.09 (d, 10.5)	5.43 (d, 5.0)	5.17 (d, 9.8)
8c	4.22 (d, 5.8)	4.23 (d, 5.6)	4.23 (d, 10.5)	4.26 (d, 5.0)	4.27 (d, 9.8)
9c					
10c					

Table 3. Continued

11c					
12c	6.30 (t, 2.1)	6.30 (d, 2.1)	6.26 (d, 2.1)	6.26 (d, 2.1)	6.24 (brs)
13c					
14c	6.13 (d, 2.2)	6.12 (d, 2.1)	6.06 (d, 2.1)	6.59 (d, 1.9)	6.60 (d, 1.6)
1d					
2d/6d	7.12 (d, 8.4)	7.13 (d, 8.6)	6.89 (d, 8.5)	7.19 (d, 8.5)	6.94 (d, 8.5)
3d/5d	6.77 (d, 8.6)	6.78 (d, 8.6)	6.73 (d, 8.5)	6.83 (d, 8.6)	6.74 (d, 8.6)
4d					
7d	5.30 (d, 5.2)	5.31 (d, 5.0)	5.12 (d, 5.1)	5.34 (d, 4.5)	5.19 (d, 5.0)
8d	4.26 (d, 5.2)	4.28 (d, 5.0)	3.47 (d, 5.1)	4.37 (d, 4.5)	3.59 (d, 5.0)
9d					
10d	5.97 (brs)	5.99 (d, 1.8)	5.83 (d, 2.1)	6.15 (d, 2.1)	6.14 (d, 2.1)
11d					
12d	6.05 (t, 2.1)	6.09 (d, 2.1)	6.06 (d, 2.1)	6.14 (d, 2.1)	6.10 (d, 2.1)
13d					
14d	5.97 (brs)	5.99 (d, 1.8)	5.83 (d, 2.1)	6.15 (d, 2.1)	6.14 (d, 2.1)
13b-Glc					
1′	4.72 (d, 7.2)				
2′	3.30 - 3.50 (m)				
3′	3.30 - 3.50 (m)				
4′	3.30 - 3.50 (m)				
5′	3.30 - 3.50 (m)				
6′	3.78 (dd, 12.2, 2.3) 3.70 (dd, 12.2, 4.8)				

ppm, *J* in Hz. [a]Recorded in 800 MHz. [b]Recorded in 600 MHz.

Table 4. ^{13}C NMR data of compounds **2**, **7, 8, 9** and **10** in CD_3OD (δ in ppm)

position	**2**[a]	**7**[b]	**8**[b]	**9**[b]	**10**[a]
1a	133.5	133.9	134.5	133.9	134.0
2a	128.5	128.5	128.0	128.2	128.2
3a	116.3	116.3	116.4	116.3	116.3
4a	158.6	158.4	158.3	158.5	158.4
5a	116.3	116.3	116.4	116.3	116.3
6a	128.5	128.5	128.0	128.2	128.2
7a	95.2	94.9	94.6	94.8	94.8
8a	57.9	57.8	58.1	58.2	58.2
9a	146.6	147.2	147.6	147.2	147.7
10a	107.4	107.3	107.2	107.0	107.2
11a	159.6	159.5	159.6	160.0	160.0
12a	102.2	101.9	101.9	102.5	102.2
13a	159.6	159.5	159.6	160.0	160.0
14a	107.4	107.3	107.2	107.0	107.2
1b	131.5	131.6	131.8	132.3	132.2
2b	126.8	126.9	126.7	125.5	125.8
3b	127.9	132.5	131.2	128.5	131.6
4b	159.6	159.5	160.6	160.2	161.2
5b	110.0	109.9	109.8	110.7	110.4
6b	130.2	130.0	129.9	126.7	126.6
7b	131.8	131.4	131.9	130.5	130.7
8b	126.3	126.7	127.0	124.2	124.3
9b	137.6	137.5	137.7	136.8	137.0
10b	123.3	120.3	120.2	120.1	121.9
11b	162.6	162.7	163.1	162.8	162.8
12b	98.1	96.8	96.7	96.6	96.9
13b	160.0	159.4	159.4	160.5	159.7
14b	110.8	108.8	109.0	107.5	104.9
1c	132.6	142.3	131.8	142.5	132.3
2c	127.9	127.8	129.2	127.9	128.8
3c	116.2	116.1	116.3	116.0	116.4

Table 4. Continued

4c	158.0	157.9	158.8	158.0	158.8
5c	116.2	116.1	116.3	116.0	116.4
6c	127.9	127.8	129.2	127.9	128.8
7c	92.5	92.2	95.0	92.2	95.0
8c	52.9	52.9	55.4	52.9	55.2
9c	142.3	132.7	148.2	132.7	140.8
10c	120.4	120.3	122.2	120.0	119.9
11c	162.5	162.6	162.4	162.7	162.6
12c	96.8	96.7	96.9	96.9	96.9
13c	160.3	160.4	160.1	159.6	160.4
14c	107.5	107.3	108.7	104.6	108.2
1d	134.2	134.2	133.9	134.6	133.4
2d	128.0	127.9	128.2	127.8	128.1
3d	116.5	116.4	116.3	116.5	116.3
4d	158.5	158.4	158.4	158.4	158.5
5d	116.5	116.4	116.3	116.5	116.3
6d	128.0	127.9	128.2	127.8	128.1
7d	95.0	94.9	94.6	94.7	94.5
8d	57.8	57.9	56.7	57.9	56.3
9d	147.6	147.6	147.6	147.8	147.5
10d	107.2	107.1	107.6	107.5	107.4
11d	159.9	160.0	159.8	160.1	159.9
12d	102.5	102.5	102.2	102.3	102.2
13d	159.9	160.0	159.8	160.1	159.9
14d	107.2	107.1	107.6	107.5	107.4
1′	102.4				
2′	74.9				
3′	77.8				
4′	71.0				
5′	77.8				
6′	62.2				

ppm, *J* in Hz. [a]Recorded in 200 MHz. [b]Recorded in 150 MHz.

Table 5. ^{1}H NMR data of compounds **13**, **14, 15** and **16** in CD_3OD (δ in ppm)

position	**13**[a]	**14**[a]	**15**[a]	**16**[a]
2				
3	6.63 (s)	6.67 (s)	6.73 (s)	6.71 (s)
4				
5				
6				
7				
8	6.51 (s)	6.71 (s)	6.83 (s)	6.80 (s)
9				
10				
1'				
2'	7.91 (d, 8.4)	7.94 (d, 8.4)	7.98 (d, 9.0)	7.97 (d, 8.8)
3'	7.06 (d, 8.5)	7.07 (d, 8.4)	7.08 (d, 9.0)	7.07 (d, 8.9)
4'				
5'	7.06 (d, 8.5)	7.07 (d, 8.4)	7.08 (d, 9.0)	7.07 (d, 8.9)
6'	7.91 (d, 8.4)	7.94 (d, 8.4)	7.98 (d, 9.0)	7.97 (d, 8.8)
1"	4.89 (m)	4.89 (d, 9.8)	4.91 (d, 9.8)	4.94 (d, 9.8)
2"	3.10 - 3.80 (m)	4.55 (m)	4.47 (m)	4.46 (dd, 9.8, 8.7)
3"	3.10 - 3.80 (m)	3.30 - 3.50 (m)	3.30 - 3.70 (m)	3.30 - 3.70 (m)
4"	3.10 - 3.80 (m)	3.30 - 3.50 (m)	3.30 - 3.71 (m)	3.30 - 3.71 (m)
5"	3.10 - 3.80 (m)	3.30 - 3.50 (m)	3.30 - 3.72 (m)	3.30 - 3.72 (m)
6"	3.10 - 3.80 (m)	3.72 (dd, 12.1, 6.1) 3.68 (dd, 12.2, 4.1	5.05 (1H, m) 3.67 (1H, m)	3.67 (1H, m) 3.36 (1H, m)
1'"	5.20 (brs)	5.24 (brs)	5.37 (d, 1.6)	5.43 (d, 1.7)
2'"	3.10 - 3.80 (m)	3.30 - 3.50 (m)	3.30 - 3.70 (m)	4.78 (1H, m)
3'"	3.10 - 3.80 (m)	3.30 - 3.50 (m)	3.30 - 3.71 (m)	3.30 - 3.70 (m)
4'"	3.10 - 3.80 (m)	3.30 - 3.50 (m)	4.53 (m)	4.67 (m)
5'"	2.53 (m)	2.38 (m)	2.44 (m)	2.42 (dq, 12.5, 6.2)
6'"	0.71 (3H, d, 6.1)	0.64 (3H, d, 6.2)	0.63 (3H, d, 6.2)	0.61 (3H, d, 6.2)
7-OMe	3.86 (3H, s)	3.92 (3H, s)	3.96 (3H, s)	3.97 (3H, s)

Table 5. Continued

4'-OMe	3.88 (3H, s)	3.87 (3H, s)	3.86 (3H, s)
6'''-OAc		2.03 (3H, s)	1.96 (3H, s)
4'''-OAc		1.76 (3H, s)	1.69 (3H, s)

ppm, *J* in Hz. [a]Recorded in 400 MHz.

Table 6. ^{13}C NMR data of compounds **13**, **14, 15** and **16** in CD_3OD (δ in ppm)

position	**13**[a]	**14**[a]	**15**[a]	**16**[a]
2	164.4	165.9	166.0	165.5
3	102.4	104.6	106.4	106.3
4	184.0	184.2	184.2	184.2
5	164.3	161.6	164.7	164.7
6	105.4	111.1	111.2	111.3
7	165.0	165.4	166.6	166.0
8	94.2	102.0	91.6	91.7
9	158.8	159.0	159.3	159.2
10	104.4	106.4	104.9	104.7
1'	124.4	124.1	124.2	124.1
2'	129.3	129.4	129.4	129.4
3'	115.6	115.7	115.8	115.8
4'	165.7	164.5	161.7	161.6
5'	115.6	115.7	115.8	115.8
6'	129.3	129.4	129.4	129.4
1''	69.9	72.1	73.1	72.4
2''	73.6	73.5	76.7	72.8
3''	78.0	81.6	81.5	81.7
4''	72.3	72.3	73.9	70.1
5''	82.5	82.5	82.6	82.7
6''	62.5	63.3	63.4	63.4
1'''	96.4	91.7	98.2	100.5
2'''	72.3	72.8	72.3	73.3
3'''	73.5	73.2	68.2	70.1
4'''	72.2	72.1	75.1	74.5
5'''	72.0	69.8	67.3	67.3
6'''	18.0	17.9	18.2	17.6
7-OMe	56.1	57.1	57.2	57.3
4'-OMe		56.2	56.1	56.1
6'''-OAc			20.83	20.8
			171.99	171.9

Table 6. Continued

4'''-OAc	20.7	20.5
	171.76	171.3

ppm, *J* in Hz. [a]Recorded in 100 MHz.

5. Sugar analysis

Compounds **1** (1 mg) and **2** (1 mg) were reacted with 1N HCl (200 μL) and deposited in a dry oven (100 ℃). After 2 hours, the solution was neutralized using a saturated Na_2CO_3 solution. Also, the results of hydrolysis of compounds were verified using TLC with the condition of *n*-BuOH : acetone : pyridine : water = 10 : 10 : 5 : 5). Thiocarbamoyl thiazolidine derivatives were then synthesized for HPLC analysis. D-glucose (1 mg), L-glucose, D-galactose and compounds are reacted with L-cysteine methyl ester hydrochloride (1mg) in the solution of pyridine (100 μL) at the oven (60 ℃). Then, *o*-tolyl isothiocyanate (100 μL) was added and the reaction time was 1hour at 60 ℃ oven (Tanaka et al. 2007).

The reaction mixtures were submitted to HPLC analysis (solvent system : aqueous 0.1% formic acid (A) and acetonitrile (B), gradient condition: 20% to 40% B in 40 min, 1ml/min) to determine the type of sugar. The t_R of the peak at 20.9 min overlapped with that of the thiocarbamoyl thiazolidine derivatives of D-glucose.

6. Neuraminidase assay procedure

The neuraminidase activity was screened using 2′-(4-methylumbelliferyl)-α-D-*N*-acetylneuraminic acid (4-MU-NANA) as the fluorescent substrate. DMSO solvent was used to dilute the concentration of all compounds and corresponding concentration in the enzyme buffer MES (32.5 mM 2-(*N*-morpholino) ethane sulfonic acid, 4 mM $CaCl_2$ pH 6.5). The assay was operated in 96-well plates containing 10 μL of virus suspensions (containing active influenza neuraminidase) and 10 μL of screening compounds. After incubation of 30 mins at 37 ℃, 30 μL of 4-MU-NANA substrate in enzyme buffer was added to each well. Then, two hours of an enzyme reaction was carried out in the incubation and stop solution (25% EtOH, 0.1 M glycine, pH 10.7) added to finish the reaction. The fluorescence intensity of the reaction solution was measured with excitation wavelength of 360 nm and emission wavelength of 440nm. Oseltamivir was used as a positive control and the results are expressed as the means ± SD of three independent experiments. Differences between group mean values were determined by one-way analysis of variance followed by a two-tailed Student's t-test for unpaired samples, assuming equal variances.

III. Results and Discussion

1. Elucidation of chemical structures of isolated compounds from the seeds of *Iris pallasii* (**1**-**12**)

1-1. Compound **1**

Compound **1** was obtained as brown amorphous powder and negative HRESIMS spectrum indicating its molecular formula of $C_{40}H_{42}O_{16}$ (m/z 777.2388 $[M-H]^-$, calcd for 777.2395, 0.9 ppm, $C_{40}H_{42}O_{16}$). The ^1H NMR data of **1** showed signals for two 4-hydroxybenzene groups at H-2a/6a [δ_H 6.96 (2H, d, J = 8.6 Hz)], H-3a/5a [δ_H 6.73 (2H, d, J = 8.5 Hz)], H-2b/6b [δ_H 6.92 (2H, d, J = 8.5 Hz)], H-3b/5b [δ_H 6.60 (2H, d, J = 8.6 Hz)] and two aliphatic protons of a dihydrobenzofuran ring at H-7a [δ_H 5.24 (1H, d, J = 6.1 Hz)], H-8a [δ_H 3.33 (1H, d, J = 6.1 Hz)]. Furthermore, presence of one 3,5-digydroxybenzene moieties deduced from signals of H-12a [δ_H 6.41 (1H, t, J = 2.1 Hz)], H-10a [δ_H 6.22 (1H, brs)] and H-14a [δ_H 6.12 (1H, brs)]. Large coupling constant of H-7b [6.25 (1H, d, J = 11.9 Hz)] and H-8b [6.07 (1H, d, J = 12.0 Hz)] indicated that the presence of cis olefinic protons. The number of 4-hydroxybenzene and the presence of above-mentioned structures, compound **1** was expected to be a viniferin type stilbenoid (Liu, Hu et al. 2013). In addition, anomeric proton signals at H-1′ [δ_H 4.73 (1H, d, J = 7.1 Hz)], H-1″ [δ_H 4.76 (1H, d, J = 7.1 Hz)] and C-1′ (δ_C 102.4), C-1″ (δ_C 102.6) confirmed the presence of two β-glucopyranose units (Figure 7). The linkage position of the hydroxybenzene moieties were confirmed from the cross-peak correlation displayed on the HMBC spectrum between H-2a [δ_H 6.96 (1H, d, J = 8.6 Hz)] and C-7a (δ_C 94.9). On the same logic, correlations of H-7b [6.25 (1H, d, J = 11.9 Hz)] and C-2b, C-9b were also identified the connection of the structures (Figure 9). The linkage position of the β-glucopyranose at C-13b, 11a were

confirmed by the expanded HMBC spectra (Figure 10). Relative configuration of 7a, 8a position were investigated by coupling constant of 1D NMR. It has been reported that if it has a *J* value of 5 to 6, it is trans form, and if it has a *J* value of 9 to 10, it is cis form. With the respect to the connection between these chiral substructures, ECD was used for the determination of absolute configuration of stilbenes (Ito and Nehira 2014). Experimental ECD spectrum of compound **1** showed the positive cotton effect at 200 – 260 nm and compared with its theoretical ECD spectra of anti-form [(2S,3S)-3-(3,5-dihydroxyphenyl)-6-hydroxy-2-(4-hydroxyphenyl)-2,3-dihydrobe-nzofuran-4-carbaldehyde]. The spectrum shows exactly the opposite trend, and therefore the absolute configuration of **1** was established as (7a *R*, 8a *R*). With above observed spectroscopic data, compound **1** was first isolated from nature and determined cis-ε-viniferin-13b-11a-O-*β*-D-diglucopyranoside (Lv et al. 2016).

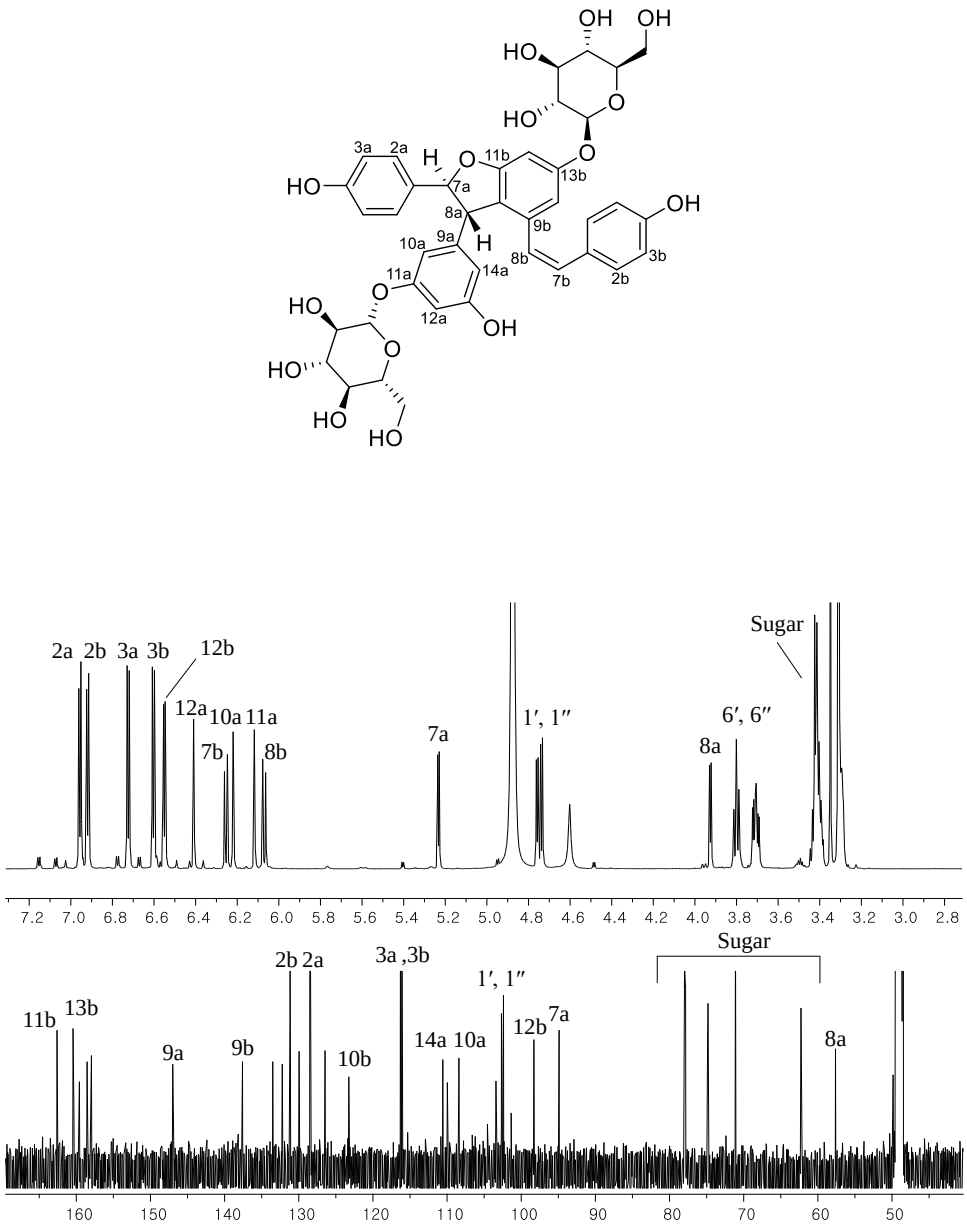

Figure 7. ^{1}H, ^{13}C NMR spectra of compound **1** in CD_3OD

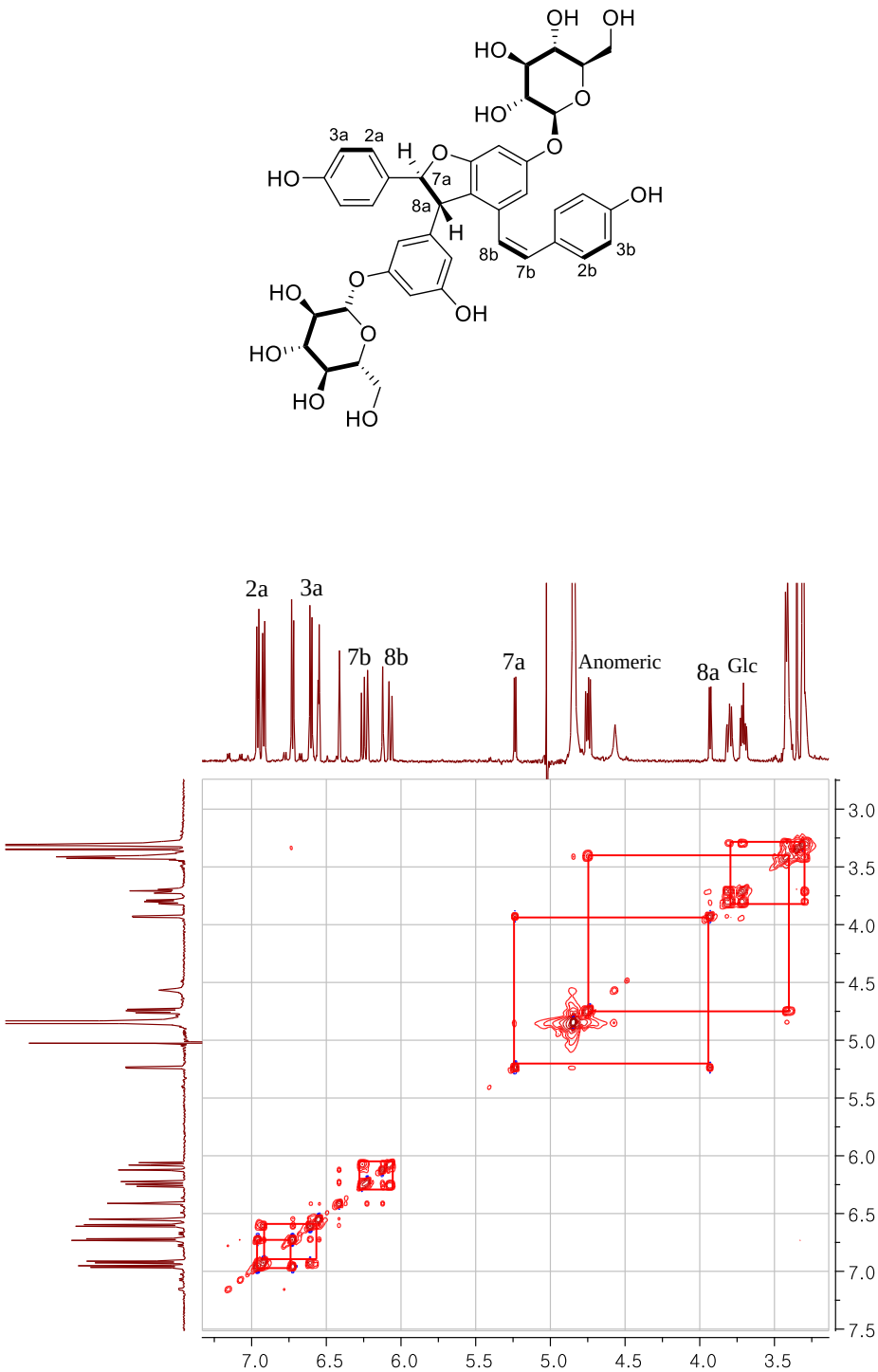

Figure 8. Key COSY spectra of compound **1**

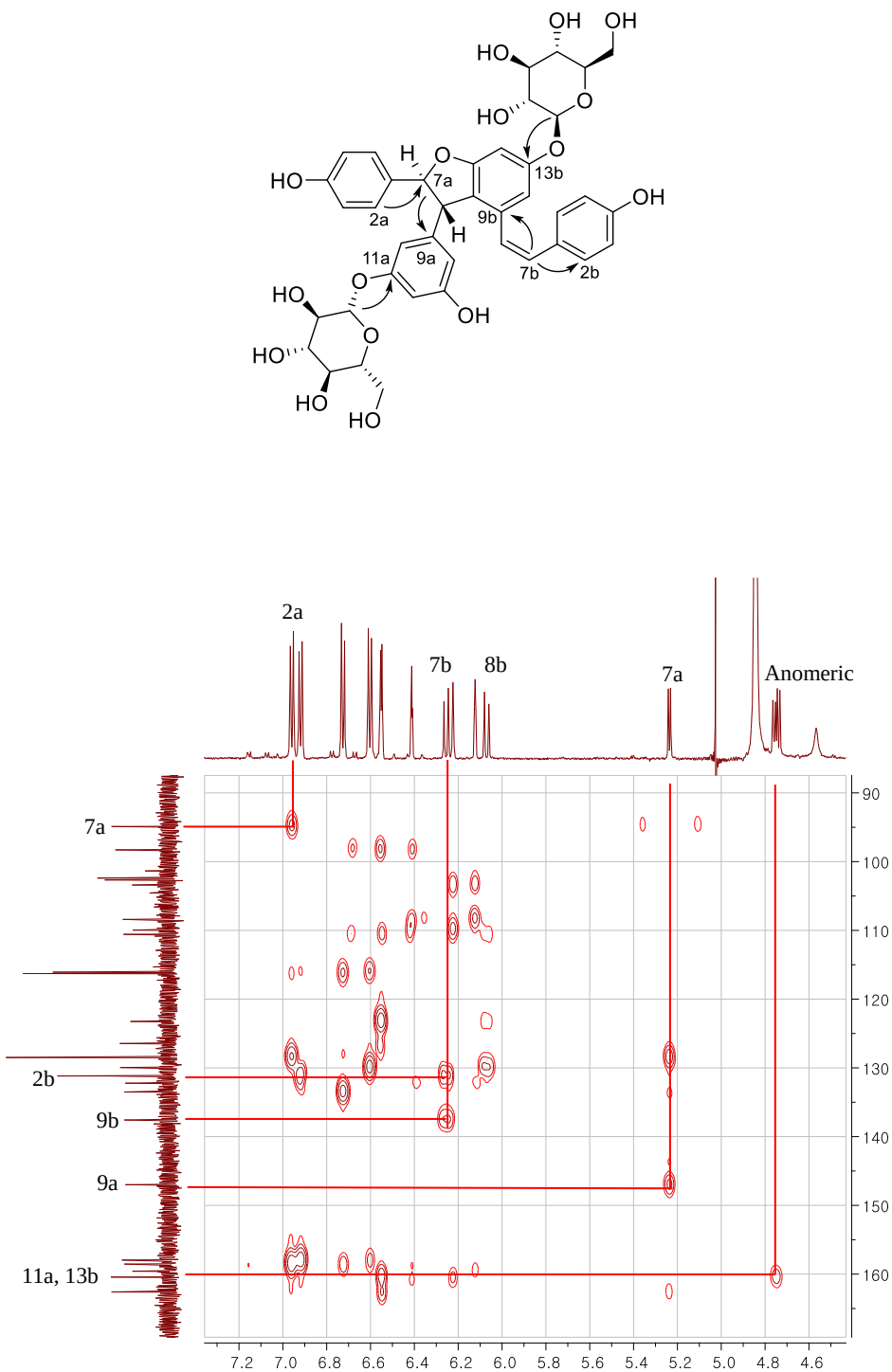

Figure 9. Key HMBC spectra of compound **1**

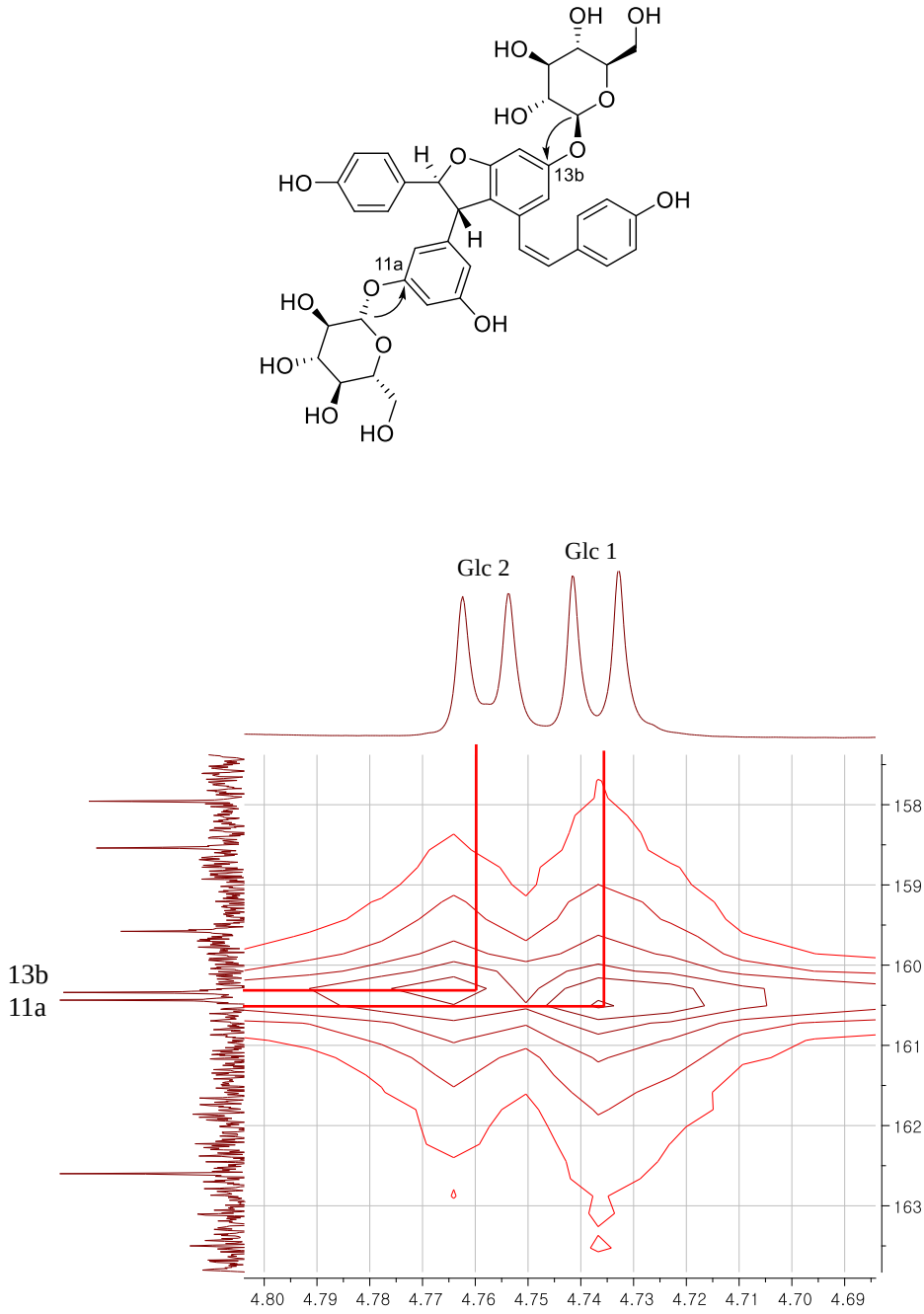

Figure 10. Expanded HMBC spectra of compound **1**

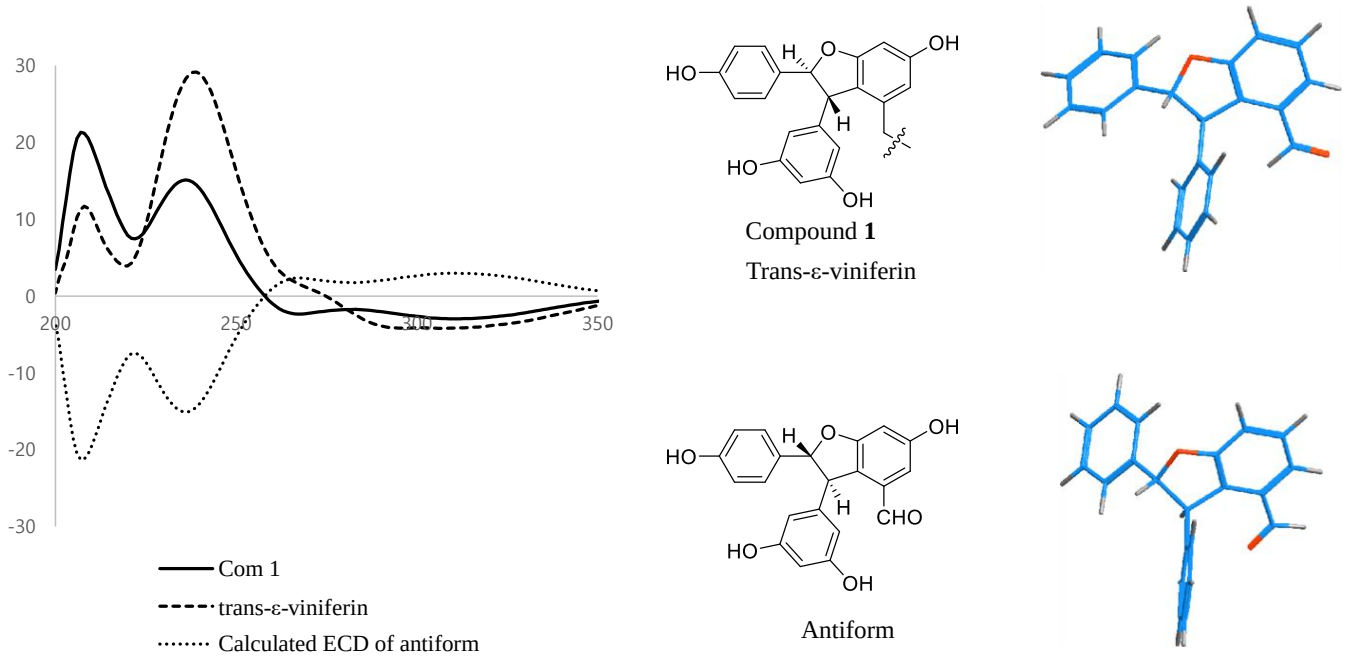

Figure 11. Comparison of ECD spectrum of compound **1** and its anti-form

1-2. Compound **2**

Compound **2** was isolated as brown amorphous powder, and negative HRESIMS data determined its molecular formula as $C_{62}H_{52}O_{17}$ (m/z 1067.3148 $[M-H]^-$, calcd for 1067, 2.1 ppm, $C_{62}H_{52}O_{17}$). Mass values suggest that there is an additional sugar in a stilbene tetramer like Vitisin A, which has 905 molecular mass that have been widely reported. The ^1H and ^{13}C NMR spectrum of **2** show that the presence of three 4-hydroxybenzene moieties at H-2a/6a [δ_H 7.00 (2H, d, J = 8.6 Hz)] and H-3a/5a [δ_H 6.74 (2H, d, J = 8.6 Hz)], H-2c/6c [δ_H 6.60 (2H, d, J = 8.5 Hz)] and H-3c/5c [δ_H 6.55 (2H, d, J = 8.6 Hz)], H-2d/6d [δ_H 7.12 (2H, d, J = 8.4 Hz)] and H-3d/5d [δ_H 6.77 (2H, d, J = 8.6 Hz)]. In addition, two characteristic triplet proton signals at H-12a [δ_H 6.10 (1H, t, J = 2.1 Hz)] and H-12d [δ_H 6.05 (1H, t, J = 2.1 Hz)] indicated that two 3,5-dihydroxybenzene structures were exist. Like compound **1**, compound **2** proton spectrum showed dihydrobenzofuran ring signals at 4 to 5 ppm. In addition, characteristic downfield carbon signals at δ_C [C-11c (162.5), C-4b (159.6)] also indicated that presence of benzofuran moieties. The ^1H-^1H COSY spectrum showed consecutive correlations in sugar units and benzofuran moieties at H-7a [δ_H 5.26 (1H, d, J = 6.5 Hz)] through H-8a [3.91 (δ_H 1H, d, J = 6.5 Hz)]. The HMBC confirmed that the location of *β*-glucopyranose by the correlation signal of H-1′ [δ_H 4.72 (1H, d, J = 7.2 Hz)] and C-13b (δ_C 160). The *β*-D-glucopyranose residue was established by the large coupling constant (7.2 Hz) of H-1′ and by comparison with a known standard using HPLC analysis after acid hydrolysis of **2**. The absolute configuration of compound **2** was established by the comparison of ECD spectrum. The aglycon of **2** is the same as the cis-vitisin B (**7**), and their ECD spectrums showed a very similar trend. Thus, compound **2** was determined as cis-vitisin B-13b-*O*-*β*-D-glucopyranoside by comparison with literature (Seki et al. 1995).

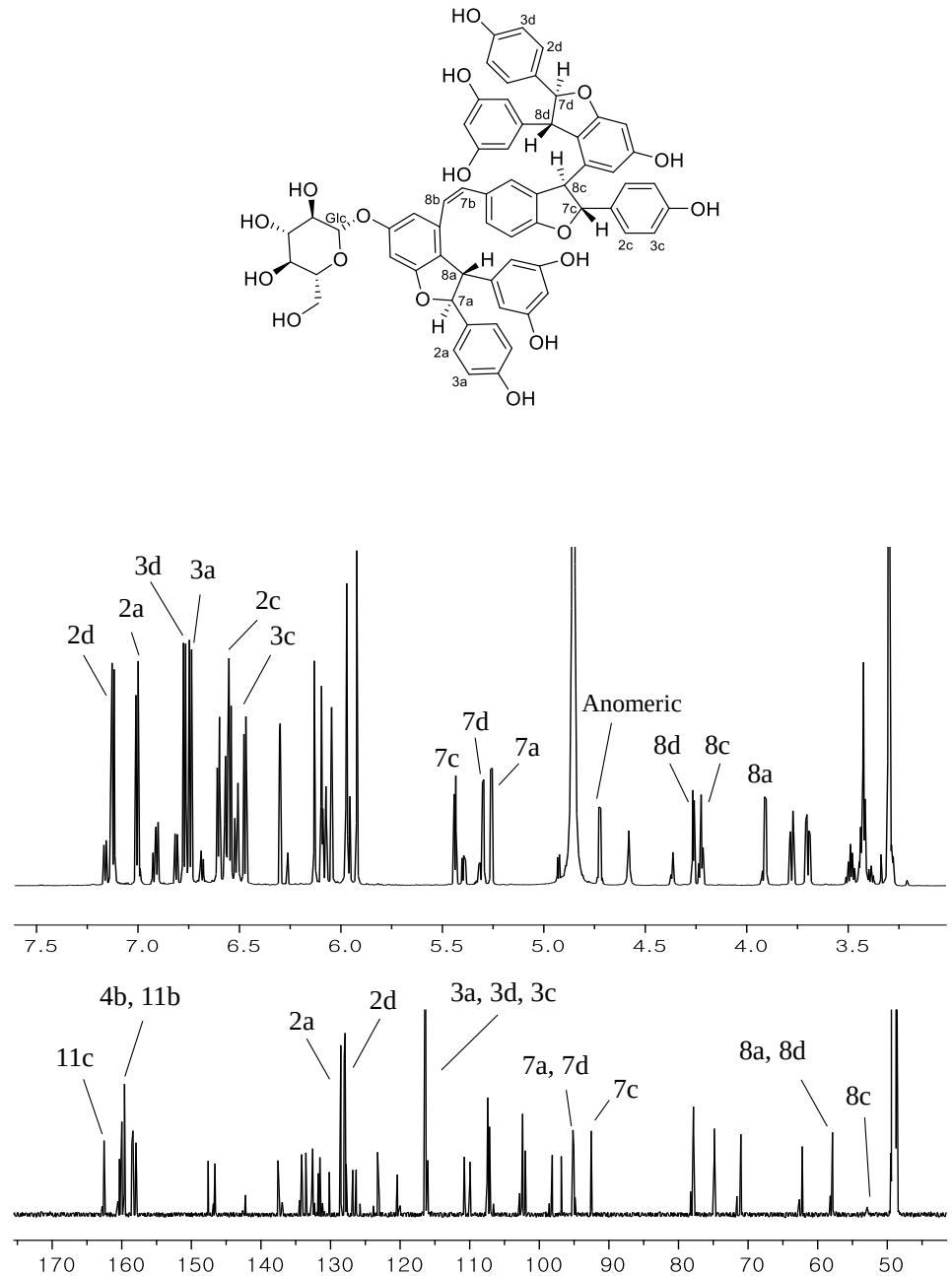

Figure 12. ^{1}H, ^{13}C NMR spectra of compound **2** in CD_3OD

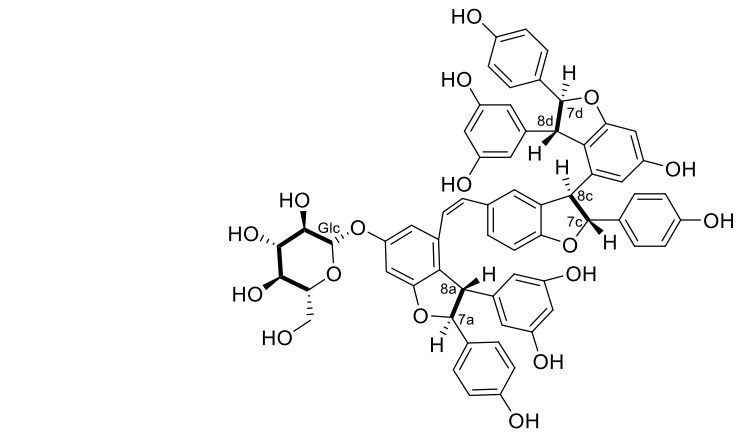

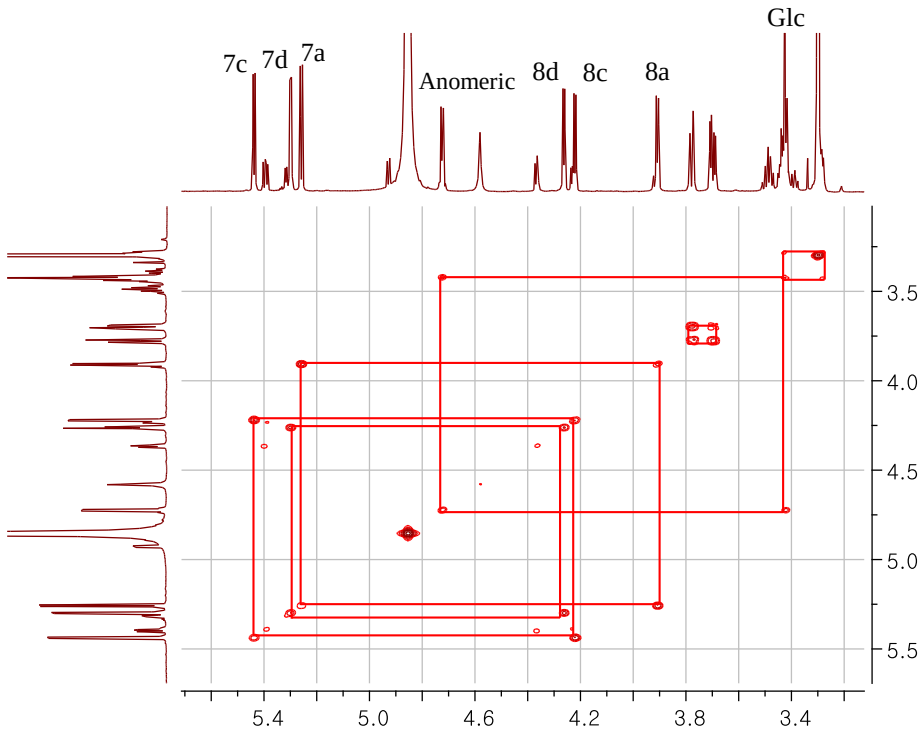

Figure 13. Key COSY spectra of compound **2**

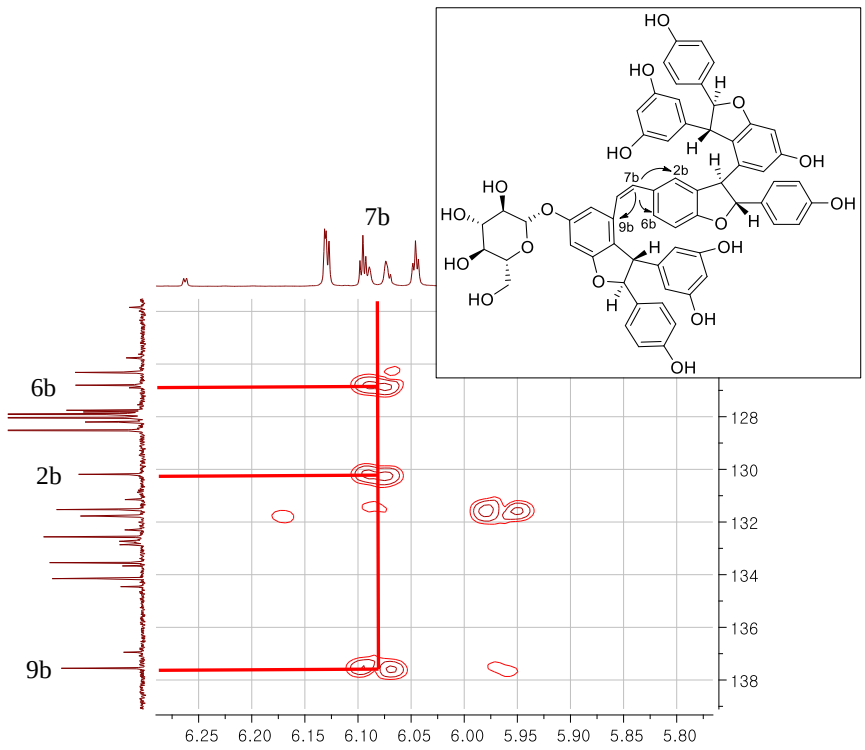

Figure 14. Key HMBC spectra of compound **2**

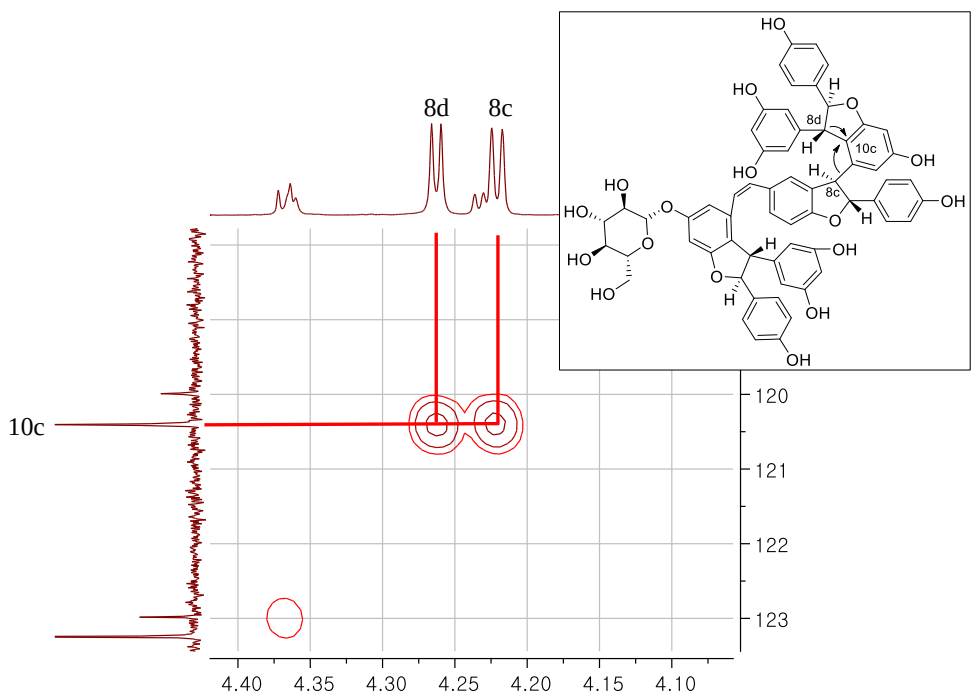

Figure 15. Key HMBC spectra of compound **2**

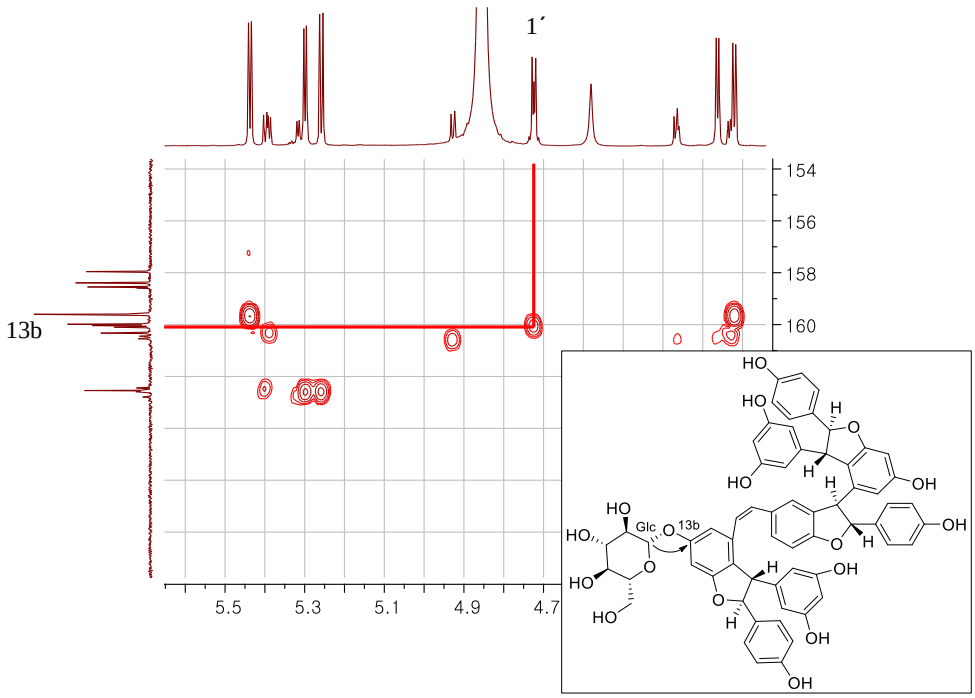

Figure 16. Key HMBC spectra of compound **2**

1-3. Compound **3**

Compound **3** was acquired as brown amorphous powder, and negative HRESIMS data determined its molecular formula as $C_{30}H_{26}O_{12}$ (m/z 453.1342 $[M-H]^-$, calcd for 453.1338, 0.9 ppm, $C_{30}H_{26}O_{12}$). The ^1H and ^{13}C NMR data of **3** proposed the structure as a resveratrol dimer, viniferin, exhibiting two 4-hydroxybenzene group at H-2a/6a [δ_H 7.17 (2H, d, J = 8.4 Hz)] and H-3a/5a [δ_H 6.79 (2H, d, J = 8.5 Hz)], H-2b/6b [7.06 (2H, d, J = 8.5 Hz)] and H-3b/5b [6.67 (2H, d, J = 8.5 Hz)], as well as two aliphatic protons of an benzofuran moiety at H-7a [δ_H 5.39 (1H, d, J = 6.6 Hz)], H-8a [δ_H 4.37 (1H, d, J = 6.6 Hz)]. Two trans olefinic proton signals at H-7b [δ_H 6.84 (1H, d, J = 16.3 Hz)], H-8b [δ_H 6.59 (1H, d, J = 16.3 Hz)] were also revealed. These

above data are accordance with those reported in published literature (Lv et al. 2015). Thus, compound **3** was elucidated as trans-ε-viniferin.

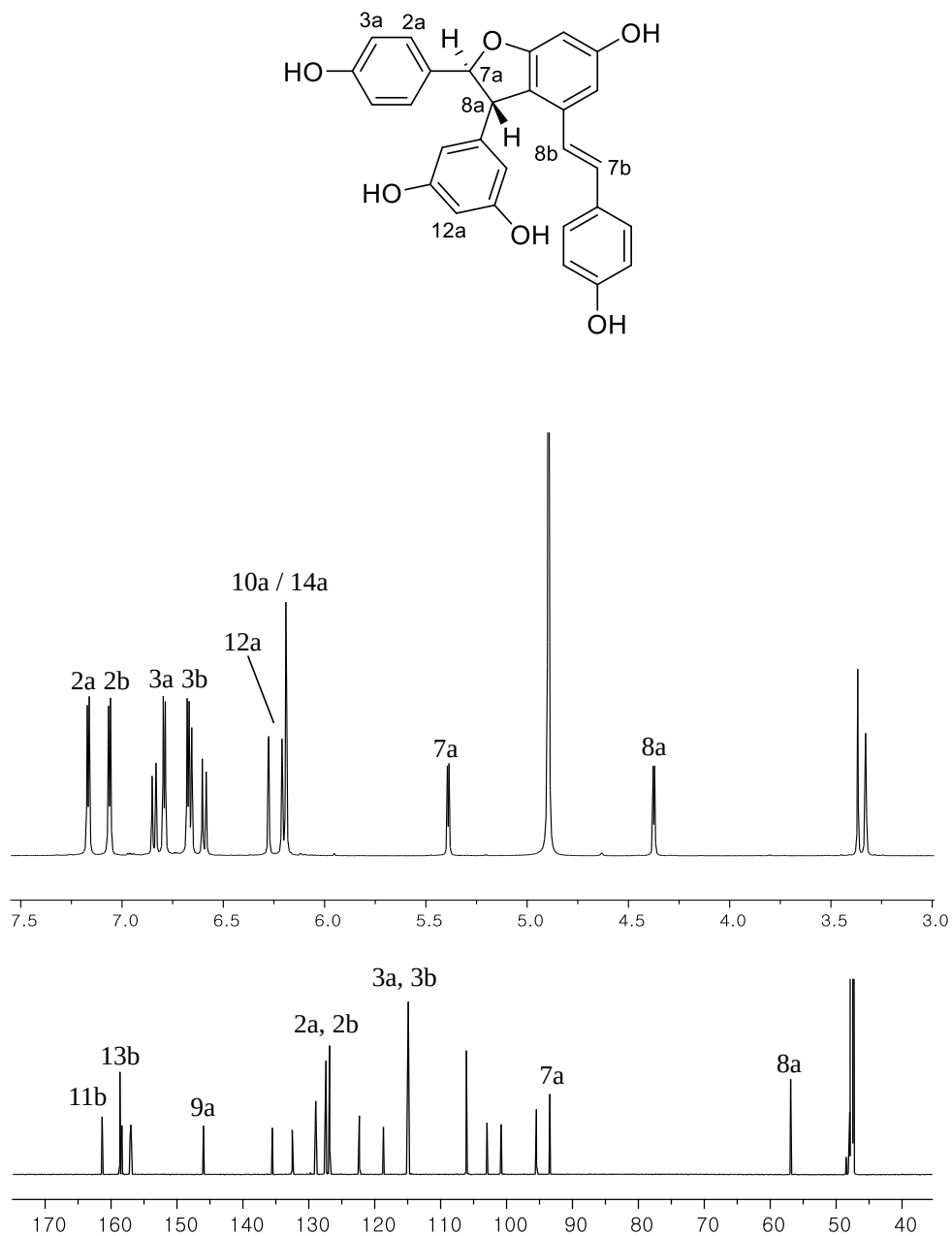

Figure 17. ^{1}H, ^{13}C NMR spectrum of compound **3** in CD_3OD

1-4. Compound **4**

Compound **4** was obtained as brown amorphous powder, and with molecular formula $C_{34}H_{32}O_{11}$, indicated by negative HRESIMS at *m/z* 615.1863 $[M-H]^-$ calcd for $C_{34}H_{32}O_{11}$ 615.1866, 0.5 ppm). The ^1H NMR data of **4** showed signals at H-2a/6a [δ_H 7.13 (2H, d, *J* = 8.4 Hz)] and H-3a/5a [δ_H 6.76 (2H, d, *J* = 8.7 Hz)], H-2b/6b [7.05 (2H, d, *J* = 8.6 Hz)] and H-3b/5b [6.64 (2H, d, *J* = 8.7 Hz)] indicating the presence of two 4-hydroxybenzene moiety. In compound **4**, compared to **3,** one glycosyl group signals at H-2′,3′,4′,5′ [δ_H 3.4 – 3.5 (1H, m)] were detected. The location of *β*-glucopyranose was deduced from the comparison of signals at H-14b [δ_H 7.01 (1H, d, J = 2.1 Hz)]. H-14b singal from compound **3** appeared at δ_H 6.66 (1H, d, J = 1.4 Hz), but from compound 4 at more downfield signals at δ_H 7.01 (1H, d, J = 2.1 Hz). Analysis of 1D proton NMR and comparing with reference, *β*-glucopyranose was attached at C-13b (Shen et al. 2009). Furthermore, two trans olefinic proton signals at H-7b [δ_H 6.91 (1H, d, J = 16.3 Hz)], H-8b [δ_H 6.59 (1H, d, J = 17.0 Hz)] were also shown. ^1H, ^{13}C NMR data exhibited two protons of dihydrobenzofuran groups at H-7a [δ_H 5.40 (1H, d, J = 6.7 Hz)], H-8a [δ_H 4.37 (1H, d, J = 6.7 Hz)] with two carbons C-7a, 8a [δ 94.9,58.2]. With above observed spectroscopic data, compound **4** was confirmed as trans-ε-viniferin-13b-*β*-glucopyranoside.

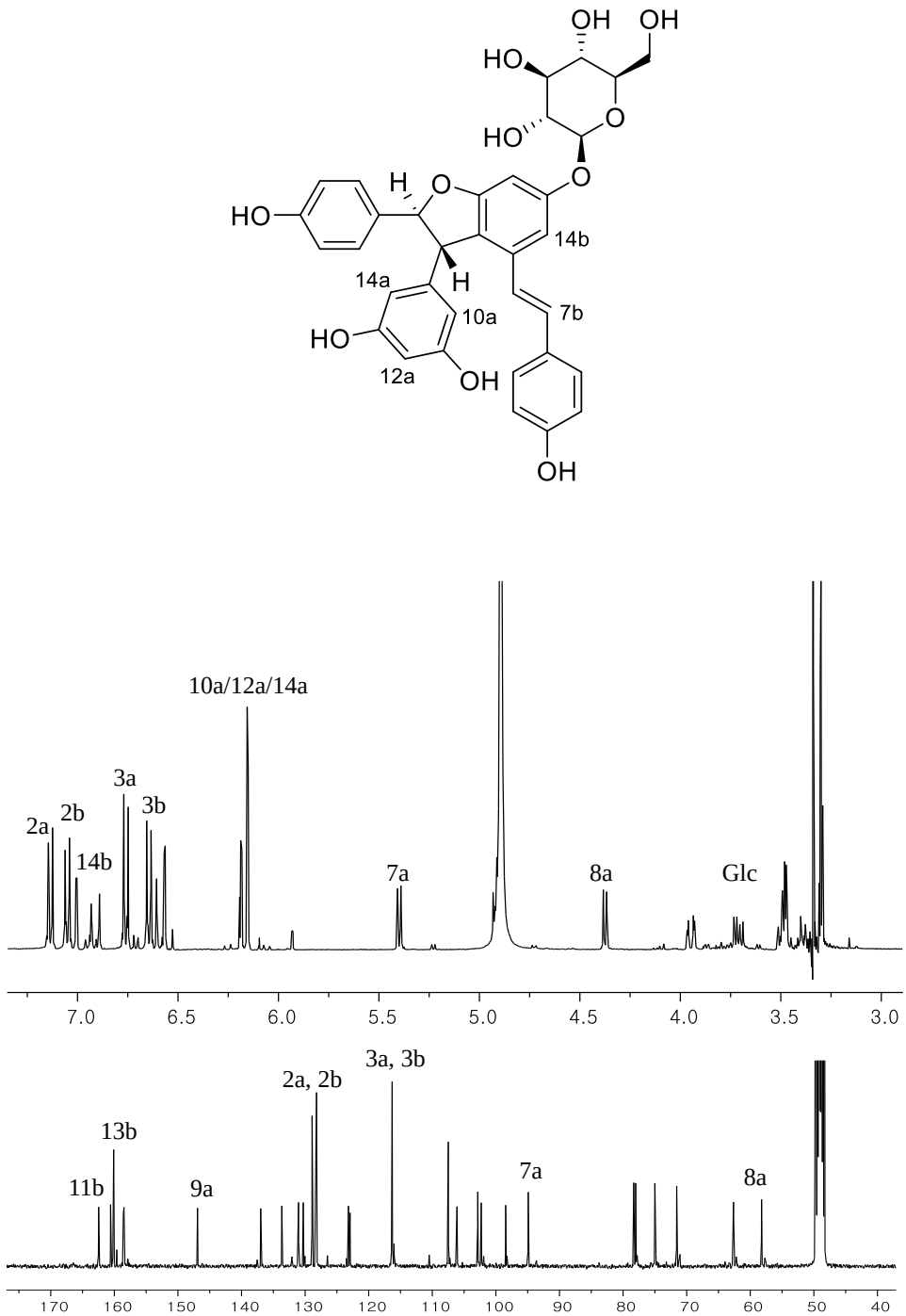

Figure 18. ^{1}H, ^{13}C NMR spectrum of compound **4** in CD_3OD

1-5. Compound **5**

Compound **5** was isolated as light brown amorphous powder. The negative HRESIMS of **5** showed a peak at *m/z* 777.2388 $[M-H]^-$ (calcd for 777.2395, 0.9 ppm, $C_{40}H_{42}O_{16}$) and yielded a molecular formula of $C_{40}H_{42}O_{16}$. With the molecular mass equal to **1**, compound **5** was inferred that the stilbene which has two sugar moieties. The ^1H and ^{13}C NMR spectra displayed benzofuran groups at H-7a [δ_H 5.39 (1H, d, J = 6.3 Hz)], H-8a [δ_H 4.48 (1H, d, J = 6.3 Hz)] with two carbons C-7a, 8a [δ 95.7, 58.7]. Except for the large coupling constants of the olefinic proton at H-7b [δ_H 6.92 (1H, d, J = 16.4 Hz)] and H-8b [δ_H 6.57 (1H, d, J = 16.4 Hz)], the 1D NMR spectral data of **5** were similar with those of compound **1**. In addition, the *J*-value of anomeric proton signal at H-1′ [δ_H 4.72 (1H, d, J = 7.3 Hz)]**,** H-1″ [δ_H 4.94 (1H, d, J = 7.3 Hz)] and the presence of anomeric carbon signal at C-1′ (103.6), and C-1″ (103.4) suggested that glucose moieties were *β*-orientated glucopyranose. Through analysis of NMR spectrum, compound **5** was confirmed as vatalbinoside C by comparison with literatures(Abe et al. 2010).

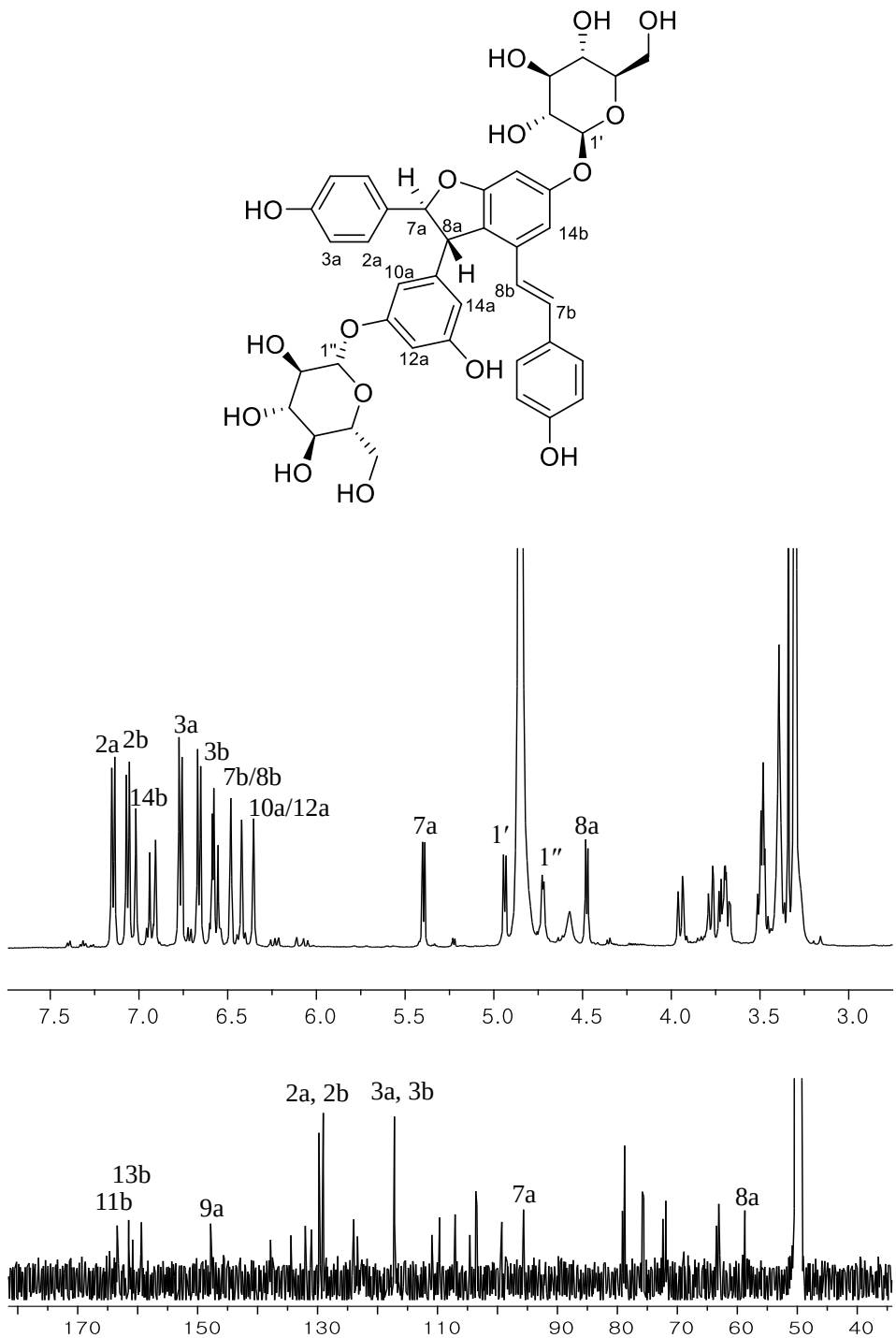

Figure 19. ^{1}H, ^{13}C NMR spectrum of compound **5** in CD_3OD

1-6. Compound **6**

Compound **6** was acquired as brown amorphous powder, and negative HRESIMS data determined its molecular formula as $C_{56}H_{42}O_{12}$ (m/z 905.2591 $[M-H]^-$, calcd for 905.2598, 0.8 ppm, $C_{56}H_{42}O_{12}$). Compound **6**, stilbene tetramer, is one of the most isolated major compounds from seeds of *Iris pallasii*. The ^1H NMR spectra exhibited typical signals of stilbene oligomer, like three 4-hydroxybenzene moieties at H-2a/6a [δ_H 7.15 (2H, d, J = 8.6 Hz)] and H-3a/5a [δ_H 6.80 (2H, d, J = 8.6 Hz)], H-2c/6c [δ_H 7.10 (2H, d, J = 8.6 Hz)] and H-3c/5c [δ_H 6.74 (2H, d, J = 8.6 Hz)], H-2d/6d [δ_H 7.03 (2H, d, J = 8.4 Hz)] and H-3d/5d [δ_H 6.65 (2H, d, J = 8.6 Hz)]. In addition, four aliphatic protons of a dihydrobenzofuran at H-7a [δ_H 5.33 (1H, d, J = 6.4 Hz)], H-8a [4.28 (δ_H 1H, d, J = 6.4 Hz)] and H-7d [δ_H 5.83 (1H, d, J = 11.6 Hz)], H-8d [4.15 (δ_H 1H, d, J = 11.5 Hz)] also detected. Unlike other tetramers, compound **6** has cycloheptane core deduced by the signals of H-7c [δ_H 5.27 (1H, d, J = 3.4 Hz)], H-8c [δ_H 5.44 (1H, d, J = 3.8 Hz)] with carbon signals at C-7c (δ_C 40.3) C-8c (δ_C 39.9). Two trans olefinic protons at H-7b [δ_H 6.34 (1H, d, J = 16.2 Hz)] and H-8b [δ_H 6.30 (1H, d, J = 16.2 Hz)] and other aromatic signals were agreement with that of the reported vitisin A spectra. Thus, compound **6** was elucidated as a vitisin A, which was previously isolatd *Vitis coignetiae* (Ito et al. 1998).

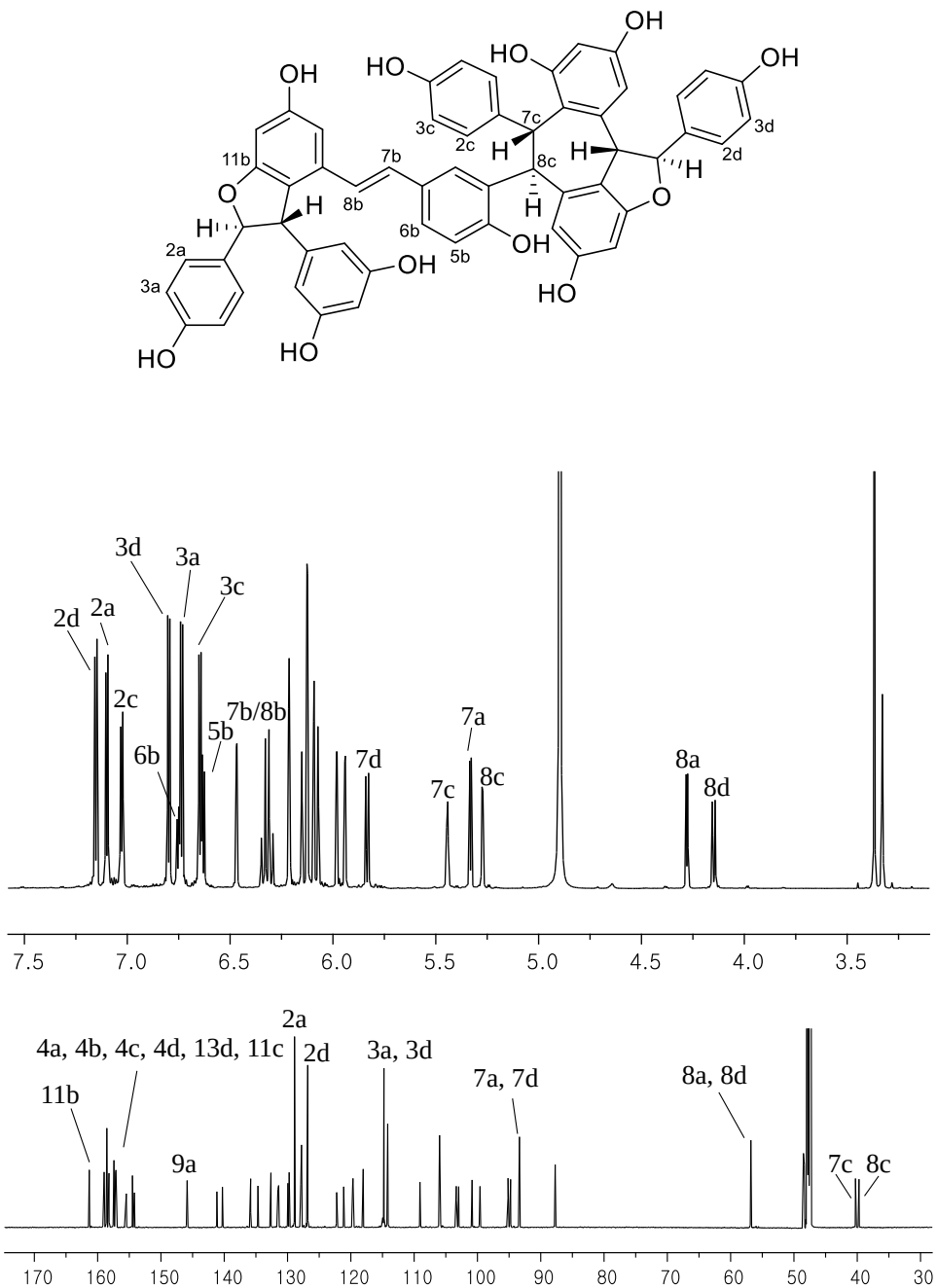

Figure 20. ^{1}H, ^{13}C NMR spectrum of compound **6** in CD_3OD

1-7. Compound **7**

Compound **7** was isolated as a light brown, amorphous powder. Its negative HRESIMS data established its molecular formula of $C_{56}H_{42}O_{12}$ (m/z 905.2589 [M-H]$^-$, calcd for 905.2598, 1.0 ppm, $C_{56}H_{42}O_{12}$) which is 162 mass values ($C_6H_{10}O_5$) less than that of **2**, suggesting that **7** is deglycosylated derivative of **2**. The ^{1}H NMR data of **7** showed three hydroxybenzene groups H-2a/6a [δ_H 7.02 (2H, d, *J* = 8.5 Hz)] and H-3a/5a [δ_H 6.75 (2H, d, *J* = 8.5 Hz)], H-2c/6c [δ_H 6.61 (2H, d, *J* = 8.5 Hz)] and H-3c/5c [δ_H 6.56 (2H, d, *J* = 8.5 Hz)], H-2d/6d [δ_H 7.13 (2H, d, *J* = 8.6 Hz)] and H-3d/5d [δ_H 6.78 (2H, d, *J* = 8.6 Hz)], two cis olefinic protons at H-7b [δ_H 6.07 (1H, d, J = 12.2 Hz)] and H-8b [δ_H 5.97 (1H, d, J = 12.2 Hz)], six aliphatic protons of benzofuran groups at H-7a [δ_H 5.22 (1H, d, *J* = 6.2 Hz)], H-8a [3.85 (δ_H 1H, d, *J* = 6.2 Hz)] and H-7c [δ_H 5.45 (1H, d, *J* = 5.6 Hz)], H-8c [4.23 (δ_H 1H, d, *J* = 5.6Hz)], H-7d [δ_H 5.31 (1H, d, *J* = 5.0 Hz)], H-8d [4.28 (δ_H 1H, d, *J* = 5.0 Hz)]. Above data are in accordance with those reported literature (Ito et al. 1999), compound **7** was elucidated as cis-vitisin B, which was once isolated from *Vitis vinifera*.

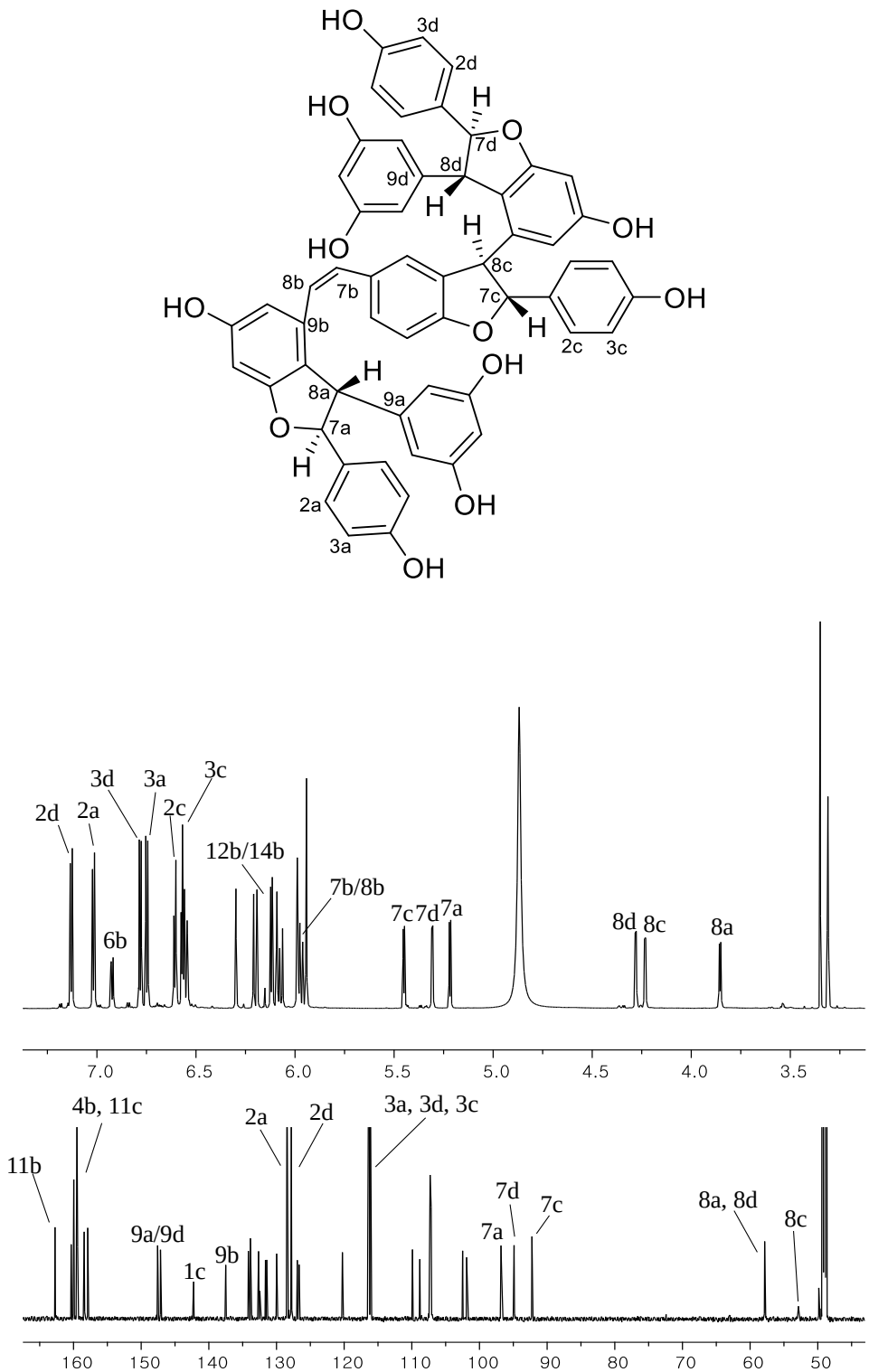

Figure 21. ^{1}H, ^{13}C NMR spectrum of compound **7** in CD_3OD

1-8. Compound **8**

Compound **8** was isolated as brown amorphous powder, and negative HRESIMS data determined its molecular formula as $C_{56}H_{42}O_{12}$ (m/z 905.2578 $[M-H]^-$, calcd for 905.2598, 0.1 ppm, $C_{56}H_{42}O_{12}$). Compound **8** has same molecular formula with **7** and has similar ^1H and ^{13}C NMR spectrum except for the coupling constants value at H-7c [δ_H 5.09 (1H, d, J = 10.5 Hz)], H-8c [4.23 (δ_H 1H, d, J = 10.5 Hz)]. In the compound **8**, the coupling constant of other benzofuran proton at H-7a [δ_H 5.21 (1H, d, J = 5.5 Hz)], H-8a [3.76 (δ_H 1H, d, J = 5.5 Hz)] to be *trans*, and H-7c between H-8c (10.5 Hz) to be *cis*, respectively. The relative stereostructure of compound **8** was confirmed by NOE, using Dreiding stereomodel (Ito and Niwa 1996). This evidence led to the relative structure of vitisin C, which was steroisomer of vitisin B at the position of 8b. Common signals of stilbene tetramer like hydroxybenzene groups at H-2a/6a [δ_H 6.99 (2H, d, J = 8.5 Hz)] and H-3a/5a [δ_H 6.74 (2H, d, J = 8.5 Hz)], H-2c/6c [δ_H 7.01 (2H, d, J = 8.5 Hz)] and H-3c/5c [δ_H 6.68 (2H, d, J = 8.5 Hz)], H-2d/6d [δ_H 6.89 (2H, d, J = 8.5 Hz)] and H-3d/5d [δ_H 6.73 (2H, d, J = 8.5 Hz)], two cis olefinic protons at H-7b [δ_H 6.17 (1H, d, J = 12.0 Hz)] and H-8b [δ_H 6.02 (1H, d, J = 12.0 Hz)], six aliphatic protons of benzofuran groups at H-7a [δ_H 5.21 (1H, d, J = 5.5 Hz)], H-8a [3.76 (δ_H 1H, d, J = 5.5 Hz)] and H-7c [δ_H 5.09 (1H, d, J = 10.5 Hz)], H-8c [4.23 (δ_H 1H, d, J = 10.5 Hz)], H-7d [δ_H 5.12 (1H, d, J = 5.1 Hz)], H-8d [3.47 (δ_H 1H, d, J = 5.1 Hz)] also confirmed that the compound **8** was cis-vitisin C (Ito and Niwa 1996).

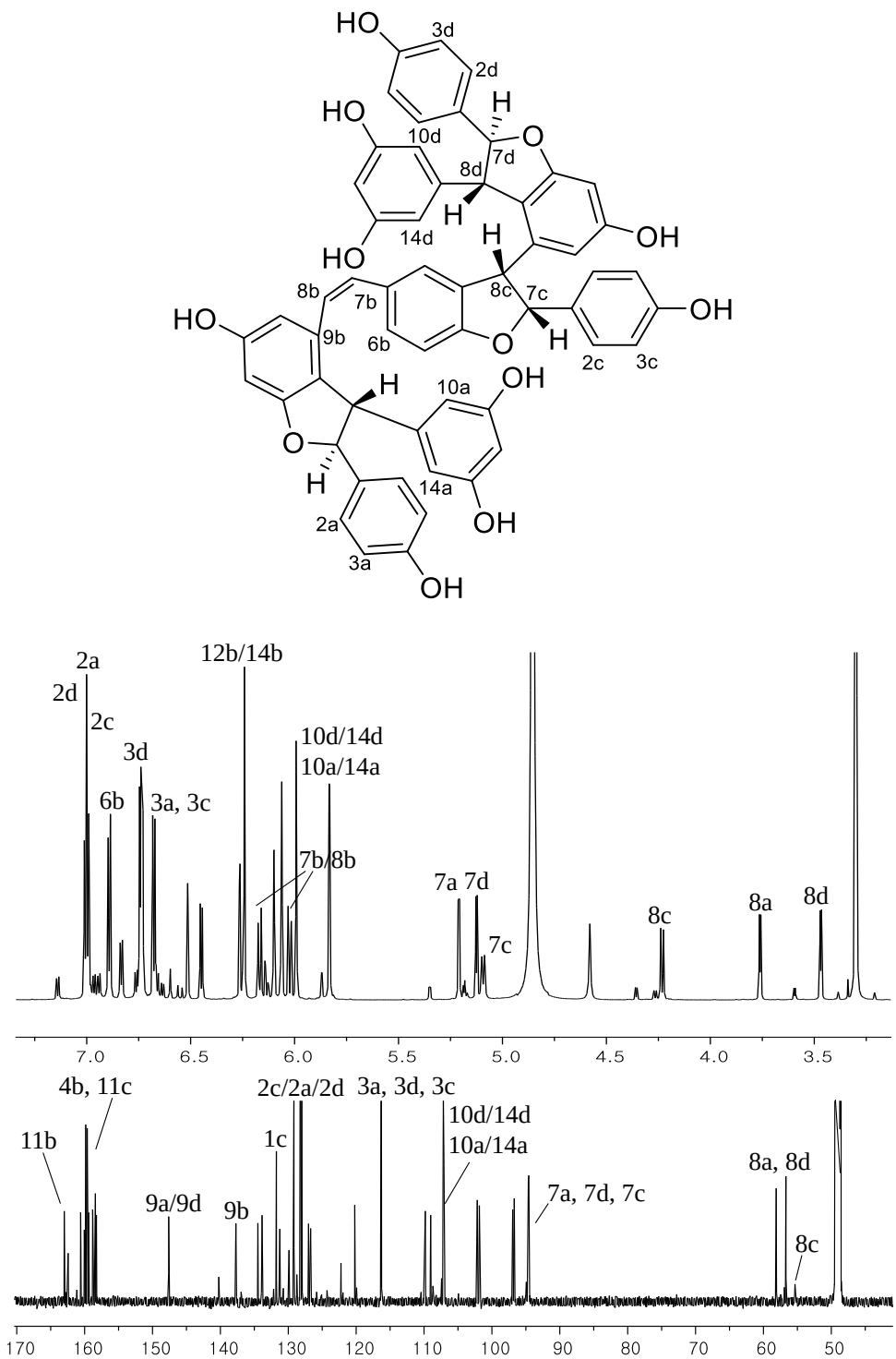

Figure 22. ^{1}H, ^{13}C NMR spectrum of compound **8** in CD_3OD

1-9. Compound **9**

Compound **9** was acquired as brown amorphous powder and had the molecular formula $C_{56}H_{42}O_{12}$ as determined by negative HRESIMS at m/z 905.2604 $[M-H]^-$ (calcd for $C_{56}H_{42}O_{12}$, 905.2598, 0.7 ppm). The ^1H NMR spectrum of compound **9** exhibited signals for six sets of ortho-coupled aromatic hydrogens at H-2a/6a [δ_H 7.14 (2H, d, J = 8.6 Hz)] and H-3a/5a [δ_H 6.77 (2H, d, J = 8.6 Hz)], H-2c/6c [δ_H 6.59 (2H, d, J = 8.4 Hz)] and H-3c/5c [δ_H 6.53 (2H, d, J = 8.7 Hz)], H-2d/6d [δ_H 7.19 (2H, d, J = 8.6 Hz)] and H-3d/5d [δ_H 6.83 (2H, d, J = 8.6 Hz)] as well as two sets of AX2-type meta-coupled aromatic hydrogens at H-10a/14a [δ_H 5.99 (2H, d, J = 1.6 Hz)], H-12a [δ_H 6.07 (1H, d, J = 2.1 Hz)] and H-10d/14d [δ_H 6.15 (2H, d, J = 2.1Hz)], H-12d [δ_H 6.14 (1H, d, J = 2.1 Hz)]. These signals suggested that the presence of three dihydrobenzofuran moieties bearing 4-oxyphenyl and 3,5-dihydroxybenzen groups which is characteristic for oligostilbenes biosynthesized from resveratrol molecules (Oshima, Kamijou et al. 1995). By comparing reference, compound **9** was elucidated as vitisin B, which was previously reported (Oshima et al. 1995).

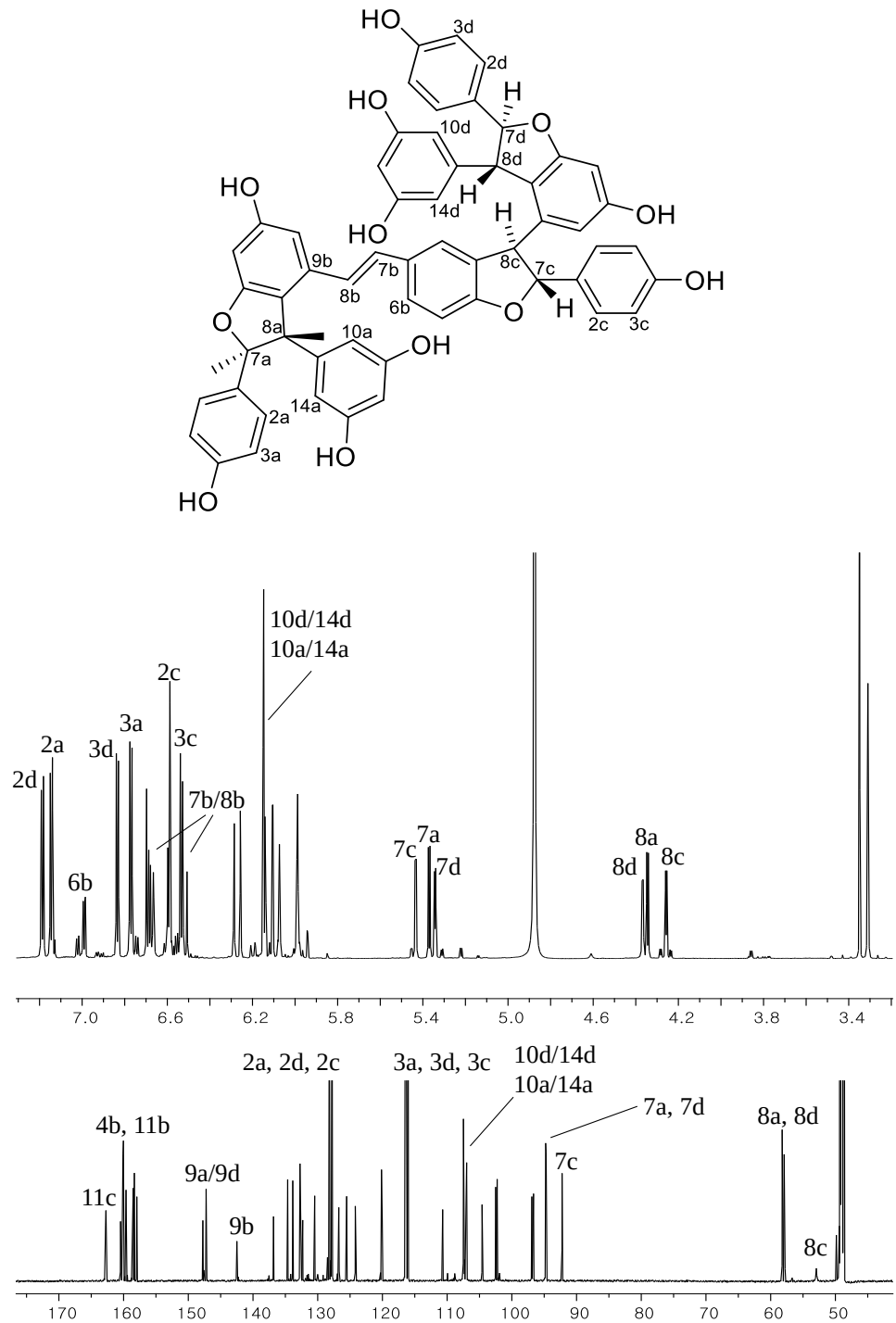

Figure 23. ^{1}H, ^{13}C NMR spectrum of compound **9** in CD_3OD

1-10. Compound **10**

Compound **10** was obtained as brown amorphos powder, and negative HRESIMS data determined its molecular formula as $C_{56}H_{42}O_{12}$ (m/z 905.2704 $[M-H]^-$, calcd for 905.2598, 0.8 ppm, $C_{56}H_{42}O_{12}$). The ^1H and ^{13}C NMR spectrum of **10** suggested main skeletons as stilbene tetramer, showing trans olefinic protons at H-7b [δ_H 6.17 (1H, d, J = 12.0 Hz)] and H-8b [δ_H 6.02 (1H, d, J = 12.0 Hz)]. Similar with those of compound **8**, the large coupling constant of H-7c [δ_H 5.09 (1H, d, *J* = 10.5 Hz)], H-8c [4.23 (δ_H 1H, d, *J* = 10.5 Hz)] is the evidence of *cis* form at the C-8c. Except for the stereochemistry at the benzofuran moiety, the 1D and 2D NMR spectral data of **10** were almost same to those of compound **9**. By comparing reference, compound **10** was identified as Vitisin C, which was previously reported (Ito and Niwa 1996).

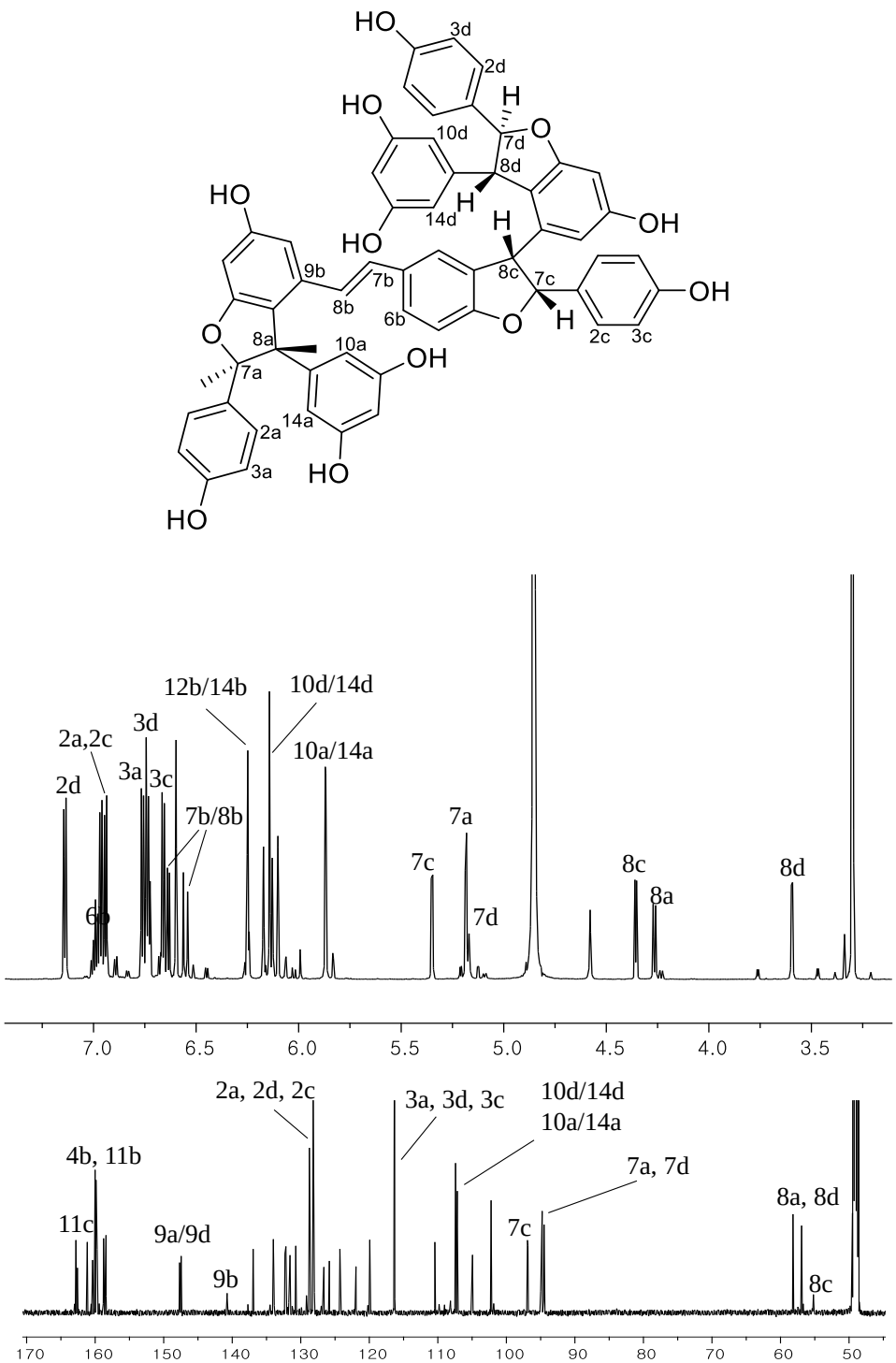

Figure 24. ^{1}H, ^{13}C NMR spectrum of compound **10** in CD_3OD

1-11. Compound **11**

Compound **11** was isolated as yellowish amorphous powder, and had the molecular formula $C_{15}H_{14}O_6$ as determined by (-)-HRESIMS at 289.0701 $[M-H]^-$ (calcd for 289.0712 3.5 ppm, $C_{15}H_{14}O_6$). The ^1H NMR data of **11** exhibited three aromatic proton signal of ABX system at H-2′ [δ_H 6.83 (1H, d, J = 1.8 Hz)], H-5′ [δ_H 6.75 (1H, d, J = 8.1 Hz)], H-6′ [δ_H 6.71 (1H, dd, J = 8.1, 1.8 Hz)], meta coupling protons at H-6 [δ_H 5.86 (1H, d, J = 2.5 Hz)] and H-8 [δ_H 5.93 (1H, d, J = 2.5 Hz)]. Through NMR spectrum, compound **11** was characterized as catechin (Oszmianski et al. 1990).

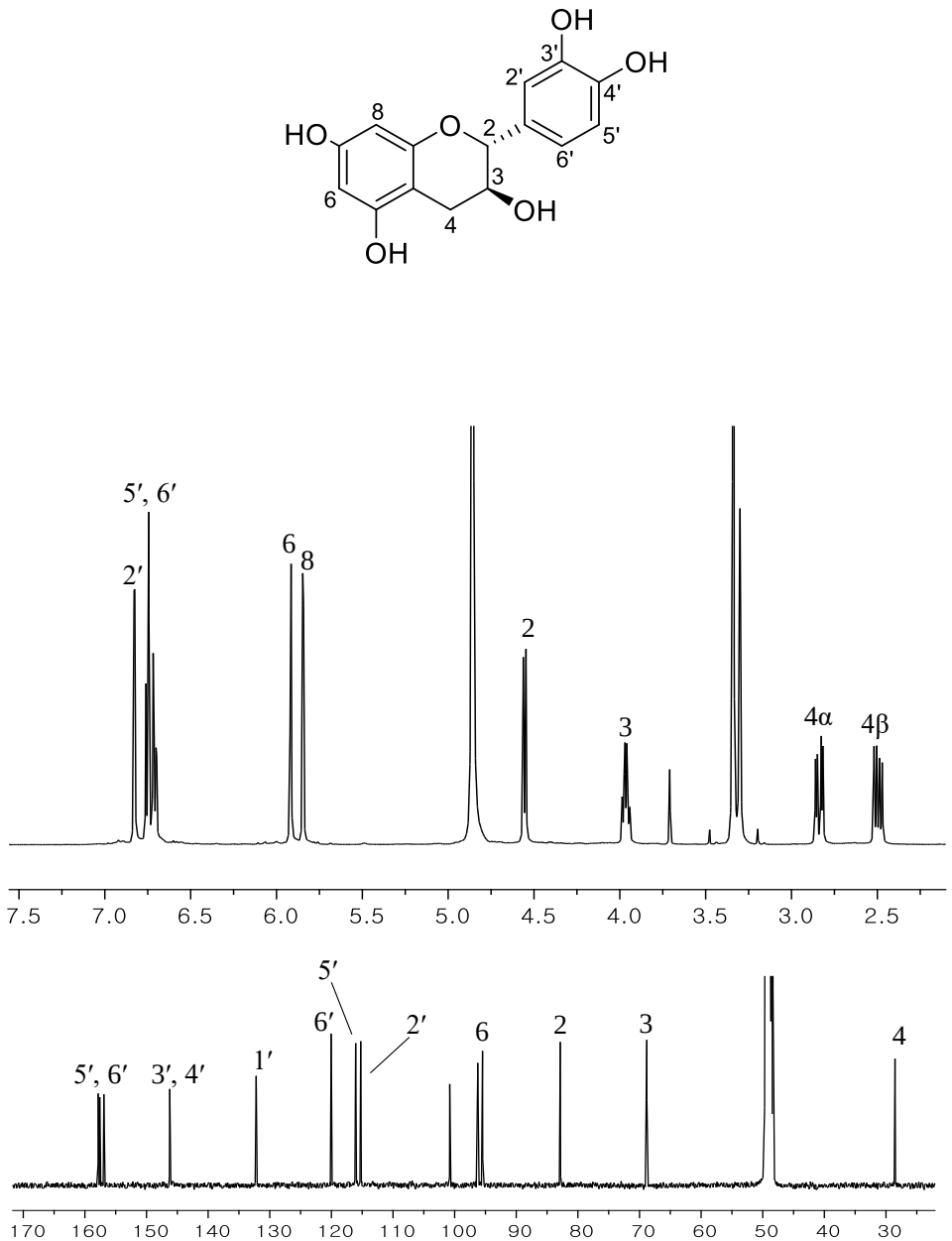

Figure 25. ^{1}H, ^{13}C NMR spectrum of compound **11** in CD_3OD

1-12. Compound **12**

Compound **12** was isolated as brown amorphous powder, and had the molecular formula $C_{30}H_{26}O_{12}$ as determined by (-)-HRESIMS at 577.1334 $[M-H]^-$(calcd for 577.1346 2.1 ppm, $C_{30}H_{26}O_{12}$). In the mass spectrum, the molecular weight of **12** was estimated to be twice that of **11** catechin dimers. The ^1H NMR data of **12** also exhibited two sets of ABX system signals at H-2‴ [δ_H 6.74 (1H, d, J = 1.8 Hz)], H-5‴ [δ_H 6.68 (1H, d, J = 8.2 Hz)], H-6‴ [δ_H 6.47 (1H, dd, J = 8.2, 1.8 Hz)] in upper ring and H-2′ [δ_H 6.59 (1H, d, J = 1.8 Hz)], H-5′ [δ_H 6.68 (1H, d, J = 8.2 Hz)], H-6′ [δ_H 6.26 (1H, dd, J = 8.2, 1.8 Hz)] in terminal ring. In addition, meta coupled protons at both A ring also detected at H-6 [δ_H 6.08 (1H, s)] and H-6″ [δ_H 5.89 (1H, d, J = 2.4 Hz)] and H-8″ [δ_H 5.79 (1H, d, J = 2.4 Hz)]. By comparing reference, compound **12** was elucidated as procyanidin B_3, which was previously reported (Oszmianski et al. 1990).

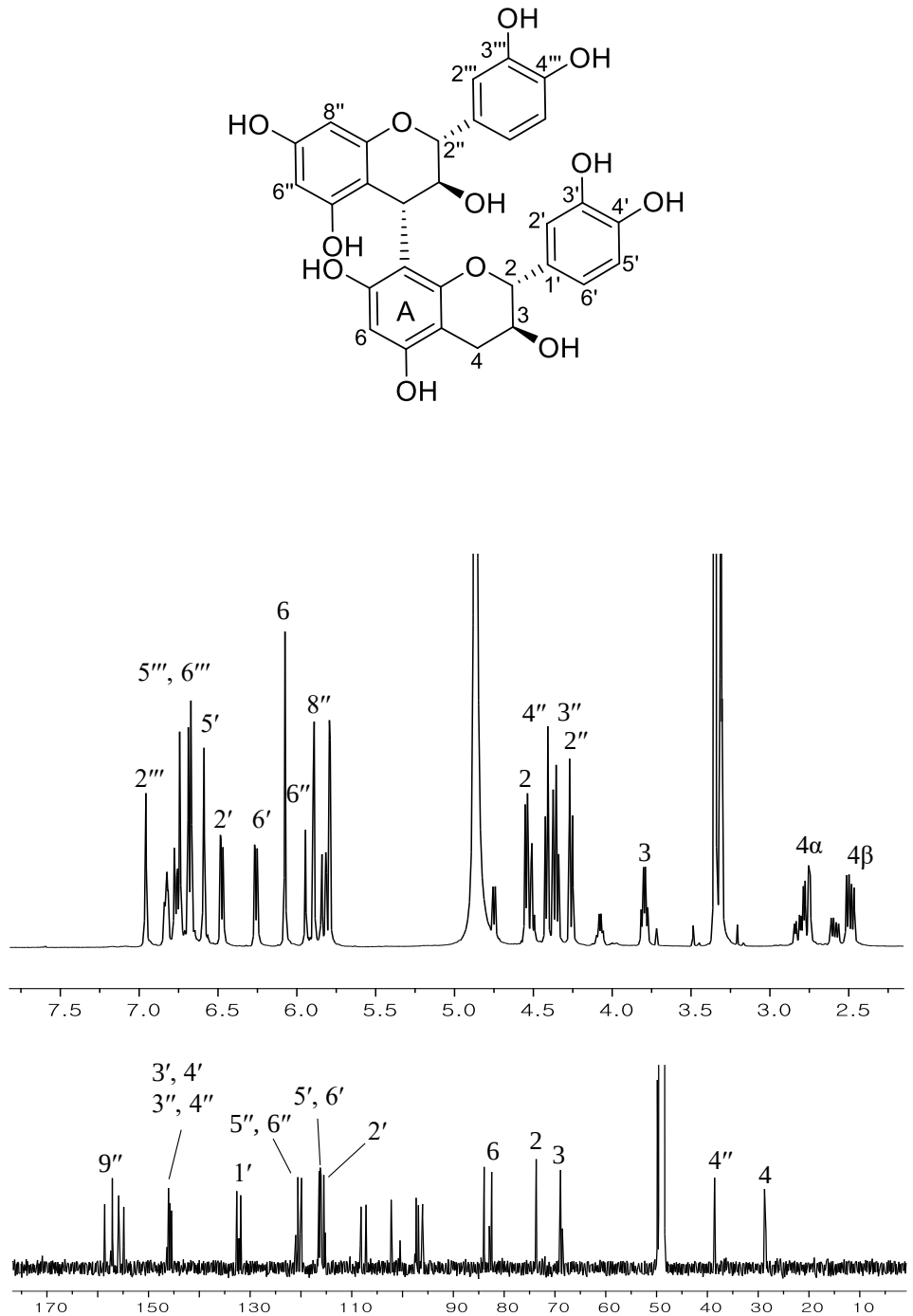

Figure 26. ^{1}H, ^{13}C NMR spectrum of compound **12** in CD_3OD

2. Elucidation of chemical structures of isolated compounds from the flos and leaves of *iris pallasii* (13-16)

Compound **13** was isolated as yellowish amorphous powder and showed characteristic UV absorption of flavones at maxima 213, 273, 335nm. The molecular formula of compound **13** was determined to be $C_{28}H_{32}O_{14}$ by negative HRESIMS data (m/z 591.1725 $[M-H]^-$, calcd for 591.1714, 1.9 ppm, $C_{28}H_{32}O_{14}$) and MS fragmentation also suggest that **13** was a C-glycoside type flavonoid. The proton NMR spectrum of **1** exhibited the signals of AA′BB′ system of 4′-hydroxy B-ring at H-2′/6′ [δ_H 7.91 (2H, d, J = 8.4 Hz)] and H-3′/5′ [δ_H 7.06 (2H, d, J = 8.45 Hz)], singlet signals for H-3 [δ_H 6.63 (1H, s)] and H-8 [δ_H 6.51 (1H, s)] confirmed the flavonoid core structure. Furthermore, the observation of anomeric protons at H-1″ [δ_H 4.89 (1H, d, J = 9.8 Hz)] and H-1‴ [δ_H 5.20 (1H, brs)] indicated the presence of the disaccharide moiety in **13,** additional chemical shifts at anomeric carbon signals at C-1″ (δ_C 69.9) and C-1‴ (δ_C 96.4) were proved the *C*- and *O*-glycones respectively. In the upfield of ^{1}H NMR spectrum, H-7-OMe singlet [δ_H 3.86 (3H, s)] evidenced the presence of one CH_3 group in the structure. The broad methyl signals at H-6‴ [δ_H 0.71 (3H, d, J = 6.1 Hz)] and C-6‴ (δ_C 18.0) suggested the presence of the rhamnosyl units, which was further confirmed by the reference. The other sugar residue was predicted to be *β*-D-glucopyranosyl based on the J value at H-1″ [δ_H 4.89 (1H, d, J = 9.8 Hz)]. Thus, compound **13** was identified as 2″-*O*-Rhamnosylswertisin (Whaley et al. 2017).

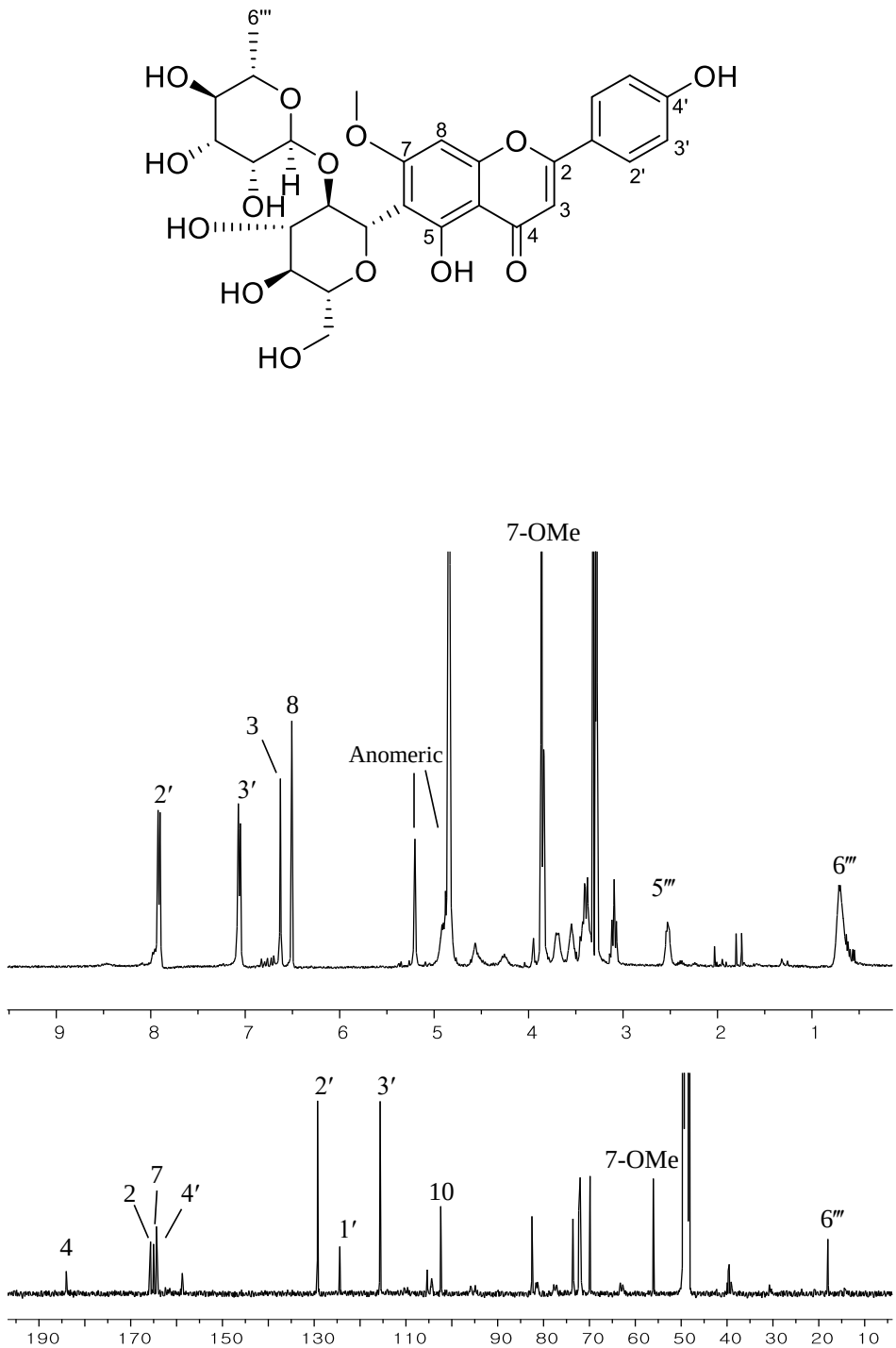

Figure 27. ^{1}H, ^{13}C NMR spectrum of compound **13** in CD_3OD

Compound **14** was obtained as yellowish amorphous powder, and negative HRESIMS data determined its molecular formula as $C_{29}H_{34}O_{14}$ (m/z 605.1879 [M-H]$^-$, calcd for 605.1879, 1.5 ppm, $C_{29}H_{34}O_{14}$), containing one additional C, two additional H compared to compound **13**. And this suggests that the CH_3 group was attached at the core flavonoids. The UV and NMR spectrum of compound **14** resembled those of compound **13** except for the H-4′-OMe [δ_H 3.88 (3H, s)] and the location of methoxy group determined to be the C-4′ (δ_C 164.5) positions by strongly downfield ^{13}C-NMR spectra. Thus, proton NMR spectrum of **14** suggested main skeleton as flavone, showing 4′-substituted B-ring at H-2′/6′ [δ_H 7.94 (2H, d, J = 8.4 Hz)] and H-3′/5′ [δ_H 7.07 (2H, d, J = 8.4 Hz)], singlet signals for H-3 [δ_H 6.67 (1H, s)] and H-8 [δ_H 6.71 (1H, s)]. Compound **14** also shown two anomeric protons at H-1″ [δ_H 4.89 (1H, d, J = 9.8 Hz)], H-1‴ [δ_H 5.24 (1H, brs)] and one of sugar is determined rhamnose by the signals at H-6‴ [δ_H 0.64 (3H, d, J = 6.2 Hz)] By comparing reference, compound **14** was elucidated as embinin, which was previously reported (Hilsenbeck and Mabry 1983).

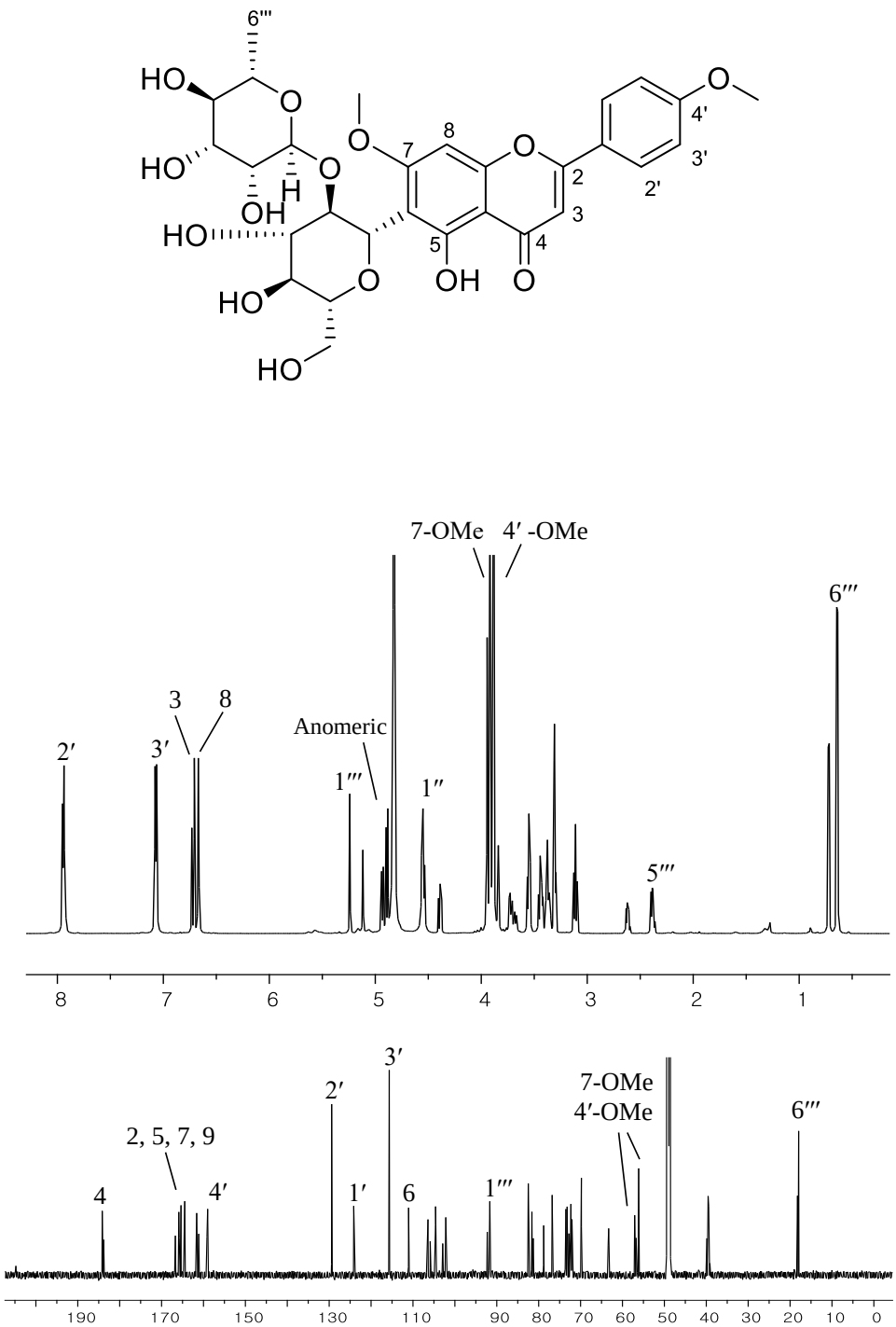

Figure 28. ^{1}H, ^{13}C NMR spectrum of compound **14** in CD_3OD

Compound **15** was isolated as yellowish amorphous powder. (-)-HRESIMS data determined its molecular formula as $C_{33}H_{38}O_{16}$ which was indicated by *m/z* value of 689.2087 $[M-H]^-$ (calcd for 605.1879, 1.5 ppm, $C_{29}H_{34}O_{14}$). The UV spectra of **15** shown the flavonoid type absorption [λ_{max} (log ε) 213 (4.5), 273 (4.3), 331 (4.4) nm]. Duplicated signals can be observed in the NMR spectra, indicating the presence of rotamers caused by rotational hindrance around the glycosyl-flavone C-C linkage (Lewis, Maxwell et al. 2000). Based on molecular formula and NMR spectra, compound **15** considered to be acetylated derivative of **14** (embinin). There was a pair of singlet signals for H-7-OMe [δ_H 3.96 (3H, s)], H-4′-OMe [δ_H 3.87 (3H, s)] and 4′-substituted B-ring at H-2′/6′ [δ_H 7.94 (2H, d, J = 8.4 Hz)] and H-3′/5′ [δ_H 7.07 (2H, d, J = 8.4 Hz)] like other flavone structures. Unlike embinin (**14**), additional signals for an acetoxy group at [δ_H 2.03 (3H, s)] and at (δ_C 20.8, 171.9) were found in NMR spectrum. The obvious downfield shift of H-4‴ [δ_H 4.53 (1H, m)] in **15** compared that of embinin H-4‴ (δ_H 3.31 – 3.50) suggest that the location of acetoxy group at C-4‴. Likewise, H-6″ [δ_H 5.05, 3.67 (1H, m)] were more downfield with that of embinin H-6″ [δ_H 3.78, 3.67 (1H, m)]. Thus, the structure of compound **15** was elucidated as 6″-4‴-*O*-diacetyl-embinin which was compared with previously reported (Whaley et al. 2017).

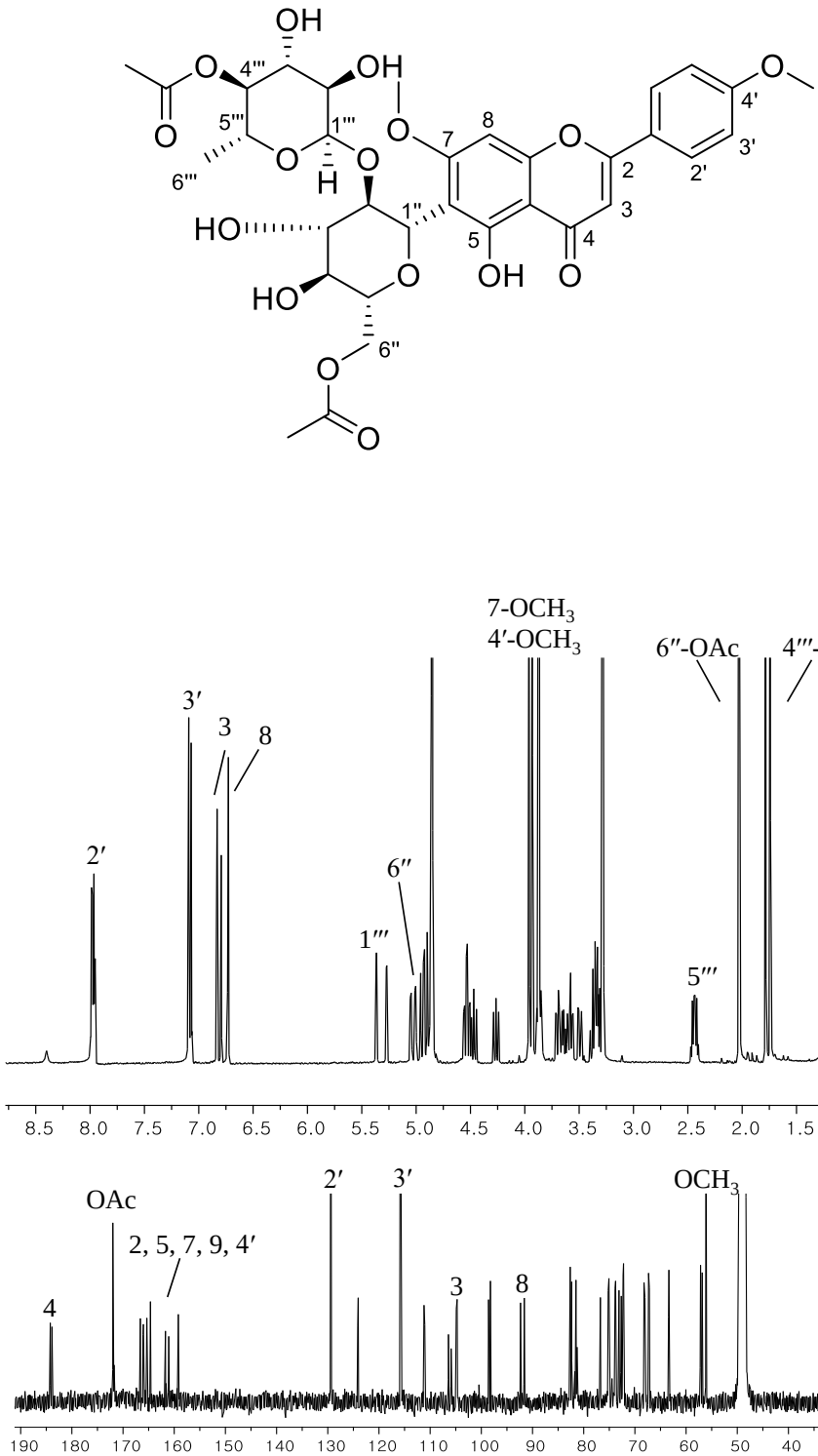

Figure 29. ^{1}H, ^{13}C NMR spectrum of compound **15** in CD_3OD

Compound **16** was obtaned as yellowish amorphous powder with molecular formula $C_{33}H_{38}O_{16}$ indicated by (-)-HRESIMS (*m/z*: 689.2087 $[M-H]^-$ calcd for 605.1879, 1.5 ppm, $C_{29}H_{34}O_{14}$). Like compound **15**, duplicated signals also observed in the NMR spectra, indicating the rotamers. Compound **16** and compound **15** both shared similar UV and NMR spectra except for H-2‴ [δ_H 4.78 (1H, m)] and H-6″ [δ_H 3.67, 3.36 (1H, m)]. It suggests that **16** was *O*-diacetyl derivative of embinin as well. Furthermore, the NMR data of rhamnosyl residue in **16** were more complicated to those of **15** which indicated that acetoxy moieties are all attached in the rhamnose. The above findings suggested the two acetoxy groups to be located at the C-2‴ and C-4‴ position. This assumption was further confirmed by reference data (Whaley et al. 2017). Thus, compound **16** was confirmed 2‴-4‴-*O*-diacetyl-embinin.

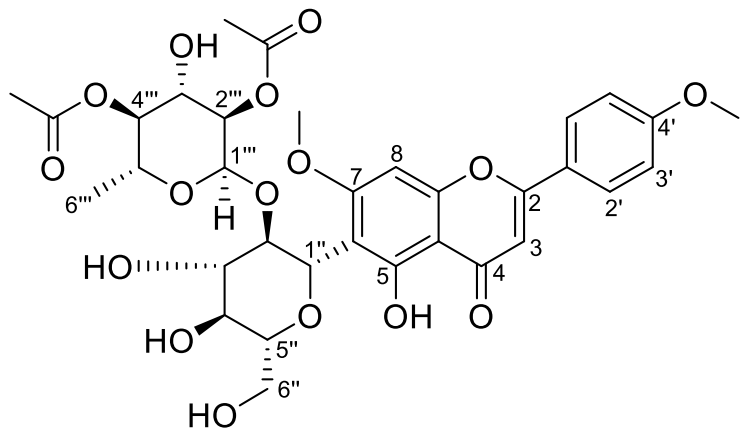

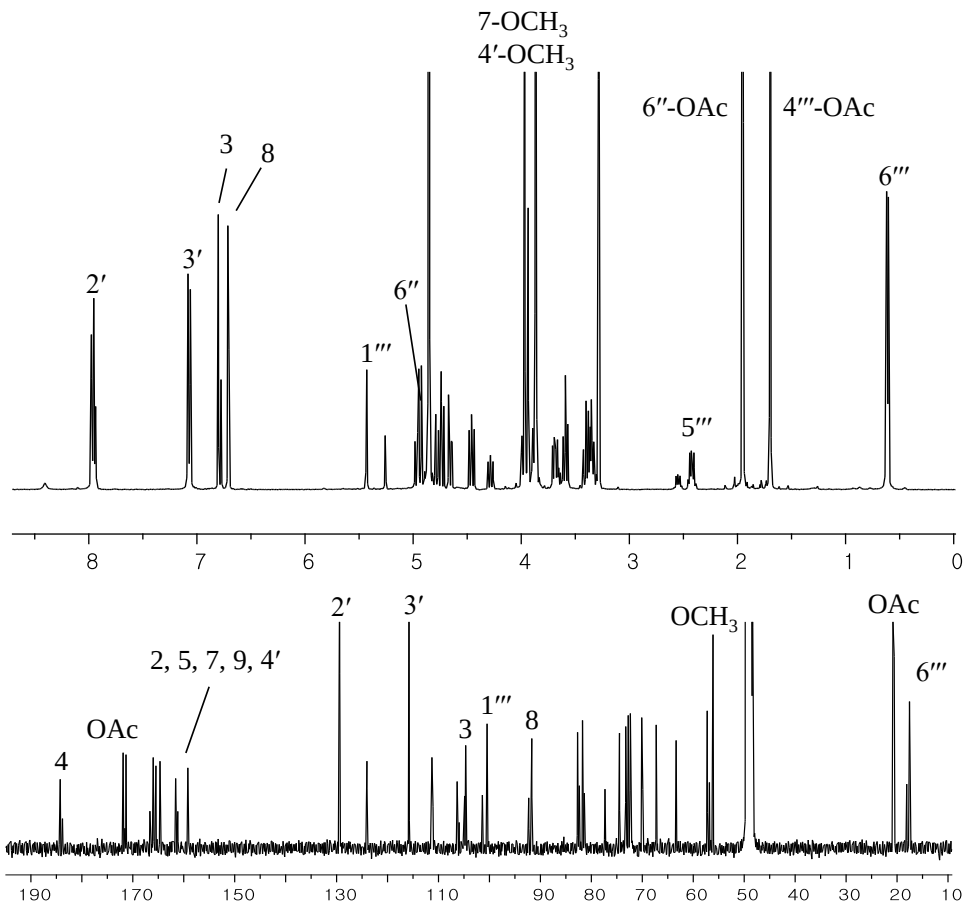

Figure 30. ^{1}H, ^{13}C NMR spectrum of compound **16** in CD_3OD

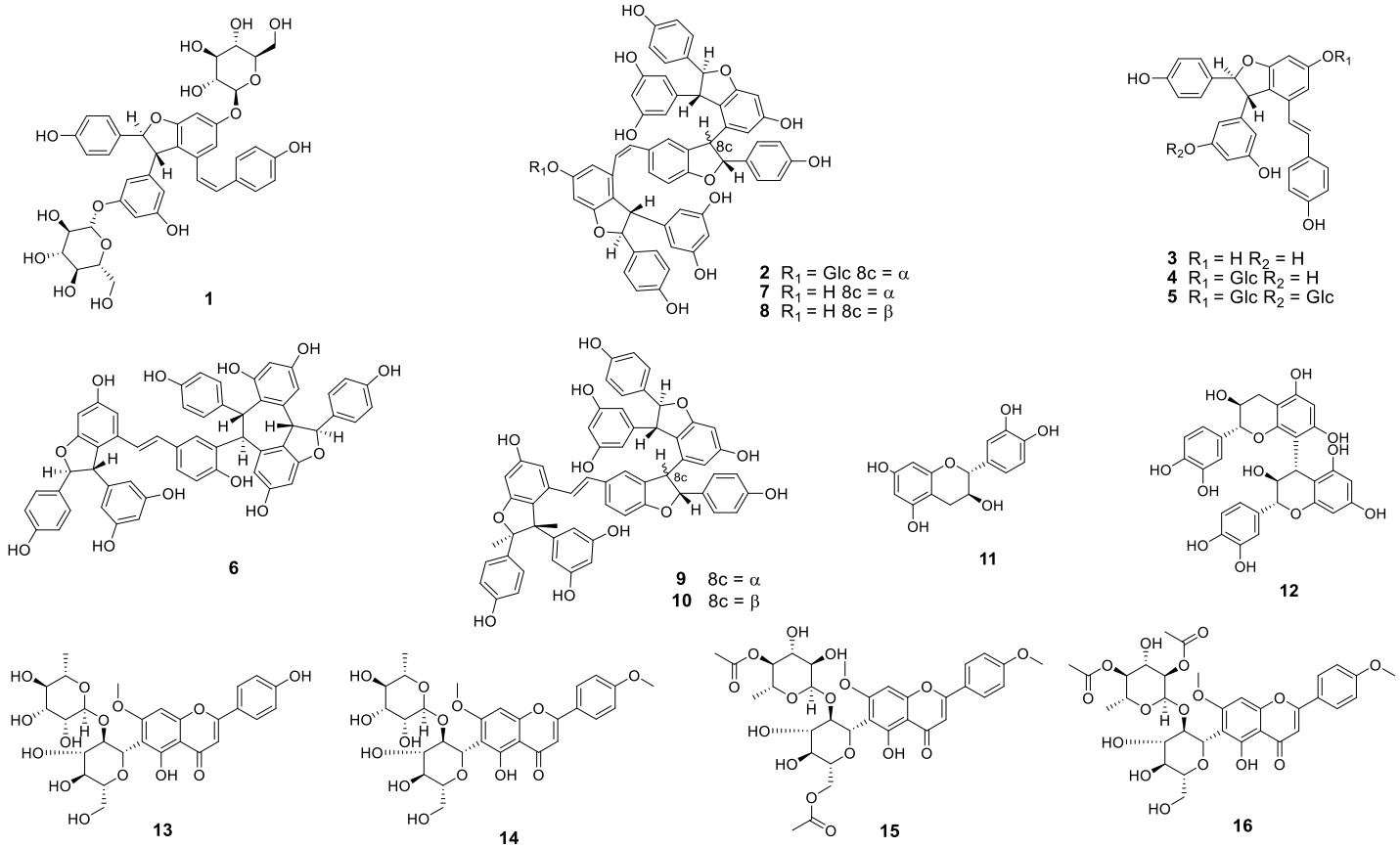

Figure 31. Structures of compounds isolated from *Iris pallasi*

3. Neuraminidase inhibitory activities of isolated compounds

The neuraminidase assay was tested before the isolation steps to estimate the degree of its neuraminidase inhibition activity. The ethanolic extracts of *Iris pallasii* which concentrations are 100, 50, 25 μg/ml were used and compared with the oseltamivir. Total extracts of *Iris pallasii* were showed moderate inhibitory activity against H1N1 virus (Figure 31). Then, all isolated compounds (**1-16**) were also screened for their inhibitory activities against neuraminidase (NA) from H1N1 influenza virus by NA inhibition assay. Tamiflu (Oseltamivir), well known flu treatment, was used as positive control for its superior ability to suppress neuraminidase. As shown in the Figure 32, compounds **7** – **10** corresponding to stilbene tetramers showed more potent neuraminidase inhibition effects than other stilbenoids either flavonoids. They showed no or weak inhibition until the concentration of 100 μM. Among stilbene tetramers (**7** – **10**), compounds **9** and **10** were evaluated much higher inhibitory activities than compound **7** – **8**. The IC_{50} of **9** showed 21.47 μM, which has most significant inhibitory activities in other compounds (Table 7). The structure-activity relationships for inhibition of neuraminidase by isolated compounds suggest that greater number of stilbene units in the structure, the better the activity. Comparing at the same size, the trans form is more active than cis form. In addition, inhibition is not significant if sugar moiety is attached to structure. These SAR results are based solely on activity results, so additional docking experiments will be required to ensure a more accurate model.

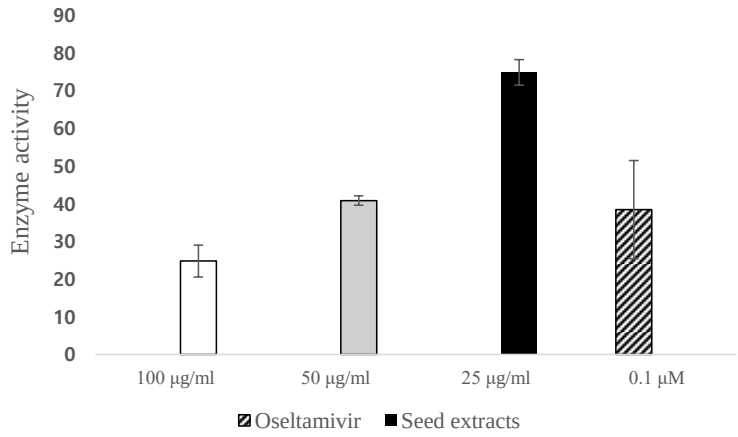

Figure 32. Neuraminidase inhibitory activities of Seeds extracts (100, 50, 25 µM)

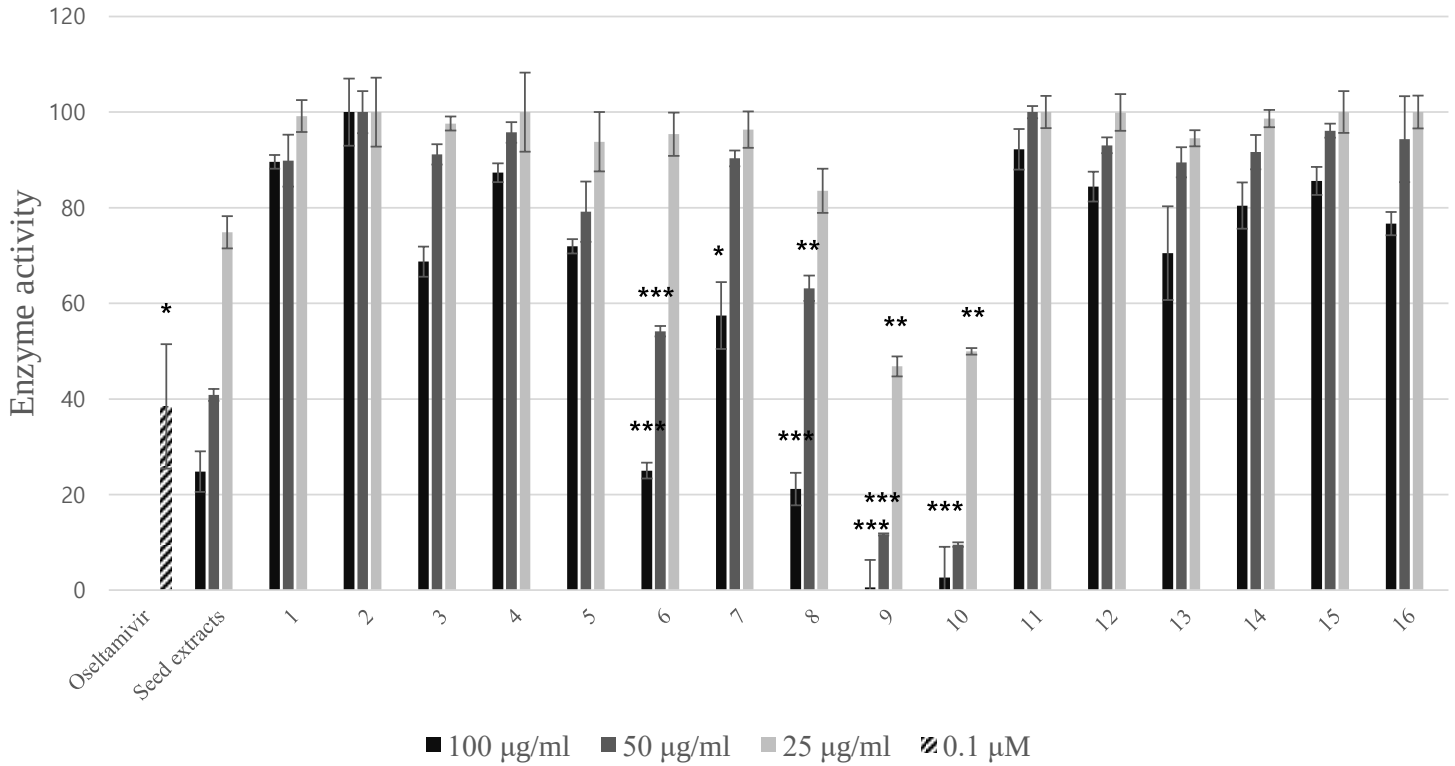

Figure 33. Neuraminidase inhibition assay of compounds **1-16**

Each value expressed as the mean ± SD (n= 2), *$p < 0.05$, **$p < 0.01$ and ***$p < 0.001$ compared only to the DMSO control. Oseltamivir was used as positive control.

Table 7. Inhibitory effects (IC_{50}) of selected compounds on neuraminidase

Compound	IC_{50}[a] (μM)
7	109.13 ± 1.26
8	76.55 ± 4.89
9	21.47 ± 2.34
10	28.64 ± 3.39
Oseltamivir[b]	0.080 ± 6.62

[a]IC_{50} was defined as the concentration (μM) which resulted in 50% inhibition of neuraminidase against H1N1 virus.

Oseltamivir[b] were used as a positive control

IV. Conclusion

Sixteen compounds (**1**-**10** stilbenoids, **11**-**12** catechins, **13**-**16** flavonoid glycosides) were isolated from the *I. pallasii* by various chromatographic methods. Among them, *cis*-ε-viniferin-13b-11a-O-*β*-D-diglucopyranoside (**1**), *cis*-vitisin B-13b-*O*-*β*-D-glucopyranoside (**2**) were reported for the first time from nature. Fourteen known compounds, *trans*-ε-viniferin (**3**), *trans*-ε-viniferin-13b-glycoside (**4**), vatalbinoside C (**5**), vitisin A (**6**), *cis*- vitisin B (**7**), *cis*-vitisin C (**8**), vitisin B (**9**), vitisin C (**10**), catechin (**11**), procyanidin B3 (**12**), 2"-O-rhamnosylswertisin (**13**), embinin (**14**), 6",4"'-diacetyl embinin (**15),** 2"',4"'-diacetyl embinin (**16**) were isolated. Especially, stilbene derivatives are isolated at the seeds and flavonoids derivatives were found in flower and leaves. Flavonoids isolated from this study were characterized by the presence of rotamer signals at a certain rate. And trans form of stilbenes were separated at a higher rate than the cis form, the trans form would have existed more in the plants. All the isolated compounds were tested for their inhibitory activities against neuraminidases from influenza viral strain (H1N1). Among the tested compounds, compounds **9** and **10** showed potent neuraminidase inhibitory activity. (IC_{50}: 21.47, 28.64 μM)

V. References

Abe N., Ito T., Ohguchi K, Nasu M., Masuda Y., Oyama M., Nozawa Y., Ito M and Iinuma M. J.., 2010. Resveratrol oligomers from *Vatica albiramis*. *Journal of Natural Products* 73, 1499-1506.

Flamini R., De Rosso M. and Bavaresco L., 2015. Study of grape polyphenols by liquid chromatography-high-resolution mass spectrometry (UHPLC/QTOF) and suspect screening analysis. *Journal of Analytical Methods in Chemistry*, 350259-350259.

Frank, J. H., Powder-George Y. L., Ramsewak R. S., and Reynolds W. F., 2012. Variable-temperature ^{1}H-NMR studies on two C-glycosylflavones. *Molecules* 17, 7914.

Goldblatt P., 2000. Phylogeny and classification of the Iridaceae and the relationships of *Iris*. *Annali di Botanica* 58, 2239-3129.

Gorham J. and Coughlan S. J., 1980. Inhibition of photosynthesis by stilbenoids. *Phytochemistry* 19, 2059-2064.

Hilsenbeck R. A. and Mabry T. J., 1983. C-glycosylflavones from *Siphonoglossa sessilis*. *Phytochemistry* 22, 2215-2217.

Ito J., Gobaru K., Shimamura T., Niwa M., Takaya Y. and Oshima Y., 1998. Absolute configurations of some oligostilbenes from *Vitis coignetiae* and *Vitis vinifera* 'Kyohou'. *Tetrahedron Letters* 54, 6651-6660.

Ito J. and Niwa M., 1996. Absolute structures of new hydroxystilbenoids, vitisin C and viniferal, from *Vitis vinifera* 'Kyohou'. *Tetrahedron Letters* 52, 9991-9998.

Ito J., Takaya Y., Oshima Y. and Niwa M., 1999. New oligostilbenes having a benzofuran from *Vitis vinifera* 'Kyohou'." *Tetrahedron Letters* 55, 2529-2544.

Ito T. and Nehira T., 2014. Dehydroxylation of stilbenoid oligomers: Absolute configuration determination via comparison of experimental and theoretical electronic circular dichroic spectra. *Tetrahedron Letters* 55, 314-318.

Lewis K. C., Maxwell A. R., McLean S., Reynolds W. F. and Enriquez R. G., 2000. Room-temperature (^{1}H, ^{13}C) and variable-temperature (^{1}H) NMR studies on spinosin. *Magnetic Resonance Chemistry* 38, 771-774.

Liu W. B., Hu L., Hu Q., Chen N., Yang Q. S. and Wang F. F., 2013. New resveratrol oligomer derivatives from the roots of *Rheum lhasaense*. *Molecules* 18, 7093.

Lv H., Wang H., He H., Ding C., Wang X. and Suo Y., 2015. Separation and purification of four oligostilbenes from *Iris lactea* Pall. *var. chinensis* (Fisch) Koidz. by high-speed counter-current chromatography. *Journal of Chromatography B* 988,127-134.

Lv H., Zhou W., Wang X., Wang Z., Suo Y. and Wang H., 2016. Extraction and separation of vitisin D, ampelopsin B and cis-vitisin A from *Iris lactea* Pall. *var. chinensis* (Fisch)0 Koidz. by alkaline extraction–acid precipitation and high-speed counter-current chromatography. *Journal of Chromatographic Science* 54, 744-751.

Oshima Y., Kamijou A., Ohizumi Y., Niwa M., Ito J., Hisamichi K. and Takeshita M., 1995. Novel oligostilbenes from *Vitis coignetiae*. *Tetrahedron Letters* 51, 11979-11986.

Oszmianski J., Lee C. J., 1990. Isolation and HPLC determination of phenolic compounds in red grapes. *American Journal of Enology and Viticulture* 41, 204-206.

Paulson J. C. and Kawasaki N., 2011. Sialidase inhibitors dampen sepsis. *Nature biotechnology* 29, 406-407.

Rahman, A. U., Choudhary M. I,. Alam M. N., Ndognii P. O., Badarchiin T. and Purevsuren G., 2000. Two new quinones from *Iris bungei*. *Chemical and Pharmaceutical Bulletin* 48, 738-739.

Reeves G., Chase M. W., Goldblatt P., Rudall P., Fay M. F., Cox A. V., Lejeune B. and Souza-Chies T., 2001. Molecular systematics of Iridaceae: evidence from four plastid DNA regions. *American Journal of Botany* 88, 2074-2087.

Regev-Shoshani G., Shoseyov O., Bilkis I. and Kerem Z., 2003. Glycosylation of resveratrol protects it from enzymic oxidation. *The Biochemical Journal* 374, 157-163.

Seki K., Haga K. and Kaneko R., 1995. Phenols and dioxotetrahydrodibenzofuran from the seeds of *Iris pallasii*. *Phytochemistry* 38, 965-973.

Shen T., Wang X. N. and Lou H. X., 2009. Natural stilbenes: an overview. *Natural Product Reports* 26, 916-935.

Tanaka T., Nakashima T., Ueda T., Tomii K. and Kouno I., 2007. Facile discrimination of aldose enantiomers by reversed-phase HPLC. *Chemical and Pharmaceutical Bulletin* 55, 899-901.

Vannozzi A., Dry I. B., Fasoli M., Zenoni S. and Lucchin M., 2012. Genome-wide analysis of the grapevine stilbene synthase multigenic family: genomic organization and expression profiles upon biotic and abiotic stresses. *BMC Plant Biology* 12, 130-130.

Vogt T., 2010. Phenylpropanoid biosynthesis. *Molecular Plant* 3, 2-20.

Whaley A. K., Ebrahim W., El-Neketi M., Ancheeva E. U., Ozkaya F. C., Pryakhina N. I., Sipkina N. U., Luzhanin V. G., Liu Z. and Proksch P., 2017. New acetylated flavone C-glycosides from *Iris lactea*. *Tetrahedron Letters* 58, 2171-2173.

Wong S., Oshima Y., Pezzuto J., Fong H. and Farnsworth M., 1986. Plant anticancer agents XXXIX: Triterpenes from *Iris Missouriensis*. *Journal of Pharmaceutical Sciences*, 317-320.

Xiao J., Capanoglu E., Jassbi A. R. and Miron A., 2016. Advance on the flavonoid C-glycosides and health benefits. *Critical Reviews in Food Science and Nutrition* 56, S29-S45.

Yuk H. J., Ryu H. W., Jeong S. H., Curtis-Long M. J., Kim H. J., Wang Y., Song Y. H. and Park K. H., 2013. Profiling of neuraminidase inhibitory polyphenols from the seeds of *Paeonia lactiflora*. *Food and Chemical Toxicology* 55, 144-149.

국문초록

타래붓꽃 (*Iris pallasii*)는 붓꽃과 (Iridaceae)에 속하는 식물로써 중국, 한국, 일본 그리고 러시아 등지에 분포하는 통년성 초본이다. 우리나라에도 많은 종류의 붓꽃이 자생하고 있으며 예로부터 한방에서 황달, 설사, 혈토, 대하, 인후염 등의 증상치료를 위해 사용되어져 왔다. 이전의 생리활성 연구에 따르면 마린자의 아세틸콜린 에스터라아제에 대한 억제효과 때문에 치매 치료제의 후보군으로도 지목된 바 있다. 현재까지 붓꽃과에 속하는 식물들로부터 flavonoid, stilbenoid, triterpenoid, catechin, quinone 등의 물질들이 분리 보고 되어있으며, 붓꽃의 씨앗에 관한 연구는 상대적으로 이루어지지 않아 본 연구에서는 붓꽃의 씨앗으로부터 UPLC-DAD/ESI-qTOF-MS 를 통해 확인한 sitlbenoid 계열의 화학 성분을 분리하고자 하였다. 이후 꽃과 잎 부위에 대한 분리 연구도 추가적으로 수행해 보았다. 타래붓꽃의 씨앗인 마린자의 EtOAc 층 분획과 BuOH 층 분획에서 다양한 chromatography 기법으로 12 종의 화합물을 분리하였으며, 구조의 동정에는 각종 이화학적 특성 및 분광학적 데이터가 활용되었다. 분리된 화학물 중 화합물 **1** 은 *β*-D-diglucopyranose 기가 붙은 viniferin 계열 stilbenoid 화합물이며, 화합물 **2** 도 *β*-D-diglucopyranose 기가 붙은 stilbene tetramer 계열 화합물이다. **1, 2** 모두 천연에서는 처음 분리 보고되는 물질이며, 화합물 **13 – 16** 은 acetyl 기 및 glucose 와 rhamnose 를 포함한 flavonoid 계열 화합물로, 네 화합물 모두 NMR 데이터에서 일정한 비율의 (2:1) major peak 와 minor peak 을 확인할 수 있었다. 이 외에도 분리된, *trans*-ε-viniferin (**3**), *trans*-ε-viniferin-13b-*β*-D-glucopyranose (**4**), vatalbinoside C (**5**), vitisin A (**6**), *cis*- vitisin B (**7**), *cis*-vitisin C (**8**), vitisin B (**9**), vitisin C (**10**), catechin (**11**), procyanidin B3 (**12**), 2"-*O*-rhamnosylswertisin (**13**), embinin (**14**), 6",4"'-*O*-diacetyl embinin (**15),** 2"',4"'-

O diacetyl embinin (**16**)로 동정하였으며, 화합물 **11 – 12** 는 catechin 계열, **1 – 10** 은 stilbenoid 계열, **13 – 16** 은 flavonoid 계열 물질이었다.

또한, 마린자 분획층들에 대하여 뉴라미니데이즈 억제 활성을 실시하였으며, 억제율이 높은 EA, BU 층에서 화합물 분리를 진행하였다. 이후 모든 분리된 화합물을 대상으로 활성을 테스트하였고, 이 중 stilbene tetramer 계열에 속하는 **7-10** 에서 유의미한 IC_{50} 을 얻을 수 있었다. 특히 vitisin B **(9)**는 IC_{50} 값이 21.47 μM 로 가장 높은 활성을 나타냈다.

이상의 결과로 마린자가 함유하고 있는 신규화합물 **1, 2** 를 분리하여 씨앗에서 나타나는 2 차 대사산물의 화학적 다양성을 규명하였고, stilbenoid 에서 유의한 바이러스 억제 활성을 확인함으로써 추출물의 활성은 스틸벤 화합물에 의한 것이었으며, 비슷한 계열의 다른 스틸벤 화합물에 대한 치료제 개발 가능성을 확인 할 수 있었다.

주요어: 타래붓꽃(*Iris pallasii*), Stilbenoid, flavonoid glycosides, Neuraminidase 억제 활성

학번: 2017-22999

부록

Supplementary information

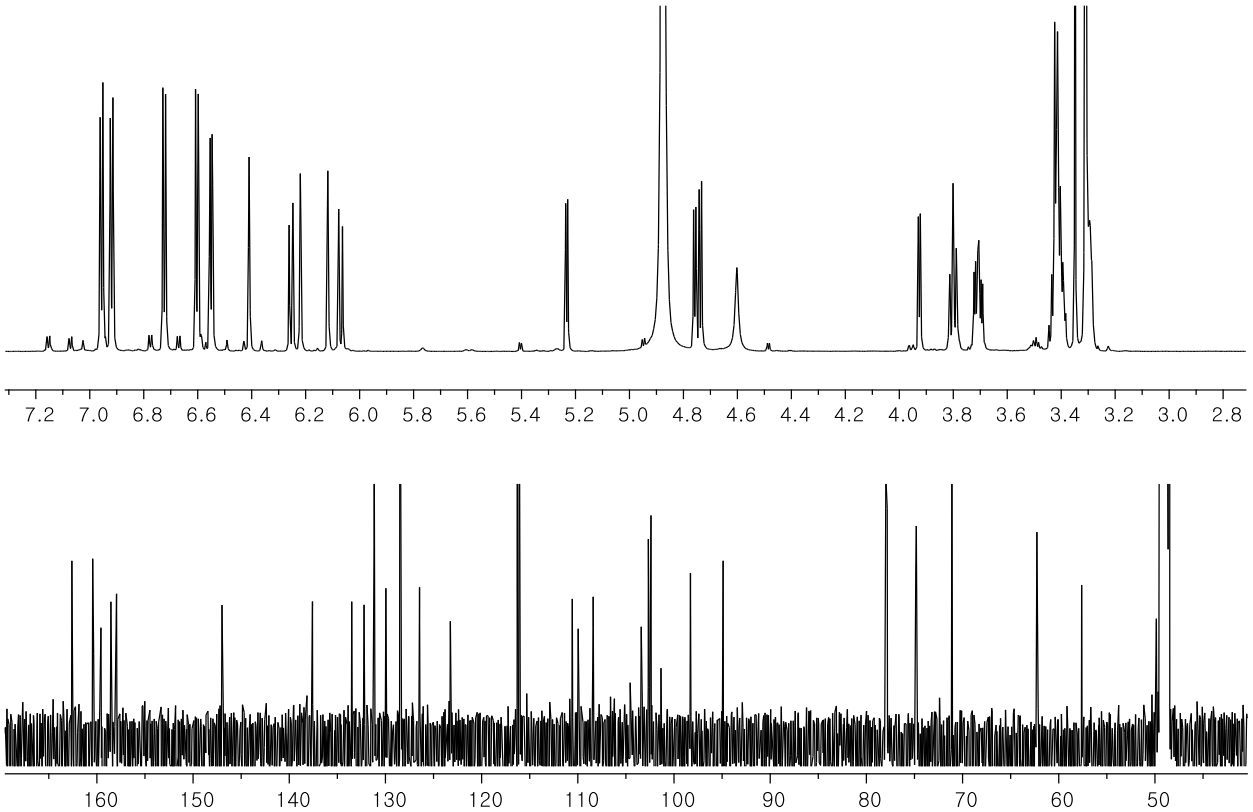

Fig. S1 ^{1}H, ^{13}C NMR spectrum of compound **1**

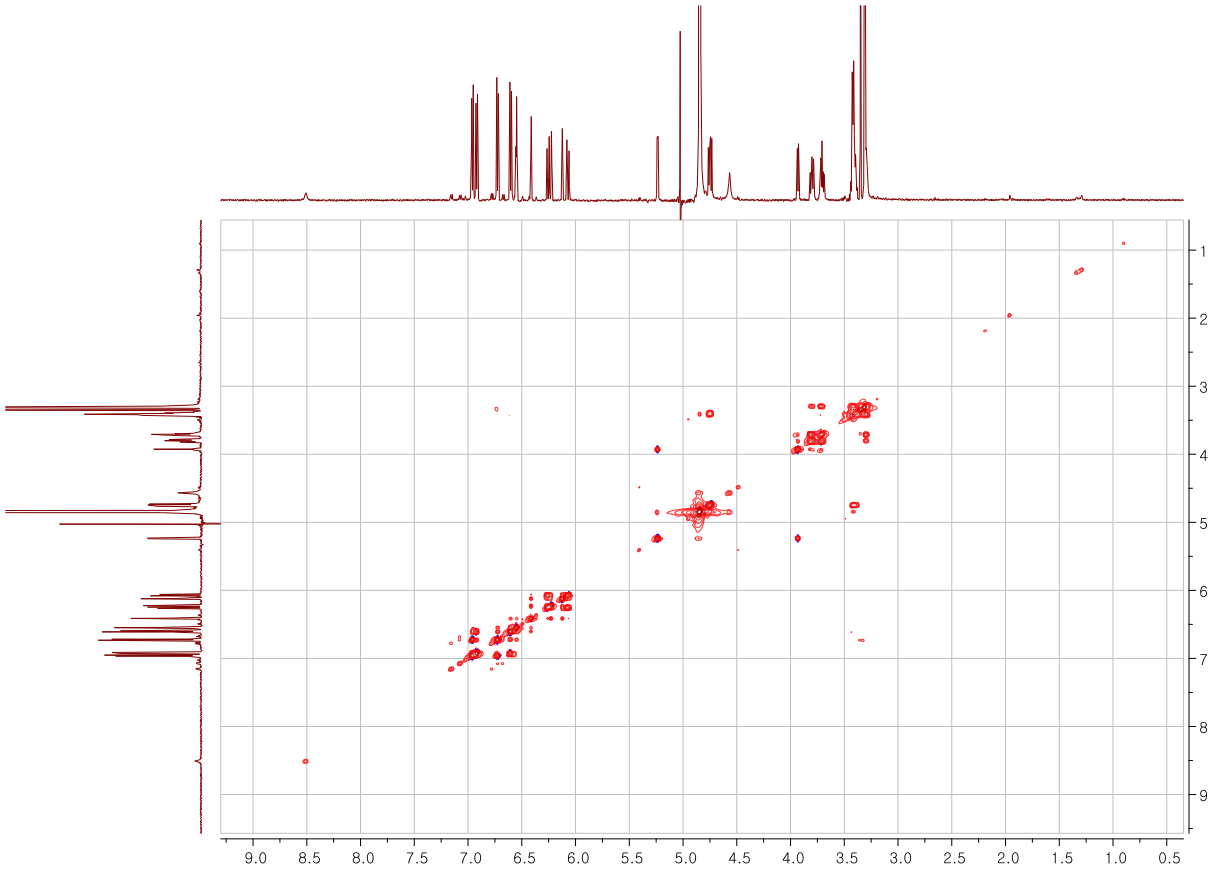

Fig. S2 COSY spectrum of compound **1**

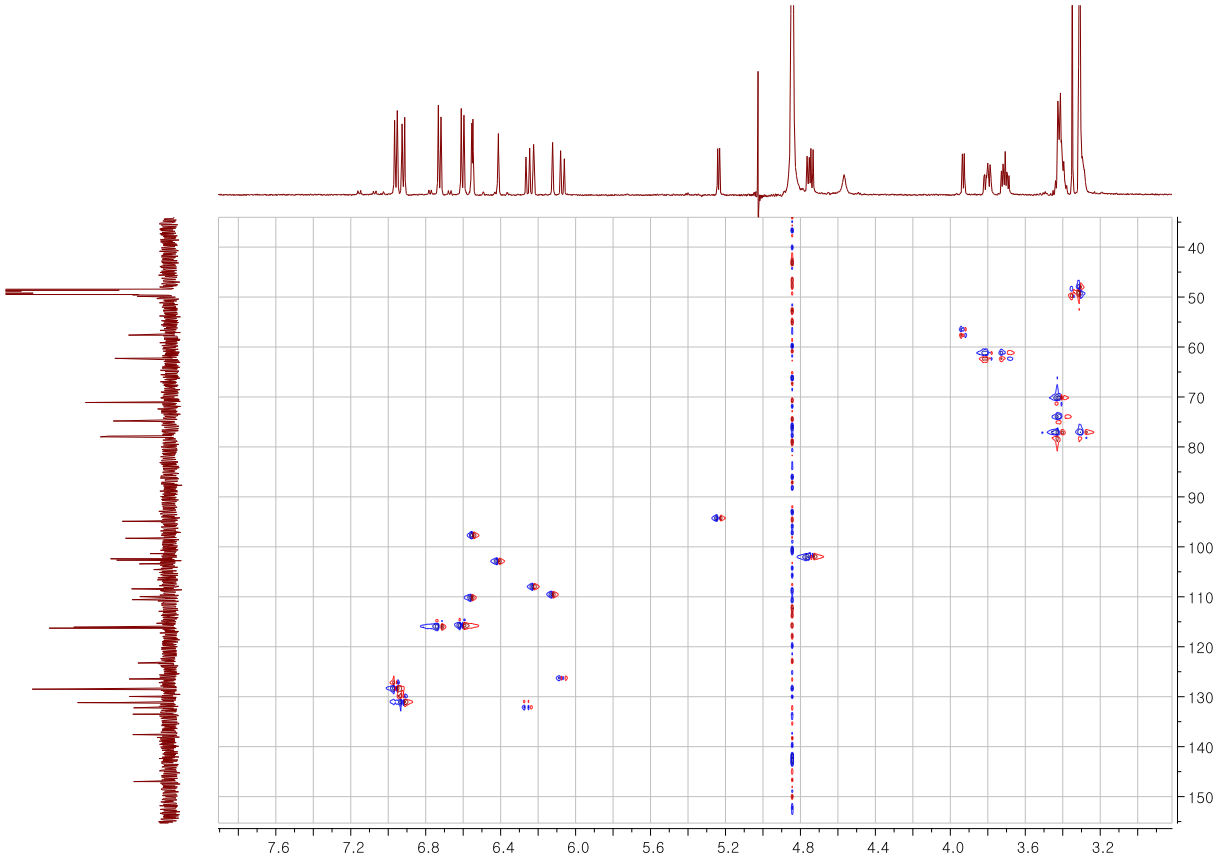

Fig. S3 HSQC spectrum of compound **1**

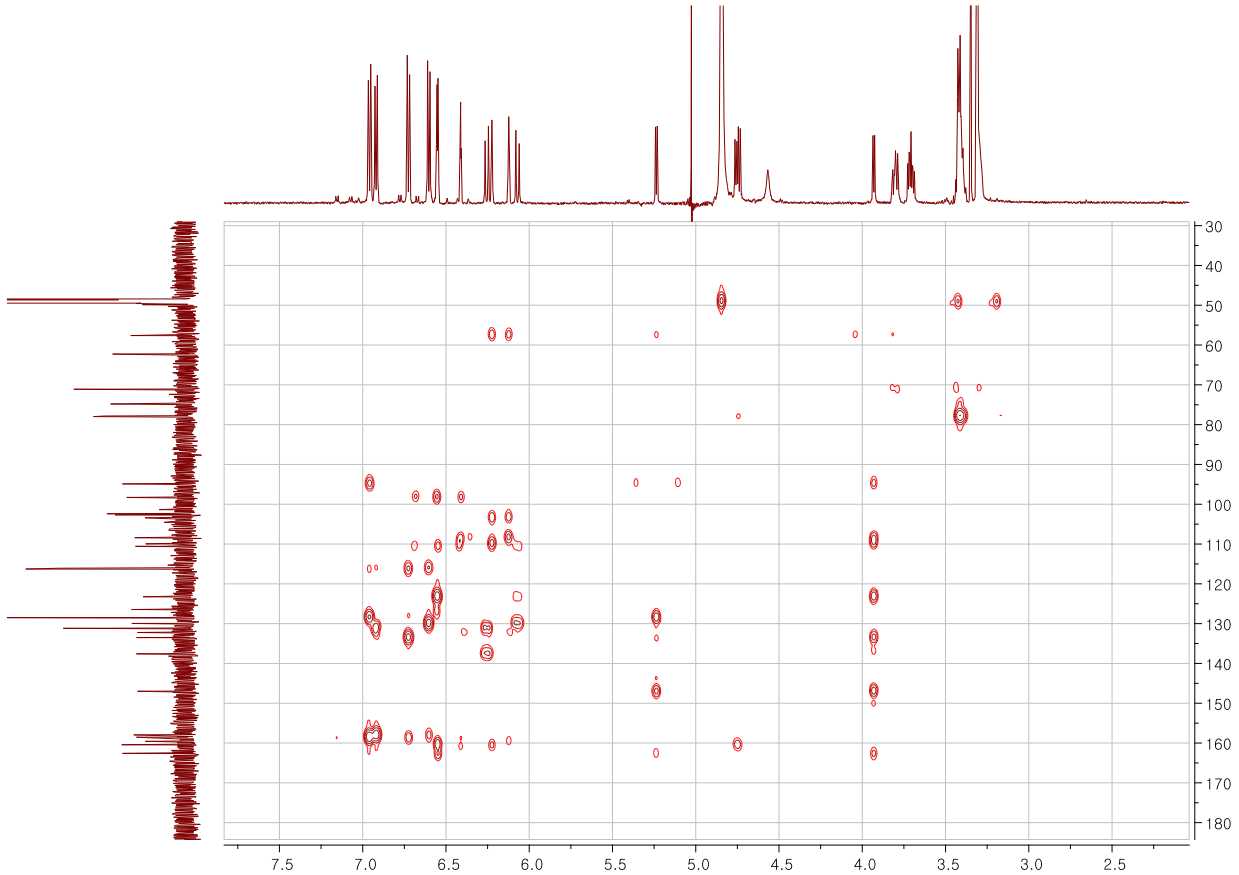

Fig. S4 HMBC spectrum of compound **1**

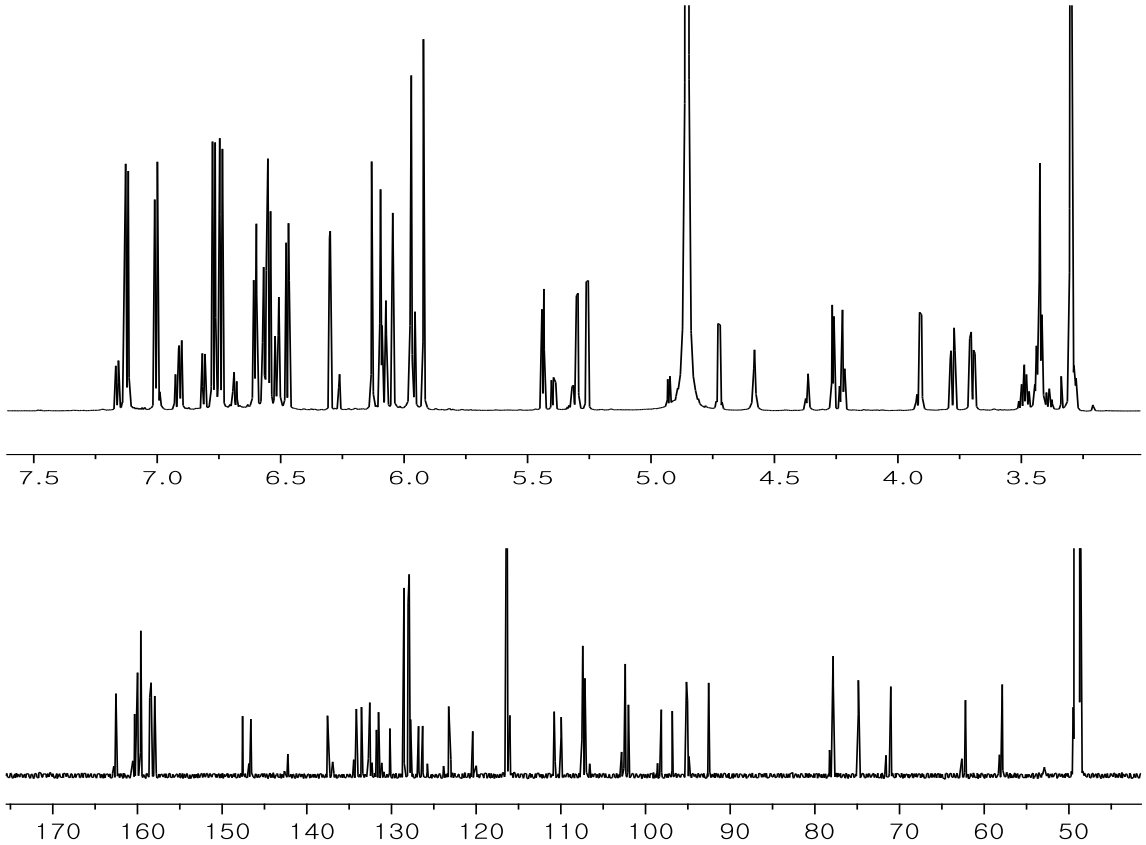

Fig. S5 ^{1}H, ^{13}C NMR spectrum of compound **2**

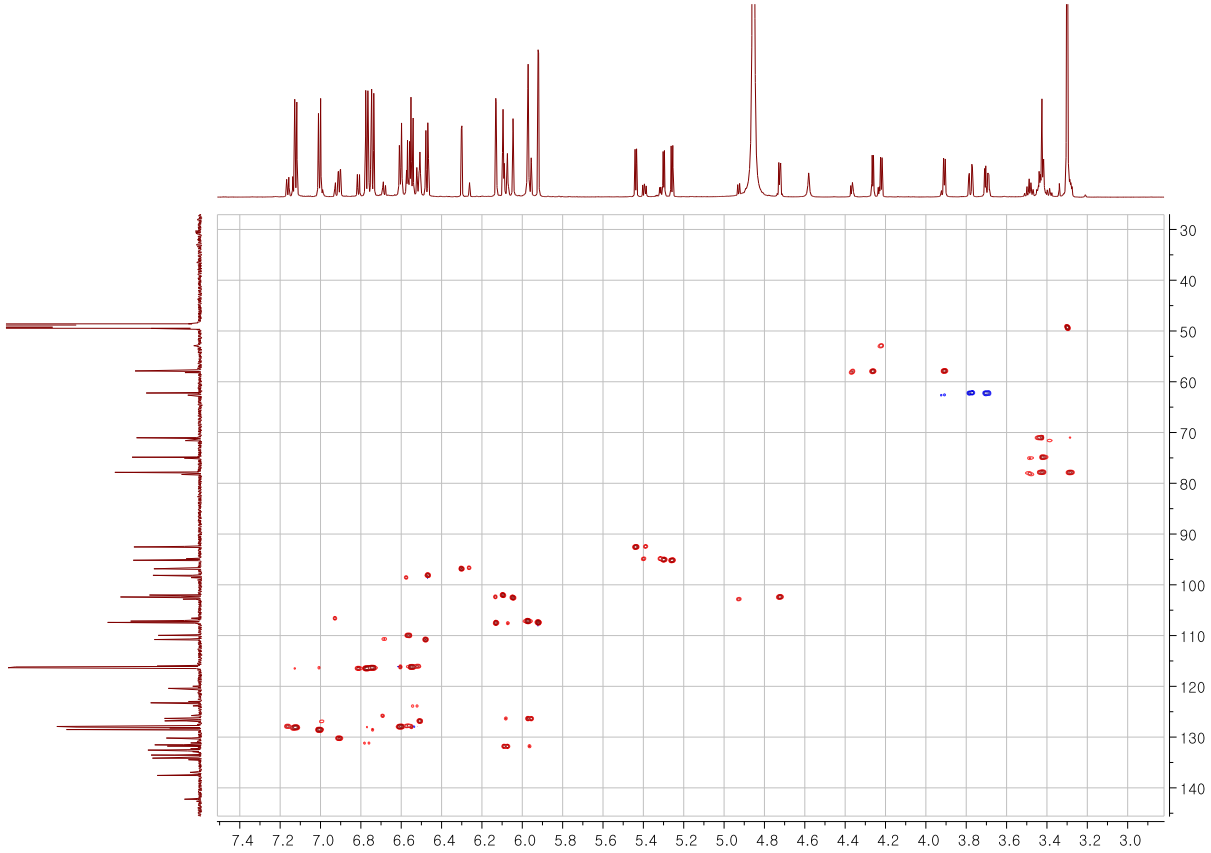

Fig. S6 HSQC spectrum of compound **2**

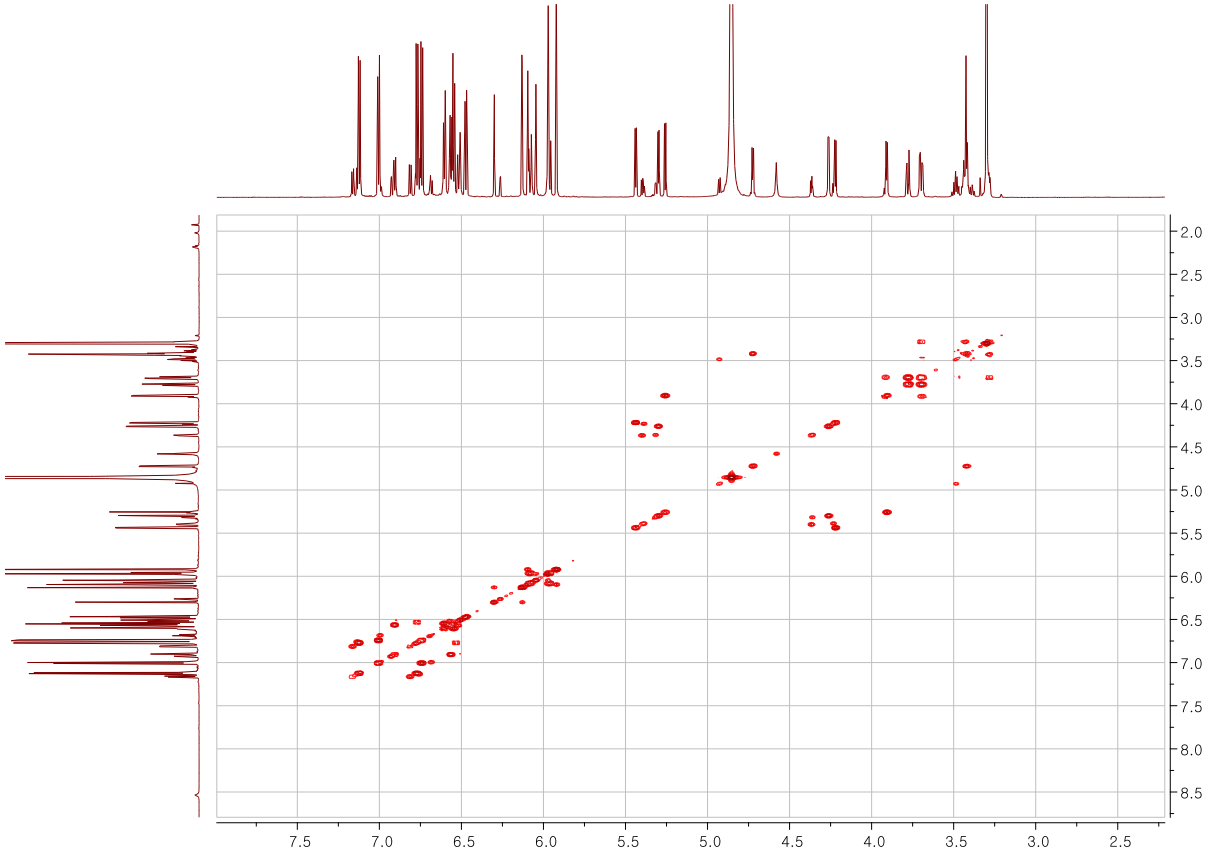

Fig. S7 COSY spectrum of compound **2**

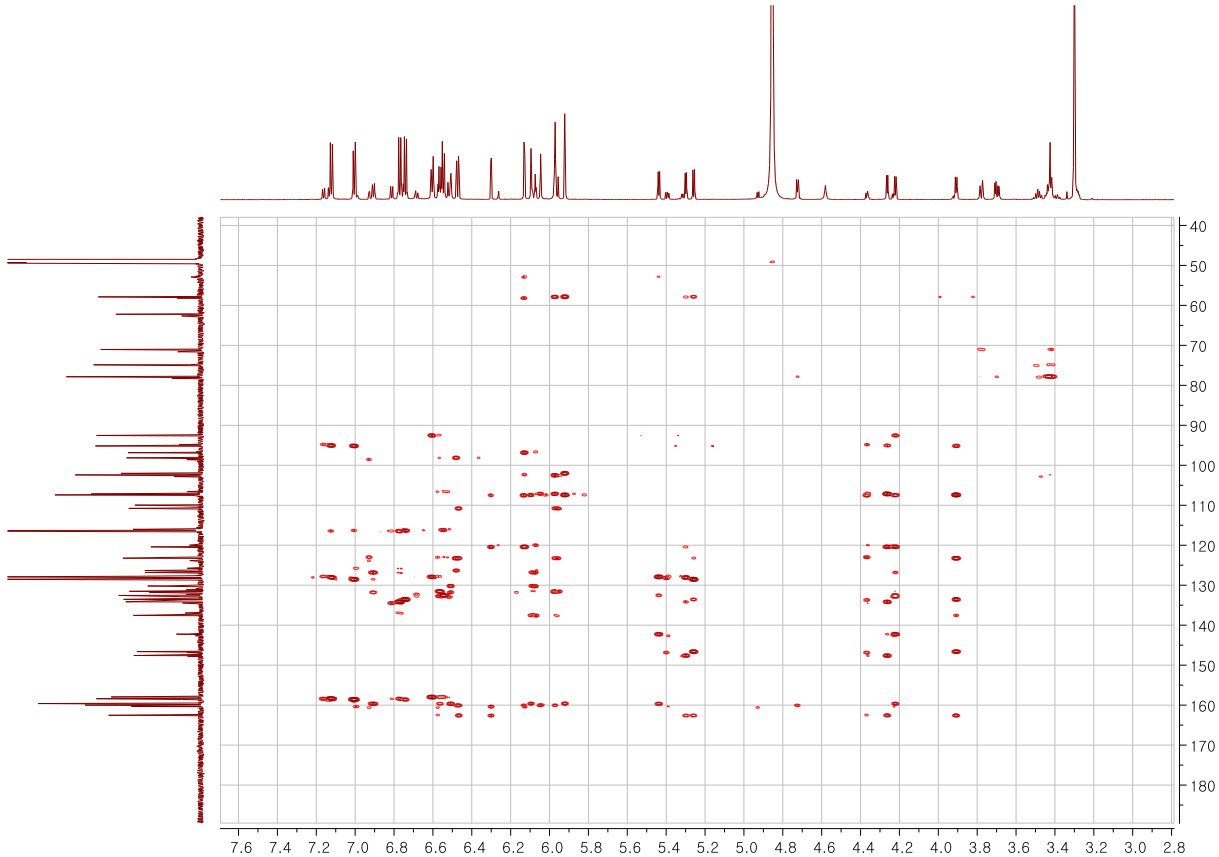

Fig. S8 HMBC spectrum of compound **2**